Semileptonic Decays and Sides of the Unitarity Triangle*

C. Bauer,[1,9] C. Bernard,[2] I. Bigi[3], M. Datta,[4] D. del Re,[5]
B. Grinstein,[6] S. Hashimoto,[7] U. Langenegger,[8] Z. Ligeti,[9]
M. Luke,[10] E. Lunghi,[11] P. Mackenzie,[12] A. Manohar,[13]
T. Moore,[14] D. Pirjol,[15] S. Robertson,[16] I. Rothstein,[17]
I. Stewart,[18] M. Voloshin[19]

[1]University of California, Berkeley; [2]Washington University; [3]Notre Dame University;
[4]University of Wisconsin, Madison; [5]University of Rome; [6]University of California, San Diego;
[7]High Energy Accelerator Research Organization (KEK); [8]Stanford Linear Accelerator Center;
[9]Lawrence Berkeley National Laboratory;[10]Toronto University;[11]ITP - University of Zurich;
[12]Fermilab;[13]University of California, San Diego; [14]University of Massachusetts
[15]Massachusetts Institute of Technology; [16]McGill University; [17]Carnegie-Mellon University;
[18]Massachusetts Institute of Technology;[19]University of Minnesota

October 2003

*This work was supported in part by the Director, Office of Science, Office of High Energy Physics, of the U.S. Department of Energy under Contract No. DE-AC03-76SF00098.

4

Semileptonic Decays and Sides of the Unitarity Triangle

Conveners: U. Langenegger, Z. Ligeti, I. Stewart

Authors: C. Bauer, C. Bernard, I. Bigi, M. Datta, D. del Re, B. Grinstein, S. Hashimoto, U. Langenegger, Z. Ligeti, M. Luke, E. Lunghi, P. Mackenzie, A. Manohar, T. Moore, D. Pirjol, S. Robertson, I. Rothstein, I. Stewart, M. Voloshin

4.1 Theory overview

4.1.1 Continuum methods (OPE, HQET, SCET)

$\succ$ A. Manohar $\prec$

The elements of the CKM matrix enter the expressions for the decay rates and mixing amplitudes of hadrons. In some cases, the the theoretical expressions are free of strong interaction effects, for example the CP asymmetry in $B \to J/\psi K^0_S$, so that measuring the CP asymmetry directly gives the value of $\sin 2\beta$, with the error in the result given by the experimental error in the measurement. In most cases, however, the experimentally measured quantities depend on strong interactions physics, and it is absolutely essential to have accurate model-free theoretical calculations to compare with experiment. A number of theoretical tools have been developed over the years which now allow us to compute B decays with great accuracy, sometimes at the level of a few percent or better. These calculations are done using effective theory methods applied to QCD, and do not rely on model assumptions.

Inclusive decays can be treated using the operator product expansion (OPE). The total decay rate is given by twice the imaginary part of the forward scattering amplitude, using the optical theorem. In heavy hadron decays, the intermediate states in the forward scattering amplitude can be integrated out, so that the decay rate can be written as an expansion in local operators. The expansion parameter is $1/m_B$, the mass of the decaying hadron. OPE techniques have been well-studied in the context of deep-inelastic scattering, where the expansion in powers of $1/Q^2$ is called the twist expansion. In inclusive B decays, the leading term in the $1/m_B$ expansion gives the parton decay rate, and non-perturbative effects enter at higher orders in $1/m_B$.

The OPE can be combined with heavy quark effective theory (HQET) for greater predictive power in heavy hadron decays. HQET is an effective theory for heavy quarks at low energies, and the HQET Lagrangian has an expansion in powers of $1/m_b$, the inverse heavy quark mass. The HQET Lagrangian is written in terms of the field b_v, which annihilates a b quark moving with velocity v. One usually works in the rest frame of the heavy quark $v = (1, 0, 0, 0)$. At leading order ($m_b \to \infty$), the heavy quark behaves like a static color source. As a result, the leading order HQET Lagrangian has heavy quark spin-flavor symmetry, since the color interactions of a static color source are spin and flavor independent. The $1/m_b$ terms in the Lagrangian break the spin and flavor symmetries, and are treated as perturbations. Since this is an effective theory, radiative corrections can be included in a systematic way. Most

quantities of interest have been computed to $1/m_b^3$ in the $1/m_b$ expansion, and radiative corrections to the leading term are typically known to order α_s^2 or $\alpha_s^2\beta_0$. In a few cases, the order α_s corrections are known for the $1/m_b$ terms. The calculations can be pushed to higher orders, if this is experimentally relevant.

The OPE can be combined in a natural way with HQET for inclusive heavy hadron decays, since both involve an expansion in $1/m_b$. This allows one to write the inclusive decay rates in terms of forward matrix elements of local operators. At leading order, the decay rate can be written in terms of the operator $\bar{b}\gamma^\mu b$, the b quark number current in full QCD. The matrix element of this operator in B hadrons is one to all orders in $\Lambda_{\rm QCD}/m_b$ and all orders in α_s. At leading order, the inclusive decay rates of all b hadrons is the same. At order $1/m_b$, the only operator allowed by dimensional analysis is the operator $\bar{b}_v(iv\cdot D)b_v$, whose matrix element vanishes by the equations of motion. This is an important result—non-perturbative corrections first enter at order $\Lambda_{\rm QCD}^2/m_B^2$, which is of order a few percent. At order $1/m_b^2$, the inclusive rate depends on two non-perturbative parameters λ_1 and λ_2 which are the heavy quark kinetic energy and hyperfine energy, respectively. The same parameters $\lambda_{1,2}$ enter other quantities such as the hadron masses. For example, the B^*–B mass difference gives $\lambda_2 = 0.12$ GeV^2. As the data become more precise, various HQET parameters are pinned down with greater precision, increasing the accuracy with which the decay rates are known.

HQET can also be applied to study exclusive decays. Heavy quark spin-flavor symmetry puts constraints on the form factors; *e.g.*, heavy quark symmetry provides an absolute normalization of the form factor at zero-recoil for the semileptonic decay $B \to D^{(*)}$, up to corrections of order $1/m_b^2$. The reason is that at zero recoil the decay proceeds by a b quark at rest turning into a c quark at rest. Since the strong interactions at leading order in $1/m$ are flavor-blind, the form-factor at zero-recoil is unity. Corrections to this result follow from the $1/m$ symmetry breaking terms. It is known that there are no $1/m$ corrections, so the first corrections are order $1/m^2$. As for inclusive decays, the $1/m^2$ corrections are a few percent, so the exclusive decay can be used to obtain V_{cb} to a few percent.

Heavy to light decays such as $B \to \pi\pi$, which is required for a determination of $\sin 2\alpha$, are more difficult to treat theoretically. Here the B meson decays into two fast moving light hadrons, and it is difficult to treat strong interactions in this kinematic regime. A recently developed effective theory, soft-collinear effective theory (SCET) is being used to deal with this situation. SCET is an effective theory that describes fast moving quarks with momentum proportional to the light-like vector n by collinear fields ξ_n. In the case of $B \to \pi\pi$, there are two back-to-back light-like vectors n and $\overline{n}$ giving the directions of the two pions. The SCET fields needed to describe this process are collinear quarks and gluons in the n and $\overline{n}$ directions, ξ_n, A_n, $\xi_{\overline{n}}$, $A_{\overline{n}}$, as well as soft quarks and gluons that describe the light degrees of freedom in the B meson. The non-perturbative interactions of ξ_n and A_n produce the pion moving in the n direction, and the interactions of $\xi_{\overline{n}}$ and $A_{\overline{n}}$ produce the pion moving in the $\overline{n}$ direction. If one neglects the soft fields, the n and $\overline{n}$ fields do not interact, so there are no final state interactions between the pions in $B \to \pi\pi$, and the factorization approximation for the decay is valid. Soft gluons interact with all modes in the effective theory, and introduce final state interactions. The extent to which this affects the decay amplitude and final state interaction phase-shift is being investigated.

SCET is also applicable in inclusive decays where the final hadronic state has small invariant mass, and is jet-like. An example is the endpoint of the photon spectrum in $B \to X_s\gamma$ decay, or electron spectrum in $B \to X_u e\nu$ decay. SCET allows one to systematically resum the Sudakov double logarithmic radiative corrections which become very large in the endpoint region.

The effective theories discussed here will be used later in this chapter to obtain detailed predictions for decay rates and form factors.

4.1.2 Lattice QCD and systematic errors

≻C. Bernard, S. Hashimoto, P. Mackenzie ≺

Systematic errors of lattice QCD computations come from a variety of sources. Many of these are associated with an extrapolation from a practical lattice calculation (at finite lattice spacing, unphysically heavy quark mass values, and finite spatial volume) to the real, continuum, infinite volume world, where the quark masses take their physical values. There are also lattice systematics that are not directly connected to an extrapolation. These include the perturbative error in connecting lattice currents to their continuum counterparts, and the "scale error" coming from the need to determine the lattice spacing in physical units.

One possible lattice systematic that will not be included below is quenching, the omission of virtual (sea) quark loops. Although the quenched approximation has been used in most lattice computations to date, one must remember that it is an *uncontrolled* approximation, not systematically improvable. Indications are that it produces errors of 10 to 20% on the phenomenologically interesting quantities we discuss in this report. However, these are uncontrolled and hence unreliable error estimates and completely unsuitable for use in connection with the precise experimental results that a Super B Factory will make possible. We therefore consider only lattice computations in which the effects of three light flavors (u, d, and s) of virtual quarks are included.

It is important to distinguish here between quenching and "partial quenching." Partial quenching [1, 2, 3] is a somewhat misleading term in this context and simply means that the valence quark masses in the lattice simulation are not necessarily chosen equal to the sea quark masses. As emphasized by Sharpe and Shoresh [3], as long there are three light virtual flavors in a partially quenched simulation, real-world, full ("unquenched") QCD results can be extracted. This is not surprising, since the real-world situation is just a special case (valence masses = sea masses) of the partially quenched simulation. In fact, partial quenching is often *preferable* to simple unquenching because it separates the valence and sea mass contributions and allows one to use the information contained in the correlations, for fixed sea masses, of the results for different valence masses. Partial quenching will be assumed in lattice errors estimates given in Section 4.5.2 and 4.6.1.

We now discuss the relevant lattice systematic effects in more detail.

Chiral extrapolation

The computer time required for a lattice simulation rises as a large power of $1/m_{u,d}$ as these masses approach their physical values. One must therefore work with larger masses and extrapolate to the real world. Chiral perturbation theory (χPT) determines the functional form of the extrapolation and makes it possible to get good control of the associated systematic error. (In the partially quenched case one must use the corresponding "partially quenched chiral perturbation theory" (PQχPT) [1].)

As the physical values of the u, d quark masses are approached, there is significant curvature in essentially all interesting quantities that involve light quarks. The curvature comes from chiral logarithms that are proportional to $m_\pi^2 \ln(m_\pi^2/\Lambda_\chi^2)$. This implies that one must get to rather small quark mass (probably $m_{u,d} \sim m_s/4$ to $m_s/8$) to control the extrapolation. If only large masses are available ($m_{u,d} \gtrsim m_s/2$), we will be limited to 10% or even 20% errors, a point that has been emphasized recently by several groups [4, 5, 6].

Thus it does little good to include virtual quark loop effects unless the u, d quark masses in the loops are significantly lighter than $m_s/2$. To achieve this goal in the near term appears to require use of staggered quarks, in particular an "improved staggered" [7] action. This fermion discretization is computationally very fast, and has a residual (non-singlet) chiral symmetry that prevents the appearance of "exceptional configurations"—thereby allowing simulation at much lighter quark masses than are currently accessible with other discretizations. There are, however, some theoretical and practical problems with staggered fermions, which we address in Section 4.1.2 below.

Discretization

The lattice takes continuous space-time and replaces it with discrete points separated by lattice spacing a. The leading a dependence for small a depends on the lattice action: improved staggered quarks have errors proportional to $\alpha_S a^2$. There are also formally subleading errors that can be quite important numerically. These are so-called "taste

violations," discussed in Section 4.1.2, which are $\mathcal{O}(\alpha_S^2 a^2)$. Precise (few percent) lattice calculations with staggered light quarks will likely require detailed control of such taste violations.

Heavy quarks introduce additional discretization errors. We assume here that the heavy quarks are introduced with the standard Fermilab approach [8], which has $\mathcal{O}(\alpha_S a, a^2)$ errors. Improvement of the heavy quarks is also possible [9, 10], although it is not yet clear whether such actions will be practical in the near term. Introducing heavy quarks *via* nonrelativistic QCD (NRQCD) [11] is likely to produce comparable errors to the Fermilab approach, especially for b quarks.

Finite volume

Since we can simulate only a finite region in space-time, there will always be some finite volume errors. The size of such errors of course depends sensitively on the number of hadrons present. For this reason lattice computations with more than one hadron in the initial or final state are probably out of reach in the next five years for all but the most qualitative studies. Even on a longer time scale such calculations will continue to be very difficult.

For single hadrons, currently feasible volumes are enough to reduce finite volume errors to the few percent level (without major sacrifice on discretization errors). Typically a volume $V \gtrsim (2.5\,\mathrm{fm})^3$ is sufficient. We can do even better for single-particle quantities whose mass dependence is determined by χPT, which also predicts the volume dependence (for large volume). This allows us to correct for finite volume effects and reduce the errors to a negligible level. We will therefore ignore finite volume effects for single-particle states from here on.

Setting the scale

In simulations, the lattice spacing a is determined after the fact by comparing the result for a one dimensional quantity with experiment. (This is equivalent to fixing Λ_{QCD} or α_S.) Therefore, the lattice error in the quantity used to set the scale will infect all other dimensionful results. The best we can do today is probably from $\Upsilon(2S-1S)$ or $\Upsilon(1P-1S)$ splittings [12, 13], which lead to a roughly 2% scale error on other quantities, after extrapolation to the continuum [14]. The scale error is usually negligible on dimensionless quantities (like form factors or f_{B_s}/f_B), but is not strictly zero because the error can enter indirectly through the determination of quark masses or momenta.)

Perturbation theory

Most interesting quantities require a weak-coupling perturbative calculation (or equivalent nonperturbative lattice computation) to match lattice currents (or, more generally, operators) to their continuum counterparts. The light-light leptonic decay constants (*e.g.*, f_π, f_K) are exceptions: staggered lattice PCAC implies that the lattice axial current is not renormalized, so lattice and continuum currents are the same. This is not true, however, for heavy-light quantities such as f_B or semileptonic form factors. To date, all such matching calculations have been done only to one loop, leaving large errors ($\sim$10%). Some reduction (perhaps by a factor of 2) in these errors may be possible using simple nonperturbative information [15]. However, it is not obvious that this technique will be successful in the current case of interest: light staggered quarks and heavy Fermilab quarks. So the range of possible errors from a one loop calculation is $\sim$5–10%. For simplicity, we use 7.5% as the nominal one-loop error in Sections 4.5.2 and 4.6.1 below; one should keep in mind that the uncertainty on this error is significant.

To do better, two-loop perturbative calculations are required. But lattice perturbation theory is very messy, since the actions are complicated and there is no Lorentz invariance. "Automated perturbation theory" [16] is probably required. There do not appear to be any fundamental impediments to this approach; however, some practical problems still need to be overcome. In particular, the issue of infrared regulation is important. Currently, "twisted boundary conditions" on the lattice fields in finite volume are used to regulate the IR divergences. In order to match to the continuum, one should the use same twisted boundary conditions there. However continuum perturbation theory (*e.g.*, dimensional regularization) with twisted boundary conditions is difficult, especially beyond one loop. Since the time scale on which the two-loop calculations will become available is therefore not clear, we present future error estimates both with and without assuming the existence of two-loop matching. Luckily, many interesting quantities, *e.g.*, ratios like f_{B_s}/f_B, are independent or nearly independent of perturbation theory.

Issues with staggered fermions

Staggered fermions carry an extra, unwanted quantum number, "taste," which is 4-fold remnant of the lattice doubling symmetry. Taste symmetry is believed to become an exact SU(4) in the continuum limit, but is broken at finite lattice spacing. The taste degree of freedom is not a problem for valence quarks, since one may choose specific tastes by hand. But for sea quark effects, the only known method for eliminating the taste degree of freedom in simulations is to take the fourth root of the staggered fermion determinant. Because of taste violations, this is not an exact reduction at finite lattice spacing and is a non-local operation. Therefore some authors worry that it could introduce non-universal behavior and lead to the wrong theory in the continuum limit. Although there is no proof that the fourth-root procedure is correct, there are several pieces of evidence in its favor [12]. In particular, if the taste symmetry does become exact in the continuum limit (which few doubt), then the fourth-root procedure is correct to all orders in perturbation theory.

There is also a practical issue with staggered fermions: It is difficult to control the chiral extrapolations unless one takes taste violations explicitly into account. Because taste violations are an artifact due to finite lattice spacing, this represents an entanglement of chiral and discretization errors. To help disentangle these errors, one can fit the lattice data to "staggered chiral perturbation theory" (SχPT) instead of ordinary continuum χPT. SχPT has been worked out for the π-K system [17, 18, 19]; it is necessary to obtain precise results for f_π, f_K, and the $\mathcal{O}(p^4)$ chiral parameters [14]. SχPT for heavy-light mesons is being worked out [20]. It is not yet clear whether the number of new chiral parameters due to taste violations in the heavy-light case will be sufficiently small that it will be as useful as in the light-light case.

In estimating the expected precision of lattice computations (Sections 4.5.2 and 4.6.1), we give two versions: "SχPT" assumes that the heavy-light SχPT works as in the light-light case and is similarly useful; "No SχPT" assumes that SχPT is not useful because of a proliferation of parameters, and one must disentangle chiral and continuum extrapolations without its help (probably by extrapolating to the continuum first and then using ordinary χPT).

All estimates given below for the expected precision of lattice computations assume the that the staggered fermions with the fourth-root procedure produce standard QCD in the continuum limit. If this assumption turns out to be incorrect, there are safer but slower methods that could be used instead. The most likely choice appears to us to be domain wall fermions (DWF), which are of order 100 times slower. (The precise factor is not known, largely because DWF have not yet been used in extensive unquenched simulations.) From Moore's law alone, this could delay by as much as a decade the attainment of lattice computations with the desired level of precision. However, despite the fact that DWF have $\mathcal{O}(a^2)$ errors, formally larger than improved staggered fermion $\mathcal{O}(\alpha a^2)$ errors, the coefficient of a^2 seems quite small, giving discretization errors smaller than for improved staggered fermions. In addition, the DWF discretization errors are not entangled with chiral extrapolation errors. Therefore, a delay of order five years, not ten, seems to us a better estimate.

Gold-plated quantities

Given the above issues and systematic errors, only a small number of hadronic quantities are likely to be computed with high (few percent) precision on the lattices in the next decade. Such quantities are called "gold plated" [12]. To be gold-plated, a quantity must involve:

- At most one hadron in initial and final state.
- Stable hadrons, not near thresholds. Unstable particles require very large volumes and untested techniques to treat decay products correctly; the same applies to the virtual decay products of stable particles near thresholds. Thus, for example, semileptonic form factors for $B \to \rho$ are excluded.
- Connected graphs only (valence quark lines connecting the initial and final state). Disconnected graphs are difficult and noisy. The η is probably excluded, because one needs to include η-η' mixing, which is governed by disconnected graphs.

- Low momenta only. Momenta $|\vec{p}|a \gtrsim 1$ lead to unacceptable discretization errors, so we are probably limited to $|\vec{p}| \lesssim 1\mathrm{GeV}$. This implies $q^2 \gtrsim 17\ \mathrm{GeV}^2$ for $B \to \pi$ semileptonic form factors. (The minimum available lattice momentum for fixed lattice size may also require $|\vec{p}| \gtrsim 350\ \mathrm{MeV}$ or more.)
- A controlled chiral extrapolation.

The gold-plated lattice quantities relevant to the Super B Factory are heavy-light leptonic decay constants (f_B, f_{B_s}), bag parameters for $B - \overline{B}$ and B_s-$\overline{B}_s$ mixing (B_B and B_{B_s}), and the semileptonic form factors for $B \to \pi$ and $B \to D$. In addition, the semileptonic form factors for $B \to D^*$ may also be possible because model dependence from the unstable D^* multiplies $\mathcal{F}(1) - 1$ and may be negligible.

4.2 Experimental overview

For precision studies of (inclusive) semileptonic B decays it is often necessary to apply an event selection procedure providing an event sample enriched in B decays and suppressing events from continuum $q\overline{q}$ production (where $q = u, d, s, c$). Traditionally, this has been implemented with the requirement of a high-momentum lepton, *e.g.*, $p > 1.4\ \mathrm{GeV}$ as measured in the center-of-mass system (CMS), indicating the semileptonic decay of a B-meson. With the arrival of B factories, a new paradigm has become possible: event selection based on the fully reconstructed (hadronic or semileptonic) decay of one of the B mesons [21]. In this approach, the fully reconstructed B_{reco} meson constitutes a "tag", and—in the $\Upsilon(4S)$ CM frame—the signal decay is observed in the "recoil" of the B_{reco} candidate. This approach yields lower backgrounds because of a cleaner environment and offers excellent possibilities to determine background control samples directly in data.

4.2.1 Recoil Physics

≻– D. del Re –≺

The study of semileptonic B meson decays $B \to X\ell\overline{\nu}$ in the recoil of a fully reconstructed B meson presents many advantages. First of all, it assures a very clean environment to study the properties of the recoil. One of the two B mesons from the decay of the $\Upsilon(4S)$ is reconstructed either in a hadronic or semileptonic decay mode. The remaining particles of the event originate from the decay of the other (recoiling) B meson. In the case of a semileptonic decay of the recoiling B, the only missing particle is a neutrino. This implies that a requirement on the net charge of the event (charge conservation) can be applied. In the case of hadronic tags, the missing mass (possibly scaled with the missing energy) of the entire event should be consistent with zero. Moreover, since the kinematics are over-constrained, the resolution on the reconstructed quantities, such as the mass of the hadronic system m_X, can be improved with kinematic fitting. The momentum of the recoiling B is also known (up to a twofold ambiguity for the case of semileptonic tags) and therefore the lepton momentum can be boosted into the B rest frame. The charge and the flavor of the B is known. Decays of B^0 and the B^+ mesons can be studied separately. The correlation between the charge of the lepton and the flavor of the B can be used to reduce backgrounds from $B \to \overline{D} \to \ell$ events.

The only drawback is that the overall efficiency of this method is very low and is dominated by the B reconstruction efficiency, a problem that is not longer relevant at very high luminosities. For this reason, the recoil approach seems to be ideal in a Super B Factory, since this is the method with the smallest experimental uncertainty.

Hadronic tags

The sum of a few, very pure fully reconstructed hadronic modes (as done, for instance, in the *BABAR* B lifetime analysis [22]) assures very high purity with minimum event selection bias, albeit at a very low efficiency. On the other hand, a fully inclusive approach with high multiplicity reconstructed modes is not feasible since the level of combinatorics would be too high. A compromise implemented by the *BABAR* experiment (see Ref. [23]) considers

only a restricted mode set with a limit on the number of particles used and employs an algorithm that is as inclusive as possible in combining the particles, neglecting the intermediate states, when possible.

B mesons decay predominantly into hadronic final states involving $\overline{D}$ mesons. Because the dominant B decay modes are $B^- \to D^{(*)0}Y^-$, $B^0 \to D^{(*)-}Y^+$, only these modes[1] are considered, where the $Y^\pm$ system consists of at most 5 charged tracks and two π^0 mesons. For each possible track and π^0 composition of the $Y^\pm$ system, several subsamples are identified depending on the possible resonant states in that sample. For instance, $B \to \overline{D}^{(*)}\pi^+\pi^0$ is subdivided into two kinematic region, one with $m(\pi^+\pi^0) < 1.5\,\mathrm{GeV}/c^2$, dominated by $B \to \overline{D}^{(*)}\rho^+$ decays and one containing the rest of the events. This allows us to isolate samples in which the signal is enhanced with respect to the combinatorial background (the $m(\pi^+\pi^0) < 1.5\mathrm{GeV}/c^2$ sample, in the example above). Enumerating the D decay modes separately, we must consider 1153 different modes.

In order to discriminate fully-reconstructed B candidates from the combinatorial background, two kinematic variables are used. The *energy difference* ΔE is defined as

$$\Delta E = E_B^* - \sqrt{s}/2\,, \tag{4.1}$$

where E_B^* is the energy of the B čandidate in the $\Upsilon(4S)$ CM frame and $\sqrt{s}$ is the CM energy. The ΔE distribution for signal decays peaks at zero, while the continuum and part of the $B\overline{B}$ background can be parameterized with a polynomial distribution. The resolution of this variable is affected by the detector momentum resolution and by the performance of particle identification (since a wrong mass assignment implies a shift in ΔE). Therefore it depends strongly on the reconstructed B mode and can vary from $20\ \mathrm{MeV}$ to $40\ \mathrm{MeV}$ depending on the charged track and π^0 multiplicity in the reconstructed mode. We therefore apply a mode-dependent ΔE selection, as tight as $-45 < \Delta E < 30\ \mathrm{MeV}$ for modes with charged tracks only and as loose as $-90 < \Delta E < 60\ \mathrm{MeV}$ for modes with two π^0 mesons.

The *beam energy-substituted mass* is defined as

$$m_{ES} = \sqrt{(\sqrt{s}/2)^2 - p_B^{*2}}\,, \tag{4.2}$$

where $\sqrt{s}$ is the total energy of the e^+e^- system in the CMS and p^* is the B candidate momentum in the CMS. Since $|p_B^*| \ll \sqrt{s}/2$, the experimental resolution on m_{ES} is dominated by beam energy fluctuations. To an excellent approximation, the shapes of the m_{ES} distributions for B meson reconstructed in a final state with charged tracks only are Gaussian. The presence of neutrals in the final state can introduce tails, due to preshowering in the material in front of the calorimeter or due to leakage outside the active detector volume.

Since the m_{ES} resolution is dominated by beam energy uncertainty while momentum resolution dominates the ΔE resolution, the two variables are practically uncorrelated.

As an estimator of the quality of a reconstruction mode we define the purity as the ratio of the integral of the signal component in the m_{ES} fit over the total number of events in the signal region ($\mathcal{P} = S/(S+B)$). We also define the integrated purity $\mathcal{P}_{\mathrm{int}}$ of a given mode as the purity of all the modes that have greater or equal $\mathcal{P}$. These quantities are computed before any other selection criteria and are to be considered as labels of the decay mode. In events with several B_{reco} candidates differing only by their submode, we choose the one with the highest value of $\mathcal{P}$. If there are multiple candidates in the same submode, the minimum ΔE criterion is used and one candidate per submode is selected. The $\mathcal{P}$ variable is also utilized to choose which of the 1153 modes is actually used in the analysis; the final yields depend on this choice. For instance for the analysis presented in [23], a cut on $\mathcal{P}$ has been optimized and a large set of modes with low $\mathcal{P}$ have been removed. The resulting m_{ES} distribution for an integrated luminosity of $80\,\mathrm{fb}^{-1}$ is shown in Fig. 4-1(a). In Table 4-1 the corresponding yields for four different levels of purity are summarized. As shown, this reconstruction method can provide close to $4000 B/\,\mathrm{fb}^{-1}$ of fully reconstructed B_{reco} mesons ($1500\,B^0/\,\mathrm{fb}^{-1}$ and $2500\,B^+/\,\mathrm{fb}^{-1}$). The corresponding purity is about 26%, which is not an important issue, as the combinatorial background

[1] Charge conjugate states are implied throughout.

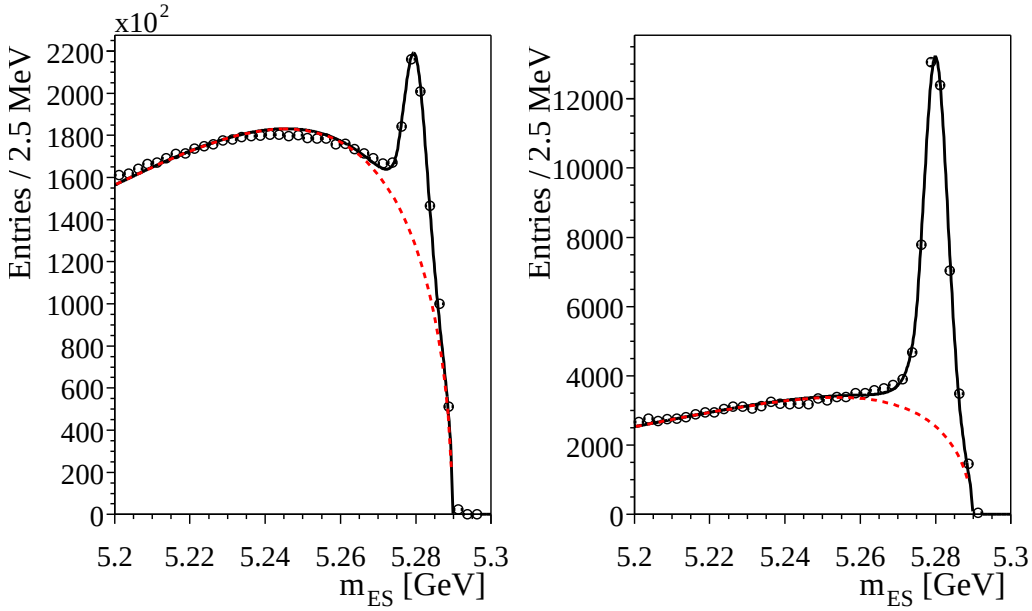

Figure 4-1. *Fit to the m_{ES} distributions of fully reconstructed hadronic B meson decays with (left) no requirement on the recoil and (right) the requirement of one lepton with $p^* > 1.0$ GeV in the recoil. Both plots are for an integrated luminosity of $80\,\mathrm{fb}^{-1}$.*

depends strongly on the recoil itself. The situation improves a lot once requirements on the recoil are applied. For instance, the requirement of a lepton with a moderate momentum of $p > 1.0$ GeV removes most of the non-$b\bar{b}$ events, while leaving the m_{ES} signal shape essentially unchanged, as illustrated in Fig. 4-1(right).

In Fig. 4-2(left) we show the extrapolation of the number of fully reconstructed hadronic B meson decays for large integrated luminosities. The corresponding plot with the measured signal yields for a few selected processes (assuming a rough estimate of the selection efficiency on the recoil) is displayed in Fig. 4-2 (right). With 10 ab^{-1}, even rare decays such as $B \to K\nu\nu$ or $B \to \pi\tau\nu$ have sufficient statistics to be observed.

Table 4-1. *Yields for fully reconstructed hadronic B decays for $80\,\mathrm{fb}^{-1}$ at different levels of the single mode purity $\mathcal{P}$ and integrated purity $\mathcal{P}_{\rm int}$.*

Channel	$\mathcal{P}_{\rm int} > 80\%$	$\mathcal{P}_{\rm int} > 50\%$	$\mathcal{P} > 10\%$	**Selection as in** [23]
$B^+ \to D^0 X$	19120 ± 170	54120 ± 370	95204 ± 660	100650 ± 640
$B^0 \to D^+ X$	11070 ± 130	25720 ± 260	55830 ± 480	62960 ± 550
$B^+ \to D^{*0} X$	18600 ± 170	44270 ± 330	75350 ± 580	82660 ± 640
$B^0 \to D^{*+} X$	20670 ± 170	50300 ± 340	55560 ± 390	46380 ± 310
Total B^+	37720 ± 240	98390 ± 500	170560 ± 880	183310 ± 905
Total B^0	31740 ± 210	76020 ± 430	111390 ± 620	109340 ± 630
Total	69460 ± 320	174410 ± 660	281950 ± 1080	292650 ± 1100

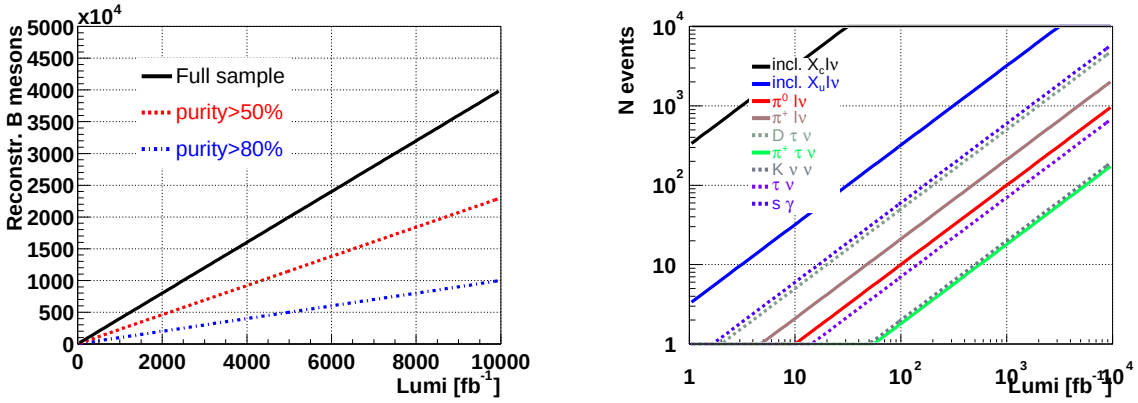

Figure 4-2. *Left: yields of fully reconstructed hadronic B meson decays for different levels of purity as a function of the integrated luminosity. Right: number of selected signal events for different processes as a function of the integrated luminosity. We assume a rough estimate of the selection efficiency on the recoil. The purity of the selected sample can vary depending on the process.*

Semileptonic tags

≻– D. del Re, M. Datta –≺

An alternative method of event tagging employs the reconstruction of semileptonic decays. The technique has a higher efficiency compared to the fully hadronic approach, but it has some disadvantages due to a smaller number of constraints. For instance, the presence of an extra neutrino does not allow the use of kinematic fits, and the momentum of the recoiling B meson is thus known only with large uncertainty. Moreover, there is no equivalent of the m_{ES} variable, and the fit of yields and the subtraction of the continuum is therefore not possible. Reconstruction efficiencies for both signal and combinatorial background must be estimated on Monte Carlo (MC) simulation and off-peak data, but can be calibrated with control samples. On the other hand, the method can still allow for a direct determination of the recoil (such as the invariant mass of the X system in $B \to Xl\nu$ decays), since all visible particles are reconstructed.

In semi-exclusive semileptonic B tags, excited neutral D modes are not explicitly reconstructed, potentially leaving unassigned neutral energy in the event. B^- candidates are reconstructed via the decay $B^- \to D^0\ell^-\overline{\nu}X$, where the X system is either nothing, a π^0 meson or a γ from the D^{*0} meson or an unreconstructed higher D meson resonance. After imposing kinematic requirements on the D^0-ℓ combination, the X is usually either nothing or a soft transition pion or photon from a higher mass charm state. The subsequent D meson decay is reconstructed as either $D^0 \to K^-\pi^+$, $D^0 \to K^-\pi^+\pi^+\pi^-$ or $D^0 \to K^-\pi^+\pi^0$. These D^0 decay modes are chosen, since they provide both the highest statistics hadronic decay modes and are the cleanest. The lepton ℓ denotes either an electron or a muon.

The exclusive semileptonic decays $B^- \to D^{*0}\ell^-\overline{\nu}_\ell$ are a cleaner subset of $D^0\ell^-\nu X$ tags. Due to the reconstruction of all the tag side visible particles, the recoil of this tagging mode is clean enough to search for signal decays with a less clean signature.

To study neutral modes $\overline{B}^0 \to D^+\ell^-\overline{\nu}$ we use the charged D meson decay $D^+ \to K^-\pi^+\pi^+$. Also, although we do not require the reconstruction of a $D^{*+}\,\ell^-\overline{\nu}$, if an acceptable D^{*+} candidate can be formed by combining a found D^0 with a soft pion, it is used in place of the D^0 candidate. If an acceptable D^{*+} candidate can be reconstructed, it is considered a suitable $\overline{B}^0$ tag. As mentioned, missing particles in the tagging B do not constitute a problem, as long as all measured particles are properly assigned. The efficiency on this method is $\sim 1\%$ of $\Upsilon(4\mathrm{S}) \to B\overline{B}$ events ($\sim 0.35\%$ for $\overline{B}^0$ and $\sim 0.65\%$ for B^-). Even though the experimental systematic uncertainties are larger in this case, this method can provide larger statistics, and can be very useful for the study of many modes with small branching

ratios. The overlap between this sample and the fully hadronic one is negligible; the two approaches can be considered uncorrelated.

4.2.2 Machine backgrounds

≻— S. Robertson —≺

Several analyses in which the signal decay mode contains one or more neutrinos rely heavily on the missing-energy signature of the unobserved neutrino(s) as part of the signal selection. In the case of $B \to X_u \ell \overline{\nu}$ decays, the neutrino four-vector may be explicitly reconstructed from the missing momentum and energy in the event, while for $B^+ \to \ell^+ \nu$, the neutrino is implicitly reconstructed by demanding that the four-vectors of all observed particle in the event other than the signal candidate lepton can be summed to form a four-vector consistent with a B^- meson. For decay modes such as $B^+ \to \tau^+ \nu$ and $B^+ \to K^+ \nu \overline{\nu}$, in which there are more than one neutrino in the final state, the signal selection similarly requires that there is large missing energy, and that all observed particles in the event can be associated with either the signal decay, or a reconstructed B^- against which it is recoiling. Two factors therefore strongly impact the performance of these analyses:

- Failure to reconstruct particles that pass outside of the geometric or kinematic acceptance of the detector.
- The presence of additional reconstructed energy in the event due to detector "noise" or reconstruction artifacts, due to physics effects such as bremsstrahlung and hadronic split-offs in the calorimeter, or due to cosmics or beam-related backgrounds.

In the next subsections, we discuss these two factors.

Acceptance and Hermiticity

Fiducial acceptance currently has the largest impact on missing energy reconstruction in *BABAR*, with an average of ~ 1 GeV of energy being missed per event. However, analyses suffering from backgrounds due to this mechanism can require that the missing momentum vector point into the detector acceptance (cf. Fig. 4-14). More problematic are backgrounds that have large missing energy due to a combination of sources, as is the case for $B^+ \to \tau^+ \nu$. In this analysis, backgrounds typically arise from events in which one or more particles pass outside of the geometrical acceptance, and additionally the event contains an unidentified K^0_L, in which case the missing momentum vector can point in any direction. For this analysis, improving the acceptance does not result in a dramatic reduction in the background rate. A study of the effect of instrumenting the *BABAR* forward B1 magnet with a "veto" detector to increase the effective geometric acceptance indicated only about a 15% reduction of background, even assuming perfect reconstruction efficiency for this detector and no occupancy due to beam backgrounds or QED processes. Some gain would potentially be realized in the signal efficiency if the tracking and/or calorimeter acceptance were increased compared with the existing *BABAR* detector.

Occupancy

Issues related to reconstruction artifacts are likely to be similar at PEP-II/*BABAR* and at a Super B Factory. Moreover, these are not expected to be the dominant source of extra energy in a high luminosity environment. Potentially the most serious issue is the presence of significant occupancy in the calorimeter, and to a lesser degree the tracking system, due to beam backgrounds and "non-physics" luminosity effects. *BABAR* data currently contains an average of ~ 1 spurious calorimeter cluster per event with a typical energy of $60 - 100$ MeV. Most of this energy is the result of single-beam lost-particle sources in the high-energy or low-energy rings, and linear scaling of these backgrounds to the anticipated Super B Factory beam currents has the effect of increasing their contribution to the level of ~ 300 MeV/event, comparable to the total "extra energy" currently observed in *BABAR* data (*i.e.*, including beam backgrounds, bremsstrahlung, hadronic split-offs, *etc.*). Consequently, the missing energy resolution probably will not

dramatically be degraded by this effect. However there is also currently a significant beam background component that scales with luminosity rather than with beam currents. This background is believed to be caused by extremely low angle radiative Bhabha scattering producing particles that scatter into machine elements in the vicinity of the Q2 septum chambers. A naive scaling of current background rates to Super B Factory luminosity would then imply extremely high occupancy in portions of the calorimeter, potentially degrading the missing energy resolution to the point that some or all of these analyses would not be not possible. Additional studies of this effect are needed; missing energy reconstruction should be an important benchmark in designing machine elements in the vicinity of the interaction region.

4.2.3 Detector Simulations

≻M. Datta, T. Moore ≺

A detailed simulation of the current *BABAR* detector has been employed for many of the high-luminosity studies presented here. The full *BABAR* simulation includes a detailed detector model using the GEANT4 toolkit [24]. GEANT 4 provides simulations for both electromagnetic and hadronic interactions. The full detector response is simulated in each sub-system so that the standard reconstruction algorithms may be applied to the simulated data. Machine backgrounds are included by overlaying random trigger events from the real data on top of the simulated events. The simulated samples of generic decays ($B\overline{B}$, $c\bar{c}$, uds, *etc.*) represent up to three times the existing data sample. Much larger equivalent samples have been produced for specific signal decay modes.

In order to study the large data samples possible at a Super B Factory, a fast MC simulation called "Pravda" has also been developed. This simulation begins by running the same event generators that are used in the full simulation. Instead of employing the detector simulation and response code, however, the detector response to the final state particles (charged tracks and neutrals) is parametrized. The charged track parametrization includes track smearing and a full error matrix. The same *BABAR* analysis code that is run on real data may also be run with the Pravda simulation.

The Pravda simulation does have some shortcomings that may or may not be important depending on the analysis considered. Because the reconstructed objects are parametrized from the true generator-level particles, there is no simulation of fake tracks and calorimeter noise. Furthermore, beam-related backgrounds are not included. This could have a significant impact on results obtained with the Pravda simulation, since we expect beam backgrounds to increase with higher luminosity. We currently have no reliable estimate of this effect, but work is underway to improve the characterization of these backgrounds. Studies of the $B^+ \to \mu^+\nu_\mu$ analysis showed optimistic predictions for the signal efficiency due to better than expected resolution on the event total energy. Nevertheless, we believe the Pravda MC was adequate for these studies. The $B^+ \to \tau^+\nu_\tau$ analysis, however, is critically dependent on the neutral energy reconstruction which was found to be inadequate in the Pravda simulation (see Section 4.6.2 for more details).

4.3 $b \to c\ell\overline{\nu}$ Inclusive and Exclusive Decays

≻I. Bigi ≺

$|V_{cb}|$ is known from inclusive and exclusive semileptonic B decays with a few percent uncertainty. The error is likely to be reduced to the 1-2% level through more data and a refined analysis of energy and mass moments in semileptonic and radiative B decays. Experimental cuts on energies and momenta introduce biases in the extracted values of the heavy quark parameters; keeping those biases under control such that one can correct for them requires low cuts. The recently proposed BPS expansion might open up a novel way to determine $|V_{cb}|$ from $B \to D\ell\nu$. If successful for $B \to De/\mu\nu$, one can use the ratio $\Gamma(B \to D\tau\nu)/\Gamma(B \to De/\mu\nu)$ as a sensitive probe for New Physics, where the BPS expansion is essential in treating the hadronic form factors. Extracting $|V_{cb}|$ from semileptonic B_s decays in $e^+e^- \to \Upsilon(5S) \to B_s\overline{B}_s$ would constitute a powerful check on our theoretical control.

We are witnessing how the study of B physics, which has been based on the paradigm of high sensitivity to subtle and potentially new features of fundamental dynamics, is now also acquiring the aspect of high numerical accuracy.

This development has been driven by two interrelated phenomena, namely the availability of magnificent experimental facilities that challenged theoretical technologies and, in doing so, inspired—actually pushed—them to become more powerful. There is every reason to expect that this fruitful interplay will continue: theoretical technologies will be further refined in response to even more detailed data.

One expression of this paradigm shift has the suggestion of a Super B Factory , an asymmetric e^+e^- collider operating near B production threshold with a luminosity of close to $10^{36}\mathrm{s}^{-1}\mathrm{cm}^{-2}$. Its justification has to be different than that more than ten years ago for the current B Factories: one has to learn to harness the much higher statistics to shape a Super B Factory into a true precision tool for exploring dynamics. This means one has to strive for

- *more accuracy* in extracting the sides of the CKM unitarity triangle,
- analyzing *more decays* – like $B \to De/\mu\nu$, D $\tau\nu$ – and
- possibly cover *new territory*, namely $e^+e^- \to \Upsilon(5S) \to B_s\overline{B}_s$.

It also means that one should not apply if one is deterred by truly hard measurements.

The '1% challenge' is the following: can we learn to predict certain observables with an $\mathcal{O}(1\%)$ accuracy, measure them, interpret the results and diagnose what they tell us about specific features of the underlying dynamics with commensurate accuracy?

In taking up this challenge, we have to be aware that assumptions that are well justified on the $\mathcal{O}(10\%)$ accuracy level might no longer be adequate on the $\mathcal{O}(1\%)$ accuracy level. Furthermore, the most convincing way that we have established control over the systematics—be they experimental or theoretical—is to determine the same basic parameter in more than one independent way. Heavy quark theory [25, 26, 27, 28] is quite well positioned to satisfy this demand, as will be illustrated below.

We expect that $|V_{cb}|$ will be determined with 1-2% accuracy soon at the current B Factories. We address it here in the Super B Factory context mainly to describe what will be the status and to illustrate at the same time the new paradigm of heavy flavor physics, which is based on two pillars:

- building a rich database involving hard measurements;
- implementing overconstraints as much as possible.

In that spirit we briefly sketch important cross checks that could be performed in $\Upsilon(5S) \to B_s\overline{B}_s$.

4.3.1 On the Heavy Quark Expansion (HQE)

B decays—mostly of the inclusive variety—can be described through an operator product expansion (OPE) in inverse powers of the heavy quark masses and of the B meson expectation values of *local* quark and gluon field operators of increasing dimension. Those are referred to as heavy quark parameters (HQP): the heavy quark masses—m_b, m_c—on the leading level, the kinetic energy and chromomagnetic moments—μ_π^2, μ_G^2—to order $1/m_Q^2$ and the Darwin and LS terms—ρ_D^3, ρ_{LS}^3—to order $1/m_Q^3$, *etc.*

The important point is that this set of HQP is 'universal' in the sense that it appears in the HQE of a host of transitions, namely $b \to c$ and $b \to u$ semileptonic, radiative and even nonleptonic ones. These HQP can be extracted from the *shape* of energy, mass, *etc.*distributions as conveniently encoded in various moments of different orders. In general there is *not* a one-to-one correspondence between these HQP and the moments; *i.e.*, the former are obtained from nontrivial linear combinations of the latter. Likewise the HQP can be determined from different types of moments, namely leptonic, hadronic or photonic moments. They can thus be greatly overconstrained, providing a high degree

of quality control over systematics on the theoretical as well as experimental side. Once the HQP are obtained from moments of $B \to X_c\ell\nu$ transitions, they can be used perfectly well for $B \to X_u\ell\nu$ and $B \to X_s\gamma$. Claiming that one needs to measure moments of $b \to u$ decays to obtain the HQP for describing them would be incorrect.

More than one treatment of the HQE with different definitions of the HQP can be found in the literature. We use 'kinetic' masses and other HQP with a hard Wilsonian cut-off scale $\mu \sim 1$ GeV. Other authors [29] studied many schemes, such as the '1S' and 'PS' masses, using HQET quantities $\lambda_{1,2}$ and four non-local correlators $\mathcal{T}_{1-4}$ together with ρ_D^3, ρ_{LS}^3 in orders $1/m_Q^2$ and $1/m_Q^3$, respectively. In any schemes there are six hadronic matrix elements that need to be determined from the data, in addition to $|V_{cb}|$. For practical applications, where only a handful of HQP truly matter, there are simple expressions relating the two sets of HQP [30]. One should keep in mind the general caveat that the role and weight of perturbative corrections is quite different in the various schemes.

4.3.2 $|V_{cb}|$

Three methods for extracting $|V_{cb}|$ from semileptonic B decays that can boast of a genuine connection to QCD have been suggested: namely the 'inclusive' one relying on $\Gamma_{SL}(B)$, the 'exclusive' one employing $B \to D^*\ell\nu$ at zero recoil, and a newcomer, namely treating $B \to D\ell\nu$ with the help of the "so-called BPS" expansion, may become competitive.

'The Golden Way': $\Gamma(B \to X_c\ell\nu)$

In the first step, one sets out to express the total $b \to c$ semileptonic width in terms of *a priori* unknown HQP and perturbative corrections, in addition to the sought-after $|V_{cb}|$ in a way that the higher-order contributions not included cannot amount to more than 1 or 2%, which then denotes the theoretical uncertainty:

$$\Gamma(B \to X_c\ell\nu) = F(|V_{cb}|; \alpha_S, HQP : m_Q, \mu_\pi^2, ...) \pm (1-2)\%|_{th} \tag{4.3}$$

This step has been completed. As shown in Ref. [31], to achieve the set goal of no more than 1–2% theoretical uncertainty at this step the following features have been included:

- all order BLM together with an estimate of second-order *non*-BLM corrections to the leading term,
- contributions through order $1/m_Q^3$,
- without ignoring, as it is usually done, contributions from HQP of the type $\langle B|(\bar{b}...c)(\bar{c}...b)|B\rangle$—*i.e.*, with local operators containing a pair of charm fields explicitly—which could be labeled 'intrinsic charm'. For otherwise there would emerge a chain of higher-dimensional operators, whose contributions scale like $\overline{\Lambda}^n/m_b^3 m_c^{n-3}$ instead of $\overline{\Lambda}^n/m_b^n$.

The main stumbling block in decreasing the theoretical uncertainty is the fact that we do not know yet even the $\mathcal{O}(\alpha_S)$ perturbative corrections of the leading nonperturbative contributions to μ_G^2 and ρ_D^3 (as well as μ_π^2 for moments).

It had been customary for a number of years to impose a constraint on the b and c quark masses that relates their difference to that of the spin-averaged B and D meson masses:

$$m_b - m_c = \langle M_B\rangle - \langle M_D\rangle + \mu_\pi^2\left(\frac{1}{2m_c} - \frac{1}{2m_b}\right) + \frac{\rho_D^3 - \overline{\rho}^3}{4}\left(\frac{1}{m_c^2} - \frac{1}{m_b^2}\right) + \mathcal{O}(1/m_Q^3)\,, \tag{4.4}$$

where $\overline{\rho}^3$ denotes the sum of two positive nonlocal correlators [32].

This procedure was legitimate and appropriate when one had to allow for very sizable uncertainties in the b quark mass and the aim was to extract $|V_{cb}|$ with no better than 10% accuracy. However now m_b is known with at least 2%

precision, and the aim for $|V_{cb}|$ is considerably higher. The relation of Eq. (4.4) then turns into a weak spot or even a liability. It should, therefore, no longer be imposed as an *a priori* constraint. One can, instead, check *a posteriori* to what degree it holds.

Using the measured value for $\Gamma_{SL}(B)$ one then obtains a value for $|V_{cb}|$ as a function of the HQP [31]:[2]

$$\begin{aligned}\frac{|V_{cb}|}{0.0417}\cdot SF \simeq\ & (1+\delta_{\Gamma_{SL},th})[1+0.30(\alpha_S(m_b)-0.22)]\times \\ & \times[1-0.66(m_b(1\ \mathrm{GeV})-4.6\ \mathrm{GeV}) \\ & +0.39(m_c(1\ \mathrm{GeV})-1.15\ \mathrm{GeV}) \\ & +0.05(\mu_G^2-0.35\ \mathrm{GeV}^2)-0.013(\mu_\pi^2-0.40\ \mathrm{GeV}^2) \\ & -0.09(\rho_D^3-0.2\ \mathrm{GeV}^3)-0.01(\rho_{LS}^3+0.15\ \mathrm{GeV}^3) \qquad (4.5)\end{aligned}$$

$$SF = \sqrt{\frac{0.105}{\mathcal{B}_{SL}(B)}\frac{\tau_B}{1.55\mathrm{ps}}}, \qquad (4.6)$$

where $\delta_{\Gamma_{SL},th}$ denotes the uncertainty in the theoretical expression for $\Gamma_{SL}(B)$. More specifically:

$$\delta_{\Gamma_{SL},th} = \pm 0.005|_{pert} \pm 0.012|_{hWc} \pm 0.004|_{hpc} \pm 0.007|_{IC}\ ; \qquad (4.7)$$

the numbers on the right hand side refer to the remaining uncertainty in the Wilson coefficient of the leading $\bar{b}b$ operator, the as yet uncalculated perturbative corrections to the chromomagnetic and Darwin contributions—this is the leading source of the present theoretical error—higher order power corrections including limitations to quark-hadron duality [33] and possible nonperturbative effects in operators with charm fields, respectively.

As a matter of practicality, the value of the chromomagnetic moment μ_G^2 is conveniently fixed by the B^*-B mass splitting.

In the second step one determines the HQP from energy and/or hadronic mass moments of different orders measured in semileptonic $b\to c$ and radiative B decays. They are of the types

$$\mathcal{M}_1(E_l) = \Gamma^{-1}\int dE_l E_l d\Gamma/dE_l \qquad (4.8)$$

$$\mathcal{M}_n(E_l) = \Gamma^{-1}\int dE_l [E_l-\mathcal{M}_1(E_l)]^n d\Gamma/dE_l\ ,\ n>1 \qquad (4.9)$$

$$\mathcal{M}_1(M_X) = \Gamma^{-1}\int dM_X^2 [M_X^2-\overline{M_D}^2] d\Gamma/dM_X^2 \qquad (4.10)$$

$$\mathcal{M}_n(M_X) = \Gamma^{-1}\int dM_X^2 [M_X^2-\langle M_X^2\rangle]^n d\Gamma/dM_X^2\ ,\ n>1\ . \qquad (4.11)$$

The DELPHI and *BABAR* analyses [34, 36] demonstrate the value of relying on several lepton energy as well as hadronic mass moments, since they provide valuable overconstraints, and, in particular, $\mathcal{M}_2(M_X)$ as well as $\mathcal{M}_3(M_X)$ are sensitive to different combinations of the relevant HQP than the other moments. The results can be stated as follows:

$$|V_{cb}|_{incl} = \frac{0.0416}{SF}\times\left[1\pm 0.017|_{exp}\pm 0.015|_{\Gamma(B)}\pm 0.015|_{HQP}\right] \qquad (4.12)$$

where the second and third errors reflect the theoretical uncertainties in Eq. (4.7) (when added in quadrature) and in the evaluations of the HQP from the moments.

One might think that the theoretical uncertainties given in Eq. (4.12) are grossly understated. For an uncertainty of $\sim 2\%$ in the value of m_b that emerged from the DELPHI analysis should contribute an uncertainty of $\sim 5\%$ in $|V_{cb}|$; *i.e.*, this source alone should produce an error larger than allowed for in Eq. (4.12). The resolution of this apparent

[2] Analogous expressions in other schemes can be found in Ref. [29], yielding similar results. (Conveners)

paradox lies in the fact that the width and the low moments depend on practically the same combination of HQP. This can be made manifest by replacing m_b in Eq. (4.6) with, say, the first lepton energy or hadronic mass moments $\langle E_l \rangle$ and $\langle M_X^2 \rangle$:

$$\begin{aligned}\frac{|V_{cb}|}{0.042} \cdot SF \simeq\ & 1 - 1.70[\langle E_l \rangle - 1.383\ \mathrm{GeV}] - 0.075[m_c(1\ \mathrm{GeV}) - 1.15\ \mathrm{GeV}] \\ & +0.085[\mu_G^2 - 0.35\ \mathrm{GeV}^2] - 0.07[\mu_\pi^2 - 0.40\ \mathrm{GeV}^2] \\ & -0.055[\rho_D^3 - 0.2\ \mathrm{GeV}^3] - 0.005[\rho_{LS}^3 + 0.15\ \mathrm{GeV}^3] \qquad (4.13) \\ \simeq\ & 1 - 0.14[\langle M_X^2 \rangle - 4.54\ \mathrm{GeV}^2] - 0.03[m_c(1\ \mathrm{GeV}) - 1.15\ \mathrm{GeV}] \\ & -0.01[\mu_G^2 - 0.35\ \mathrm{GeV}^2] - 0.1[\mu_\pi^2 - 0.40\ \mathrm{GeV}^2] \\ & -0.1[\rho_D^3 - 0.2\ \mathrm{GeV}^3] + 0.006[\rho_{LS}^3 + 0.15\ \mathrm{GeV}^3]\ ; \qquad (4.14)\end{aligned}$$

i.e., once this substitution has been made, the sensitivity to m_c has been greatly reduced, while the one to the other HQP is still rather mild.

As a '*caveat emptor*' it should be noted that the relationship between the moments and the HQP has not been scrutinized to the same degree as the one between $\Gamma_{SL}(B)$ and the HQP. Yet there are some general lessons to be drawn from it:

- One has to allow m_b and m_c to float independently of each other rather than impose the constraint of Eq. (4.4).
- Harnessing different types and different order of moments is essential to obtain the overconstraints that provide a sensible measure for the theoretical as well as experimental control one has achieved.
- The values of the HQP inferred from this analysis can be used in describing other widths as well like for $B \to X_u \ell\nu$ and $B \to X\gamma$. The only difference is that one has to use a different linear combination of moments to obtain m_b rather than $m_b - 0.65 m_c$.

The photon spectrum—cuts and biases

When measuring spectra to evaluate moments, experimental cuts are imposed on energies or momenta for good practical reasons. Yet theoretically such cuts can have a significant nontrivial impact not reproduced by merely integrating the usual OPE expressions over the limited range in energy or momentum, since there are exponential contributions of the form $e^{-c\mathcal{Q}/\mu_{had}}$ that do not appear in the usual OPE expressions; $\mathcal{Q}$ denotes the 'hardness' of the transition, μ_{had} the scale of nonperturbative dynamic (and c a dimensionless number). Such contributions are indeed quite irrelevant for $\mathcal{Q} \gg \mu_{had}$, in particular for $\mathcal{Q} \simeq m_b,\ m_b - m_c$. Yet the aforementioned cuts degrade the 'hardness' of the transition.

For $B \to X\gamma$ the first photon energy moment and the variance provide a measure of $m_b/2$ and $\mu_\pi^2/12$, respectively. Cutting off the lower end of the photon spectrum increases the former and reduces the latter in an obvious way. Yet the impact of such a cut is not fully described by the usual OPE expressions: for the degrading of the 'hardness' is not reflected there. One has $\mathcal{Q} \simeq m_b - 2E_{cut}^\gamma$; *i.e.*, for $E_{cut}^\gamma \simeq 2\,\mathrm{GeV}$ one has $\mathcal{Q} < 1\,\mathrm{GeV}$, making these exponential contributions significant; for higher cuts the OPE expressions quickly lose reliability and then even meaning.

A pilot study [35] of such effects has been performed, where it was found that they introduce a bias, *i.e.*, a systematic shift in the values of m_b and μ_π^2 extracted from the measured moments with a cut [37]. The good news is that this bias does not imply the need to increase the theoretical uncertainties, but can be corrected for; *e.g.*, for $E_{cut}^\gamma = 2\,\mathrm{GeV}$ the bias corrected and thus 'true' m_b is about 50 MeV lower than the bare value extracted from the moment using the usual OPE corresponding to a $\sim 1\%$ upward shift; likewise one finds a correction of about $0.1 - 0.15\ \mathrm{GeV}^2$ for μ_π^2, *i.e.*, a $\sim 25\,\%$ shift, which is much larger than for the leading HQP m_b.

A much more detailed study is now underway [38]. Since one is merely analyzing a correction, terms $\sim \mathcal{O}(1/m_Q^3)$ are irrelevant. Thus, there are only three relevant parameters with dimension—$M_B - m_b$, μ_π^2 and $\mathcal{Q}$—and there must be simple scaling behavior for the correction.

Some general conclusions can already be drawn:

- One should strive hard in all moment analyses to keep the experimental cuts as lows as possible.
- Such biases in the experimentally truncated moments can be corrected for rather than be invoked to inflate the theoretical uncertainties.
- Measuring moments with cuts in a range where the biases can be handled provides important cross checks of our control over the systematics.

'The Gold-Plated Way': $B \to D^* \ell\nu$ at zero recoil

The second method involves measuring the exclusive reaction $B \to D^* \ell\nu$, extrapolate it to the zero recoil point[3] for D^* and extract $|V_{cb} F_{D^*}(0)|$. The zero-recoil form factor has the important property that it is normalized to unity for $m_Q \to \infty$ and has no correction linear in $1/m_Q$:

$$F_{D^*}(0) = 1 + \mathcal{O}(\alpha_S) + \mathcal{O}(1/m_Q^2) \; . \tag{4.15}$$

At finite quark masses there are corrections that lower the form factor. The drawbacks are that it contains an expansion in powers of $1/m_c$ rather than just $1/m_b$ or $1/(m_b - m_c)$ and that non-local operators appear in higher orders. Different estimates for $F_{D^*}(0)$ can be found in the literature:

$$F_{D^*}(0) = \begin{cases} 0.89 \pm 0.06 \text{ Sum Rules [39]} \\ 0.913 \pm 0.042 \textit{ BABAR} \text{ Physics Book [40]} \\ 0.913^{+0.024+0.017}_{-0.017-0.030} \text{ Quenched Lattice QCD [41].} \end{cases} \tag{4.16}$$

The first value was obtained by applying the HQ sum rules and includes terms through $\mathcal{O}(1/m_Q^2)$; the uncertainty applies to adding errors linearly. The lattice result is obtained in the quenched approximation and includes terms through $\mathcal{O}(1/m_Q^3)$; keeping only terms through $\mathcal{O}(1/m_Q^2)$ reduces the central value to 0.89. One should also note that the lattice analysis assumes that one can rely on an expansion in powers of $1/m_c$ (an assumption that is partially checked for self-consistency).

With $|V_{cb} F_{D^*}(0)| = 0.0367 \pm 0.0013$ and using $F_{D^*}(0) = 0.90 \pm 0.05$ for convenience, one obtains

$$|V_{cb}|_{excl} = 0.0408 \cdot [1 \pm 0.035|_{exp} \pm 0.06|_{theor}] \; , \tag{4.17}$$

to be compared with

$$|V_{cb}|_{incl} = 0.0416 \cdot [1 \pm 0.017|_{exp} \pm 0.015|_{\Gamma_{SL}(B)} \pm 0.015|_{HQP}] \; . \tag{4.18}$$

The agreement between the two values represents a highly satisfying and quite non-trivial success of both the experimental and theoretical analysis. At the same time, it is our considered judgment that with $F_{D^*}(0)$ depending on an expansion in $1/m_c$, this exclusive method is running into a 'brick wall' for the theoretical uncertainty of about 5%.

[3] This extrapolation is actually quite nontrivial, and needs to be redone carefully with better data.

'The Cinderella Story': $B \to D\ell\nu$

As is now well-known, QCD possesses heavy-flavor as well as spin symmetry for $m_Q \to \infty$. At finite values of m_Q both are broken by terms $\sim \mathcal{O}(1/m_Q^2)$ in $\Gamma_{SL}(B)$ and in $F_{D^*}(0)$, as just discussed. The reaction $B \to D\ell\nu$ is usually seen as a 'poor relative' of the more glamorous $B \to D^*\ell\nu$, since its form factor has a contribution linear in $1/m_Q$ and thus $1/m_c$. It is also harder to measure, since the relevant rate is smaller, and one cannot benefit from the $D^* \to D\pi$ 'trick'. Yet we might be seeing a 'Cinderella story' in the making, namely the emergence of a novel approach allowing us to calculate the nonperturbative contributions to the form factor F_D quite reliably.

The role of the 'good fairy' could be played by the so-called 'BPS' approximation [42]. If $\mu_\pi^2 = \mu_G^2$ were to hold exactly,[4] one would have

$$\vec{\sigma}_Q \cdot \vec{\pi}_Q |B\rangle = 0 \ , \ \varrho^2 = \frac{3}{4} \tag{4.19}$$

where $\vec{\pi}_Q \equiv i\vec{\partial} + g_S\vec{A}$ denotes the covariant derivative and ϱ^2 the slope of the Isgur-Wise function.

The BPS limit cannot be exact in QCD. From the SV sum rules, we have inferred the general inequality $\mu_\pi^2 > \mu_G^2$; yet one expects the difference to be of quite moderate size. Experimentally we have, indeed,

$$\mu_G^2 = (0.35^{+0.03}_{-0.02})\ \mathrm{GeV}^2 \quad vs. \quad \mu_\pi^2 = (0.45 \pm 0.1)\ \mathrm{GeV}^2 \ , \tag{4.20}$$

which provides a measure for the proximity of the BPS limit through the ratio $(\mu_\pi^2 - \mu_G^2)/\mu_\pi^2$. This can be parametrized through the dimensionless quantity

$$\gamma_{\mathrm{BPS}} \equiv \sqrt{\varrho^2 - 0.75} \ , \tag{4.21}$$

which is smaller than 1/2 for $\varrho^2 < 1$. There are further suppression factors, yet even so the BPS treatment might provides only a qualitative description for observables that receive contributions linear in γ_{BPS}. Yet there is a whole class of quantities where the leading corrections are of order $\gamma_{\mathrm{BPS}}^2 \propto (\mu_\pi^2 - \mu_G^2)/\mu_\pi^2$. Among them is the form factor describing $B \to D\ell\nu$ at zero recoil, analogous to $F_{D^*}(0)$ described above:

$$\mathcal{F}_+ = \frac{2\sqrt{M_B M_D}}{M_B + M_D} f_+(0) \ , \tag{4.22}$$

with the usual definition:

$$\langle D(p_D)|(\bar{c}\gamma_\mu b)|B(p_B)\rangle = f_+(q^2)(p_B + p_D)_\mu + f_-(q^2)(p_B - p_D)_\mu \ , \ q = (p_B - p_D) \ . \tag{4.23}$$

In the BPS limit, $\mathcal{F}_+$ is normalized to unity: $\mathcal{F}_+ = 1 + \mathcal{O}(\gamma_{\mathrm{BPS}}^2(1/m_c - 1/m_b)^2)$. The power-suppressed contributions are then very small; the more significant effect is due to perturbative corrections which produce a slight excess over unity for $\mathcal{F}_+$ [42]:

$$\mathcal{F}_+ = 1.04 + 0.13 \cdot \frac{\mu_\pi^2(1\ \mathrm{GeV}^2) - 0.43\ \mathrm{GeV}^2}{1\ \mathrm{GeV}^2} \pm \delta|_{expon} \tag{4.24}$$

The intrinsic limitation $\delta|_{expon}$ is due to 'exponential' terms

$$\delta|_{expon} \propto \left(e^{-m_c/\mu_{had}} - e^{-m_b/\mu_{had}}\right)^2 \tag{4.25}$$

that have to exist, yet do not appear in the usual HQE expressions. A reasonable estimate for it is in the 1–2% range; *i.e.*, at present it seems possible that one could extract $|V_{cb}|$ from $B \to D\ell\nu$ at zero recoil with a higher accuracy than from $B \to D^*\ell\nu$. This requires that $\mu_\pi^2(1\ \mathrm{GeV}^2) \leq 0.45\ \mathrm{GeV}^2$ holds, *i.e.,* its value falls into the lower part of the presently allowed range. In any case, this method has to be and can be validated by comparing the value of $|V_{cb}|$ thus ~~obtained with the one from $\Gamma_{SL}(B)$~~.

[4] This is not a renormalization scale independent statement, yielding concerns that have not been fully addressed. (Conveners)

"From Rags to Riches": $B \to D\tau\nu$

A success of this method in extracting $|V_{cb}|$ opens up an intriguing avenue to search for the intervention of New Physics in $B \to D\tau\nu$. It has been noted [43] that the ratio $B \equiv \Gamma(B \to D\tau\nu)/\Gamma(B \to De/\mu\nu)$ could be changed significantly relative to its Standard Model value by a contribution from a charged Higgs exchange. Its impact can be parametrized in a two-Higgs-doublet model by the ratio $R = M_W \tan\beta / M_H$ with tanβ denoting the ratio of the two VEV's. The authors of Ref. [43] find sizable deviations from the Standard Model value of B for $R \geq 10$, which could be realized even for M_H as high as 200 – 300 GeV for sufficiently large tanβ. There is a considerable 'fly in the ointment', though. The authors argued that in the infinite mass limit the hadronic form factors drops out from B. However that is not true at finite values of the heavy quark masses. In particular there are $1/m_c$ (and $1/m_b$) corrections that are likely to be sizable; furthermore the rate for $B \to De/\mu\nu$ depends on the single form factor f_+, whereas $B \to D\tau\nu$ is also sensitive to the second form factor f_-, since m_τ is *non*negligible on the scale of M_B.

Yet the BPS expansion—once it is validated by $|V_{cb}|$—allows us to relate these form factors, and thus predict the value of $\Gamma(B \to D\tau\nu)/\Gamma(B \to De/\mu\nu)$ in the Standard Model. A 'significant' deviation—'significant' probably means larger than 10 %—provides evidence for New Physics.

Measuring $B \to \tau\nu D$ appears feasible only at a Super B Factory due to the small branching ratio of $B \to \tau\nu D$ relative to $B \to D^*\ell\nu$, the absence of the D^* 'trick' and the complication of having to identify the τ lepton.

4.3.3 Quality control

The option to run at $\Upsilon(5S) \to B_s\overline{B}_s$ might turn out to be very valuable. The motivation would *not* be to perform measurements that can be done at LHC and the Tevatron, such as searching for $B_s - \overline{B}_s$ oscillations and *CP* asymmetries in $B_s(t) \to D_s K$, $J/\psi\,\phi$; instead one would perform measurements *uniquely* possible here. One is the extraction of $|V_{cb}|$ from $\Gamma_{SL}(B_s)$ and $B_s \to D_s^*\ell\nu$ at zero recoil in close analogy to nonstrange B decays. This is another example of following Lenin's dictum "Trust is good—control is better!". For comparing $|V_{cb}|$ as inferred from B_d, B_u and B_s decays provides a powerful check of experimental systematics and even more of theoretical uncertainties like the often mentioned limitations to quark-hadron duality. Such limitations could be larger than predicted due to the accidental "nearby presence" of a hadronic resonance of appropriate quantum numbers. This would be a stroke of bad luck, but could happen. Due to the isospin invariance of the strong interactions it would affect $B_d \to X_c\ell\nu$ and $B_u \to X_c\ell\nu$ equally (unlike $B_d \to X_u\ell\nu$ *vs.* $B_u \to X_u\ell\nu$), but *not* $B_s \to X_{c\bar{s}}\ell\nu$. Such a scenario would reveal itself by yielding inconsistent values for $|V_{cb}|$ from $B_{u,d}$ and B_s semileptonic decays.

4.3.4 Conclusions

The study of heavy flavor dynamics in the beauty sector has made tremendous progress in both the quantity and quality of data, and in the power of the theoretical tools available to treat them. This progress is well-illustrated by the determination of $|V_{cb}|$. The pieces are in place to extract it from $\Gamma(B \to X_c\ell\nu)$ with 1–2% accuracy. This is being achieved by fixing the HQP appearing in the HQE through the shape of distributions in semileptonic and radiative B decays as encoded through their energy and mass moments. Analyzing $B \to D^*\ell\nu$ at zero recoil provides a valuable cross check; yet both the procedure for extrapolating to zero-recoil and the evaluation of the form factor $F_{D^*}(0)$ have to be scrutinized very carefully. Only dedicated lattice QCD studies hold out the promise to reduce the theoretical uncertainty below the 5% mark; however, that is truly a tall order, and requires a fully unquenched treatment, and a very careful evaluation of the scaling in powers of $1/m_c$.

These developments will happen irrespective of the existence of a Super B Factory . However their description is highly relevant for discussions about a Super B Factory :

- The HQP m_b, μ_π^2 etc. extracted from moments of $B \to X_c\ell\nu$ and $B \to X_s\gamma$ are the basic parameters needed for describing $B \to X_u\ell\nu$, $B \to \gamma X_d$, $B \to X\ell^+\ell^-$ *etc.*, transitions.

- Reproducing $|V_{cb}|$ within the stated uncertainty of $1-2\%$ constitutes a valuable validation for Super B Factory measurements.
- $B \to D\ell\nu$ has been put forward as a second theoretically clean exclusive mode for determining $|V_{cb}|$; to perform an accurate analysis close to the zero-recoil domain presumably requires data from a Super B Factory .
- On a more general level, it demonstrates the 'high precision' paradigm that has to be at the core of such a program. For it illustrates how alleged high accuracy can be validated through overconstraints, namely determining the basic parameters in many systematically different ways in various decays. These lessons can be fully carried over to extractions of other CKM parameters like $|V_{ub}|$ and $|V_{td}|$.
- The huge statistics and hoped-for purity of Super B Factory data are required to measure $B \to D\tau\nu$ as a sensitive probe for New Physics, most likely in the form of charged Higgs states.
- One should contemplate a run of $e^+e^- \to \Upsilon(4S) \to B_s\overline{B}_s$, not only for calibrating absolute B_s branching ratios, but also to extract $|V_{cb}|$ from B_s decays, as the final cross check of our theoretical control.

4.3.5 Experimental Prospects

≻ U. Langenegger ≺

Recent preliminary measurements of the lepton spectrum [21] and the mass moments of the hadronic system [44] presented by the *BABAR* and Belle collaborations using the recoil approach already show very competitive results compared to the the traditional B tagging with high-momentum leptons. With statistics of 200–300 fb^{-1}, the analyses will probably become systematics-limited. At the moment, there are no prospects for substantial gains at higher luminosities in the study of these decays.

4.4 $b \to u$ Inclusive Decays

4.4.1 Theory

≻– M. Luke –≺

A precise and model independent determination of the magnitude of the Cabibbo-Kobayashi-Maskawa (CKM) matrix element V_{ub} is important for testing the Standard Model at B Factories via the comparison of the angles and the sides of the unitarity triangle.

$|V_{ub}|$ is notoriously difficult to measure in a model independent manner. The first extraction of $|V_{ub}|$ from experimental data relied on a study of the lepton energy spectrum in inclusive charmless semileptonic B decay [45], a region in which (as will be discussed) the rate is highly model-dependent. $|V_{ub}|$ has also been measured from exclusive semileptonic $B \to \rho \ell \overline{\nu}$ and $B \to \pi \ell \overline{\nu}$ decay [46]. These exclusive determinations also suffer from model dependence, as they rely on form factor models (such as light-cone sum rules [47]) or quenched lattice calculations at the present time (for a review of recent lattice results, see [48]).

In contrast, inclusive decays are quite simple theoretically, and if it were not for the huge background from decays to charm, it would be straightforward to determine $|V_{ub}|$ from inclusive semileptonic decays. Inclusive B decay rates can be computed model independently in a series in $\Lambda_{\rm QCD}/m_b$ and $\alpha_s(m_b)$ using an operator product expansion (OPE) [49]. At leading order, the B meson decay rate is equal to the b quark decay rate. The leading nonperturbative corrections of order $\Lambda_{\rm QCD}^2/m_b^2$ are characterized by two heavy quark effective theory (HQET) matrix elements, usually called λ_1 and λ_2,

$$\lambda_1 \equiv \frac{1}{2m_B}\langle B|\overline{h}_v (iD)^2 h_v|B\rangle, \qquad \lambda_2(\mu) \equiv \frac{1}{6m_B}\langle B|\overline{h}_v \sigma^{\mu\nu} G_{\mu\nu} h_v|B\rangle. \tag{4.26}$$

The $B - B^*$ mass splitting determines $\lambda_2(m_b) \simeq 0.12$ GeV^2, while a recent fit to moments of the charged lepton spectrum in semileptonic $b \to c$ decay obtained [50]

$$m_b^{1S} = 4.82 \pm 0.07_E \pm 0.11_T \,{\rm GeV}, \qquad \lambda_1 = -0.25 \pm 0.02_{ST} \pm 0.05_{SY} \pm 0.14_T \,{\rm GeV}^2 \,, \tag{4.27}$$

where m_b^{1S} is the short-distance "$1S$ mass" of the b quark [51, 52]. (Moments of other spectra give similar results [53].)

Since the parton level decay rate is proportional to m_b^5, the uncertainty in m_b is a dominant source of uncertainty in the relation between $B \to X_u \ell \overline{\nu}_\ell$ and $|V_{ub}|$; an uncertainty in m_b of 50 MeV corresponds to a $\sim 5\%$ determination of $|V_{ub}|$ [51, 54]. Unfortunately, the semileptonic $b \to u$ decay rate is difficult to measure experimentally, because of the large background from charmed final states. As a result, there has been much theoretical and experimental interest in the decay rate in restricted regions of phase space where the charm background is absent. Of particular interest have been the large lepton energy region, $E_\ell > (m_B^2 - m_D^2)/2m_B$, the low hadronic invariant mass region, $m_X \equiv \sqrt{s_H} < m_D$ [55], the large lepton invariant mass region $q^2 > (m_B - m_D)^2$ [56], and combinations of these [57]. Of these, the charged lepton cut is the easiest to implement experimentally, while the hadronic mass cut has the advantage that it contains roughly 80% of the semileptonic rate [58]. However, in both of these cases, the kinematic cuts constrain the final hadronic state to consist of energetic, low invariant mass hadrons, and the local OPE breaks down. By contrast, in the large q^2 region the local OPE remains valid, although there are a number of other sources of theoretical uncertainty.

The shape function region: For the cuts $E_\ell > (m_B^2 - m_D^2)/2m_B$ and $m_X \equiv \sqrt{s_H} < m_D$, the local OPE breaks down and the relevant spectrum is instead determined at leading order in $\Lambda_{\rm QCD}/m_b$ by the light-cone distribution function of the b quark in the meson [59],

$$f(\omega) \equiv \frac{\langle B|\bar{b}\,\delta(\omega + in\cdot D)\,b|B\rangle}{2m_B}\,, \tag{4.28}$$

where n^μ is a light-like vector. $f(\omega)$ is often referred to as the shape function, and corresponds to resumming an infinite series of local operators in the usual OPE. The physical spectra are determined by convoluting the shape function with the appropriate kinematic functions:

$$\frac{1}{\Gamma}\frac{\mathrm{d}\Gamma(B \to X_u \ell \overline{\nu}_\ell)}{\mathrm{d}E_\ell} = \frac{4}{m_b}\int \theta(m_b - 2E_\ell - \omega) f(\omega)\, d\omega + \ldots \tag{4.29}$$

$$\frac{1}{\Gamma}\frac{\mathrm{d}\Gamma(B \to X_u \ell \overline{\nu}_\ell)}{\mathrm{d}s_H} = \frac{1}{m_b^3}\int \frac{2s_H^2(3\omega - 2s_H/m_b)}{\omega^4}\,\theta(\omega - s_H/m_b) f(\omega - \Delta)\, d\omega + \ldots \tag{4.30}$$

where $m_b - 2E_\ell \lesssim \Lambda_{\rm QCD}$, $s_H \lesssim \Lambda_{\rm QCD} m_b$, $\Delta \equiv m_B - m_b$, and the ellipses denote terms suppressed by powers of α_s or $\Lambda_{\rm QCD}/m_b$. $f(\omega)$ is a nonperturbative function and cannot be calculated analytically, so the rate in this region is model-dependent even at leading order in $\Lambda_{\rm QCD}/m_b$.

However, $f(\omega)$ also determines the shape of the photon spectrum in $B \to X_s\gamma$ at leading order,

$$\frac{1}{\Gamma}\frac{\mathrm{d}\Gamma(B \to X_s\gamma)}{\mathrm{d}E_\gamma} = 2f(m_b - 2E_\gamma) + \ldots \tag{4.31}$$

so $f(\omega)$ may be determined experimentally from the measured $B \to X_s\gamma$ spectrum and applied to semileptonic decay. The CLEO collaboration [60] recently used a variant of this approach to determine $|V_{ub}|$ from their measurements of the $B \to X_s\gamma$ photon spectrum and the charged lepton spectrum in $B \to X_u \ell \overline{\nu}_\ell$.

The relations (4.29–4.31) hold only at tree level and at leading order in $\Lambda_{\rm QCD}/m_b$, so a precision determination of $|V_{ub}|$ requires an understanding of the size of the corrections. The most important radiative corrections are the parametrically large Sudakov logarithms, which have been summed to subleading order [61]. In addition, contributions from additional operators which contribute to $B \to X_s\gamma$ have been calculated [62]. The perturbative corrections are typically included by convoluting the partonic rate with the shape function $f(\omega)$ [58]; however, the consistency of this approach has been questioned in [63].

The subleading twist corrections have been studied more recently [64, 65, 66, 67, 68]. In [65, 66], it was shown that there is a large $\mathcal{O}(\Lambda_{\rm QCD}/m_b)$ correction to the relation between the $B \to X_s\gamma$ spectrum and the charged lepton energy endpoint region, shifting the extracted value of $|V_{ub}|$ by $\sim 10 - 15\%$. Since this is a simple model estimate, the corresponding uncertainty is not clear. In Ref. [67] it was shown that the variation of this estimate in a number of models was quite small, suggesting a small uncertainty in $|V_{ub}|$. However, models that give larger effects do exist [68]. A second source of uncertainty arises because of the weak annihilation (WA) contribution, which will be discussed in more detail in the next section. These are formally sub-subleading twist effects, but are enhanced by a factor of $\sim 16\pi^2$ because there are only two particles in the final state. However, the relevant matrix elements vanish under the assumption of factorization; hence, as will be discussed in the next section, the size of the WA contribution is very difficult to determine reliably. The authors of [66] estimated the corresponding uncertainty in $|V_{ub}|$ to be at the $\sim 10\%$ level (with unknown sign) for a cut $E_\ell > 2.3$ GeV. For both subleading effects, the fractional uncertainty in $|V_{ub}|$ is reduced considerably as the cut on E_ℓ is lowered below 2.3 GeV.

Analogous corrections to the region between the $B \to X_s\gamma$ spectrum and the hadronic invariant mass spectrum were considered in [68], and found to be much smaller. In the range of models studied, the subleading effects were at the few percent level for a cut $m_X < 1.55\,\mathrm{GeV}$. The subleading effects are reduced as the cut is raised.

Lepton q^2 cuts: Another solution to the problem of the breakdown of the local OPE is to find a set of cuts which eliminate the charm background but do not destroy the convergence of the OPE, so that the distribution function $f(\omega)$ is not required. In Ref. [56] it was pointed out that this is the situation for a cut on the dilepton invariant mass. Decays with $q^2 > (m_B - m_D)^2$ must arise from $b \to u$ transition. Such a cut forbids the hadronic final state from moving fast in the B rest frame, and simultaneously imposes $m_X < m_D$ and $E_X < m_D$. Thus, the region selected by a q^2 cut is entirely contained within the m_X^2 cut, but because the dangerous region of high energy, low invariant mass final states is not included, the OPE does not break down [69]. The price to be paid is that the relative size of the

unknown $\Lambda_{\rm QCD}^3/m_b^3$ terms in the OPE grows as the q^2 cut is raised. Equivalently, as was stressed in [70], the effective expansion parameter for integrated rate inside the region $q^2 > (m_B - m_D)^2$ is $\Lambda_{\rm QCD}/m_c$, not $\Lambda_{\rm QCD}/m_b$. In addition, the integrated cut rate is very sensitive to m_b, with a ± 80 MeV error in m_b corresponding to a $\sim \pm 10\%$ uncertainty in $|V_{ub}|$ [70, 57].

An additional source of uncertainty arises from weak annihilation (WA) graphs [71]. WA arises at $\mathcal{O}(\Lambda_{\rm QCD}^3/m_b^3)$ in the local OPE, but, as previous mentioned, is enhanced by a factor of $\sim 16\pi^2$, but vanishes in factorization. Assuming factorization is violated at the 10% level gives a corresponding uncertainty in $|V_{ub}|$ from a pure q^2 cut of $\sim 10\%$ [71]; however, this estimate is highly uncertain.[5] In addition, since the contribution is fixed at maximal q^2, the corresponding uncertainty grows as the cuts are tightened.

The theoretical uncertainties from a pure q^2 cut may be considerably reduced by considering more complicated kinematic cuts: in [57] it was proposed that by combining cuts on both the leptonic and hadronic invariant masses the theoretical uncertainty on $|V_{ub}|$ could be minimized. For a fixed cut on m_X, lowering the bound on q^2 increases the cut rate and decreases the relative size of the $1/m_b^3$ terms (including the WA terms), while introducing only a small dependence on $f(\omega)$. Since this dependence is so weak, a crude measurement of $f(\omega)$ suffices to keep the corresponding theoretical error negligible. The sensitivity to m_b is also reduced. With the representative cuts $q^2 > 6$ GeV^2, $m_X < 1.86$ GeV, the overall theoretical uncertainty in $|V_{ub}|$ was estimated to be at the $\sim 8\%$ level, assuming a ± 80 MeV uncertainty in m_b. Tightening these cuts further increases the overall theoretical uncertainty; estimates of the theoretical uncertainty for different cuts are given in Ref. [56].

Nonfactorizable terms and the determination of $|V_{ub}|$

≻ M. Voloshin ≺

The well-known difficulty of determining the mixing parameter $|V_{ub}|$ from the inclusive semileptonic decay rate is the need to cope with the overwhelming background due to the transition $b \to c$. The suggested way to eliminate, or strongly suppress, this background is to measure the rate of the decays $B \to X_u\, \ell\, \nu$ in restricted regions of the phase space that are kinematically forbidden for $B \to X_c\, \ell\, \nu$. Such kinematical cuts however leave as 'usable' only a fraction of the total inclusive rate of the decays $B \to X_u\, \ell\, \nu$, and the nonperturbative effects discussed in this section become relatively enhanced in the restricted decay rate, while being quite small in the total probability of the decay. Namely, the discussed effects behave formally as a delta function located either at the lowest end of the spectrum of the hadronic recoil invariant mass m_X, or, equivalently, at the highest value of the q^2 for the lepton pair. In reality these effects are spread over interval determined by Λ_{QCD}, although resolving such smearing is beyond the current accuracy of the theoretical analysis.

The standard description [74, 75] of nonperturbative effects in the inclusive decay rates of a heavy hadron H_Q containing a heavy quark Q is based on the Operator Product Expansion (OPE) in inverse powers of the heavy quark mass m_Q for the effective operator

$$\mathcal{L}_{eff} = 2\,{\rm Im}\,\left[i \int d^4x\, e^{ipx}\, T\left\{ \mathcal{L}_W^\dagger(x), \mathcal{L}_W(0) \right\} \right], \tag{4.32}$$

constructed from the weak-interaction Lagrangian $\mathcal{L}_W$, in terms of which operator (at $p^2 = m_Q^2$) the total decay rate is given by[6]

$$\Gamma_H = \langle H_Q |\, \mathcal{L}_{eff}\, | H_Q \rangle\,. \tag{4.33}$$

Using in Eq. (4.32) the term

$$\mathcal{L}_{ub} = \frac{G_F\, V_{ub}}{\sqrt{2}}\, (\overline{u}\, \gamma_\mu\, (1 - \gamma_5)\, b)\, \ell_\mu \tag{4.34}$$

[5] After completion of this report, it was observed that the $\mathcal{O}(\alpha_s)$ corrections to WA may actually dominate in the endpoint regions [72], as the $\alpha_s/(4\pi)$ suppression is compensated by a $m_b/\Lambda_{\rm QCD}$ enhancement. At present there is disagreement as to whether the $\mathcal{O}(0.1)$ suppression of the tree level term discussed after Eq. (4.38) is lifted at $\mathcal{O}(\alpha_s)$ [72] or not [73].

[6] The non-relativistic normalization for the *heavy* quark states is used here: $\langle Q|Q^\dagger Q|Q\rangle = 1$.

with $\ell_\mu = \bar{\ell}\,\gamma_\mu\,(1-\gamma_5)\,\nu$ in place of $\mathcal{L}_W$, one would find the total inclusive decay rate of $B \to X_u\,\ell\,\nu$. The effective operator (4.32) is evaluated using short-distance OPE. The leading term in the expansion describes the perturbative decay rate, while subsequent terms containing operators of higher dimension describe the nonperturbative contributions. The term of interest for the present discussion is the third one in this expansion, containing a four-quark operator [74, 75, 76, 77]

$$\mathcal{L}^{(3)}_{b\to u\ell\nu} = -\frac{2\,G_F^2\,|V_{ub}|^2\,m_b^2}{3\,\pi}\,\left(O^u_{V-A} - O^u_{S-P}\right), \tag{4.35}$$

where the following notation [78] is used for the relevant four-quark operators (normalized at $\mu = m_b$):

$$\begin{aligned} O^q_{V-A} &= (\bar{b}_L\gamma_\mu q_L)(\bar{q}_L\gamma_\mu b_L)\,, \qquad & O^q_{S-P} &= (\bar{b}_R q_L)(\bar{q}_L b_R)\,, \\ T^q_{V-A} &= (\bar{b}_L t^a\gamma_\mu q_L)(\bar{q}_L t^a\gamma_\mu b_L)\,, \qquad & T^q_{S-P} &= (\bar{b}_R t^a q_L)(\bar{q}_L t^a b_R)\,. \end{aligned} \tag{4.36}$$

(The operators T, containing the color generators t^a, will appear in further discussion.)

The matrix elements of the operators O^u over the B mesons can be parameterized in terms of the meson annihilation constant f_B and of dimensionless coefficients B ("bag constants") as

$$\langle B^+|O^u_{V-A}|B^+\rangle = \frac{f_B^2\,m_B}{16}\,(B_1^s + B_1^{ns})\,, \qquad \langle B^+|O^u_{S-P}|B^+\rangle = \frac{f_B^2\,m_B}{16}\,(B_2^s + B_2^{ns})\,, \tag{4.37}$$

for the B^+ meson containing the same light quark (u) as in the operator, and

$$\langle B_d|O^u_{V-A}|B_d\rangle = \frac{f_B^2\,m_B}{16}\,(B_1^s - B_1^{ns})\,, \qquad \langle B_d|O^u_{S-P}|B_d\rangle = \frac{f_B^2\,m_B}{16}\,(B_2^s - B_2^{ns})\,, \tag{4.38}$$

for the B_d meson where the light quark (d) is different from the one in the operator. In the limit of naive factorization the "bag constants", both the flavor-singlet (B^s) and the flavor non-singlet (B^{ns}) ones are all equal to one: $B_1^s = B_1^{ns} = B_2^s = B_2^{ns} = 1$, and the matrix elements over the B mesons of the difference of the operators entering Eq. (4.35) are vanishing. However the expected accuracy of the factorization is only about 10%, which sets the natural scale for the non-factorizable contributions, *i.e.*, for the deviations from the naive factorization. (Numerical estimates of non-factorizable terms can be found in [79, 80, 81].) After averaging the operator in Eq. (4.35) one finds the contribution of the non-factorizable terms to the rates of the $B \to X_u\,\ell\,\nu$ decays in the form

$$\delta\Gamma(B^\pm \to X_u\,\ell\,\nu) = \frac{G_F^2\,|V_{ub}|^2\,f_B^2\,m_b^3}{12\,\pi}\,\frac{\delta B^s + \delta B^{ns}}{2}\,, \qquad \delta\Gamma(B_d \to X_u\,\ell\,\nu) = \frac{G_F^2\,|V_{ub}|^2\,f_B^2\,m_b^3}{12\,\pi}\,\frac{\delta B^s - \delta B^{ns}}{2}\,, \tag{4.39}$$

where $\delta B^s = B_2^s - B_1^s$ and $\delta B^{ns} = B_2^{ns} - B_1^{ns}$. These contributions can be compared with the 'bare' total decay rate $\Gamma_0 = G_F^2\,|V_{ub}|^2 m_b^5/(192\pi^3)$:

$$\begin{aligned} \frac{\delta\Gamma(B^\pm)}{\Gamma_0} &\approx \frac{16\pi^2\,f_B^2}{m_b^2}\,\frac{\delta B^s + \delta B^{ns}}{2} \approx 0.03\left(\frac{f_B}{0.2\,GeV}\right)^2\,\frac{\delta B^s + \delta B^{ns}}{0.2}\,, \\ \frac{\delta\Gamma(B_d)}{\Gamma_0} &\approx \frac{16\pi^2\,f_B^2}{m_b^2}\,\frac{\delta B^s - \delta B^{ns}}{2} \approx 0.03\left(\frac{f_B}{0.2\,GeV}\right)^2\,\frac{\delta B^s - \delta B^{ns}}{0.2}\,. \end{aligned} \tag{4.40}$$

Thus non-factorizable terms may show up in the total decay rates only at the level of few percent. Nevertheless their relative contribution in a kinematically restricted decay rate can be substantial and generally limits the precision of determination of $|V_{ub}|$ at the level of uncertainty of about 10% [82], at least until a better quantitative understanding of such terms is available.

It should be emphasized that it would be incorrect to interpret the effects of the nonfactorizable terms as due to the 'Weak Annihilation' of the 'constituent' quarks: $b\,\overline{u} \to \ell\,\nu$, since the amplitude of such a process is essentially zero for obvious chiral reasons. Rather, one might think of the discussed effects as arising from the interference and annihilation processes involving the light 'sea' quarks in the B mesons, for which the chiral suppression is not operative, and the expected smallness of order 10% arises due to the overall smallness of the 'sea' contribution.

In lieu of a good theory of the non-factorizable terms, these can be studied experimentally. One straightforward way of probing these terms is to measure the difference of the (similarly kinematically restricted) decay rates for the charged $B^{\pm}$ and the neutral B_d mesons. According to equations (4.40), this would allow the extraction of the flavor non-singlet coefficient δB^{ns}. However, the most natural place to study these terms are the decays of D mesons, where the relative contribution of the nonperturbative effects is greatly enhanced.

In particular, it is well-known that there is a noticeable difference between the lifetimes of the strange D_s and the neutral D^0 mesons: $\tau(D_s)/\tau(D^0) = 1.20 \pm 0.025$, which cannot be described by spectator dependent effects in Cabibbo-suppressed decay channels, or by the flavor SU(3) breaking [77]. Although this discrepancy can be attributed merely to the overall inaccuracy of the OPE in the inverse of the charm quark mass[7], a more constructive approach would be to attempt to describe this difference in lifetimes as due to deviations from factorization (see also in [77, 83]). In the limit of flavor SU(3) symmetry, the difference of the dominant inclusive nonleptonic decay rates of D^0 and D_s mesons can be written [75] in terms of matrix elements of four-quark operators (normalized at $\mu = m_c$) as

$$\Gamma(D^0) - \Gamma(D_s) = \frac{2\, G_F^2\, \cos^4\theta_c\, m_c^2\, f_D^2\, m_D}{9\pi}\, C_+\, C_-\, \left(-\delta B^{ns} - \frac{3}{4}\,\varepsilon_1^{ns} + \frac{3}{4}\,\varepsilon_2^{ns}\right), \tag{4.41}$$

where θ_c is the Cabibbo angle, C_+ and C_- are the well known short-distance QCD renormalization coefficients for nonleptonic weak interaction: $C_- = C_+^{-2} = (\alpha_s(m_c)/\alpha_s(m_W))^{12/25}$, and the flavor non-singlet coefficients B and ε parameterize the following differences of the matrix elements:

$$\langle T^s_{V-A}\rangle_{D_s} - \langle T^s_{V-A}\rangle_{D^0} = \frac{f_D^2\, m_D}{8}\,\varepsilon_1^{ns}\,, \qquad \langle T^s_{S-P}\rangle_{D_s} - \langle T^s_{S-P}\rangle_{D^0} = \frac{f_D^2\, m_D}{8}\,\varepsilon_2^{ns}\,, \tag{4.42}$$

where the operators T are the same as in Eq. (4.36) with the b quark being replaced by c. (The parameters ε_1 and ε_2 both vanish in the limit of factorization.) It should be also mentioned that no attempt is being made here to allow for the breaking of the flavor SU(3) symmetry, thus no distinction is made between the annihilation constants or masses of the D_s and D_0 mesons.

The expression (4.41) for the difference of the total decay rates corresponds numerically to

$$\Gamma(D^0) - \Gamma(D_s) \approx 3.3\, \left(\frac{f_D}{0.22\, GeV}\right)^2\, \left(-\delta B^{ns} - \frac{3}{4}\,\varepsilon_1^{ns} + \frac{3}{4}\,\varepsilon_2^{ns}\right)\, \mathrm{ps}^{-1}\,. \tag{4.43}$$

Comparing this estimate with the experimental value for the difference of the total decay rates: $0.41 \pm 0.05\,\mathrm{ps}^{-1}$, one arrives at an estimate of corresponding combination of the non-singlet factorization parameters:

$$-\delta B^{ns} - \frac{3}{4}\,\varepsilon_1^{ns} + \frac{3}{4}\,\varepsilon_2^{ns} \approx 0.12\,, \tag{4.44}$$

which agrees with the understanding that nonfactorizable contributions are at a level of about 10%.

The estimate (4.44) of the non-factorizable terms, however, can serve only as a semi-quantitative indicator of the magnitude of the spectator effects in the inclusive rate of the processes $B \to X_u\, \ell\, \nu$ described by a different combination of the factorization parameters in Eq. (4.39) than in Eq. (4.44). A somewhat more direct test of the relevant combination of the parameters would be possible from the difference of the total semileptonic decay rates of D_s and D^0 mesons. Indeed, in the limit of the flavor SU(3) symmetry this difference arises only in the decays due to $c \to s\, \ell\, \nu$ and is given in terms of the operators normalized at $\mu = m_c$ as

$$\Gamma_{sl}(D^0) - \Gamma_{sl}(D_s) = \frac{G_F^2\, \cos^2\theta_c\, m_c^2\, f_D^2\, m_D}{12\pi}\, (-\delta B^{ns}) \approx 1.1\, \left(\frac{f_D}{0.22\, GeV}\right)^2\, (-\delta B^{ns})\, \mathrm{ps}^{-1}\,. \tag{4.45}$$

Given that the total semileptonic decay rate of the D^0 meson is approximately $0.16\,\mathrm{ps}^{-1}$, the discussed difference can easily amount to a quite sizable fraction of the semileptonic rate, provided that $|\delta B^{ns}| \sim 0.1$.

[7] In this respect the situation is no better for the expansion of a constrained inclusive rate of the decays $B \to X_u\, \ell\, \nu$ [82].

A measurement of the difference of the inclusive semileptonic decay rates of the D^0 and D_s mesons would make it possible to more reliably predict the difference of the corresponding decay rates between B^0 and $B^\pm$ mesons: $\Gamma(B^0 \to X_u\,\ell\,\nu) - \Gamma(B^\pm \to X_u\,\ell\,\nu)$, which, according to the previous discussion, is dominantly concentrated in the upper part of the spectrum of the invariant mass of the lepton pair. At the level of accuracy of the present discussion the only difference between the theoretical expressions for B and for D mesons arises through a different normalization point of the four-quark operators in the equations (4.39) and (4.45). Taking into account the 'hybrid' evolution of the operators containing b quark down to $\mu = m_c$ gives the relation between the non-singlet factorization constants:

$$\delta B^{ns}(m_b) = \frac{8\,\kappa^{1/2}+1}{9}\delta B^{ns}(m_c) + \frac{2\,(\kappa^{1/2}-1)}{3}\,\left[\varepsilon_1^{ns}(m_c) - \varepsilon_2^{ns}(m_c)\right], \tag{4.46}$$

where $\kappa = (\alpha_s(m_c)/\alpha_s(m_b))$. However, modulo the unlikely case that the difference of the constants ε in this relation is much bigger than the difference between the constants B, the renormalization effect is quite small, and most likely is at the level of other uncertainties in the considered approach (such as the accuracy of the flavor SU(3) symmetry, higher QCD corrections, contribution of higher terms in m_c^{-1}, *etc.*). Thus with certain reservations, one can use the approximate relation $\delta B^{ns}(m_b) \approx \delta B^{ns}(m_c)$ to directly relate the differences in the inclusive semileptonic decay rates:

$$\Gamma(B^0 \to X_u\,\ell\,\nu) - \Gamma(B^\pm \to X_u\,\ell\,\nu) \approx \frac{|V_{ub}|^2}{|V_{cs}|^2}\,\frac{f_B^2}{f_d^2}\,\frac{m_b^3}{m_c^3}\left[\Gamma_{sl}(D^0) - \Gamma_{sl}(D_s)\right]. \tag{4.47}$$

A measurement of these differences of the semileptonic decay rates can provide information only on the flavor non-singlet part of the non-factorizable terms. In order to probe the singlet part of these terms one should gain insight into the absolute decay rate of individual particles rather than their differences. In doing this, it is also quite natural to discuss the semileptonic decay rates of the D mesons, where the effect is larger than for the B mesons. Neglecting the Cabibbo-suppressed transition $c \to d\,\ell\,\nu$, one can write the contribution of the non-factorizable terms to the semileptonic decay rate of either of the non-strange D mesons as

$$\delta\Gamma_{sl}(D) = \frac{G_F^2\,f_D^2\,m_c^2\,m_D}{12\,\pi}\,\frac{\delta B^s - \delta B^{ns}}{2} \approx 0.08\,\mathrm{ps}^{-1}\left(\frac{m_c}{1.4\,GeV}\right)^2\left(\frac{f_D}{0.2\,GeV}\right)^2\,\frac{\delta B^s - \delta B^{ns}}{0.2}\,. \tag{4.48}$$

Thus with 'natural' values of the parameters the effect of the non-factorizable terms easily reaches about one half of the experimental semileptonic decay rate, *e.g.*, $\Gamma_{sl}(D^0) = 0.164 \pm 0.007\,\mathrm{ps}^{-1}$. Therefore an analysis of these rates necessarily should include the non-factorizable terms even at their expected suppressed level.

The 'full' formula for the semileptonic decay rate of a D meson, that includes the QCD radiative corrections up to two loops [84], and the second term of the OPE of the effective operator (4.32) [85] reads as

$$\begin{aligned}\Gamma_{sl}(D) \;=\; & \frac{G_F^2\,m_c^5}{192\,\pi^3}\left[|V_{cs}|^2\left(1 - 8\frac{m_s^2}{m_c^2}\right) + |V_{cd}|^2\right] \\ & \times\left[1 - 2.413\,\frac{\alpha_s}{\pi} - 23.44\left(\frac{\alpha_s}{\pi}\right)^2\right]\left(1 + \frac{\lambda_1 + \mu_g^2}{2\,m_c^2}\right)\left(1 - \frac{\mu_g^2}{2\,m_c^2}\right) + \delta\Gamma_{sl}(D)\,,\end{aligned} \tag{4.49}$$

where $\alpha_s = \alpha_s(m_c)$, $\delta\Gamma_{sl}(D)$ is given by Eq. (4.48), and a certain inaccuracy has to be admitted in the treatment of the cross terms between, *e.g.*, the radiative corrections and the effect of the finite mass m_s of the strange quark or between the radiative corrections and a part of the $\mathcal{O}(m_c^{-2})$ terms. This inaccuracy, however, is at the level of other uncertainties involved in Eq. (4.49), *e.g.*, due to higher perturbative terms, or the experimental uncertainties in the data, and can be safely neglected in the present discussion. Finally λ_1 and μ_g^2 are the standard parameters of HQET. The 'chromo-magnetic' term μ_g^2 is determined from the mass difference between the heavy vector and pseudoscalar mesons: $\mu_g^2 \approx 0.37\,GeV^2$, while the 'kinetic' term is less certain and should obey the inequality [86] $(-\lambda_1) \geq \mu_g^2$.

The contribution $\delta\Gamma_{sl}(D)$ of the non-factorizable terms could be estimated from comparison of Eq. (4.49) with the data, if not for the uncertainty of the first term, arising from the value of the charm quark mass m_c. A value of about

1.4 GeV for the 'pole' mass of the charm quark originates from the charmonium sum rules [87]. If this value is used in Eq. (4.49), the first term accounts for only about one half of the experimental rate [79, 88]. In order to remedy this contradiction without involving a substantial nonfactorizable contribution it was suggested [79] that the 'pole' value of m_c should be significantly larger, $m_c \approx 1.65$ GeV, which can hardly be reconciled with the rest of phenomenology of charmonium and charmed hadrons. In particular the mass parameter m_c, entering Eq. (4.49) can be deduced from the mass formula for a pseudoscalar meson:

$$M_P = m_Q + \overline{\Lambda} - \frac{\lambda_1 + \mu_g^2}{2\, m_Q} + O(m_Q^{-2})\,, \tag{4.50}$$

provided that the parameters $\overline{\Lambda}$ and λ_1 of the HQET can be determined. One way of experimentally determining these parameters is from a measurement of the moments of the lepton energy and of the hadronic recoil mass in the dominant semileptonic B decays. This technique was recently pursued by the CLEO experiment [89]. An analysis [90] of their results in terms of Eq. (4.49) favors the 'pole' charm quark mass in the region around 1.4 GeV, and thus suggests a large contribution of the non-factorizable term, reaching up to 0.5 – 0.6 (depending on the value of $\alpha_s(m_c)$) of the experimental semileptonic decay rate.

The discussion of the non-factorizable contribution to the semileptonic decays $B \to X_u\, \ell\, \nu$ presented in this subsection can be summarized by the following main points:

- The present poor knowledge of the non-factorizable terms can become a major source of uncertainty in determination of $|V_{ub}|$, limiting the accuracy of the knowledge of this mixing parameter at about 10%.
- The most favorable way of determining the flavor non-singlet part of these terms is from a measurement of the difference of the semileptonic decay rates of the strange D_s meson and the non-strange D mesons.
- The flavor singlet part of the non-factorizable terms can be estimated from the total semileptonic decay rate of the D mesons with an improved knowledge of the parameters $\overline{\Lambda}$ and λ_1 of the HQET. The latter parameters can determined from moments of the spectra in semileptonic decays of the B mesons.

Constraining weak annihilation contributions with lattice QCD

≻– C. Bernard, S. Hashimoto, P. Mackenzie –≺

It may become feasible in the future to use lattice QCD calculaitons to constrain the size of non-factorizable amplitudes such as those due to weak annihilation. The necessary bag parameters B_1 and B_2 may be calculated using lattice QCD. There is an exploratory quenched lattice calculation by Di Pierro and Sachrajda [91]. They used the lattice HQET (static limit) and the matching between the continuum $\Delta B = 0$ four-quark operators and corresponding lattice HQET operators is done by one-loop calculation. Their results are

$$B_1(m_b) = 1.06(8), \qquad B_2(m_b) = 1.01(6), \tag{4.51}$$

which leads to $B_1 - B_2 = 0.05(10)$, assuming no error correlation. The result (4.51) is quite consistent with the vacuum saturation approximation (or the factorization).

The quantity $B_1 - B_2$ measures the violation of factorization. In the lattice calculation the sources of the violation are the perturbative matching and the non-perturbative lattice matrix elements. In the perturbative matching, the violation starts at one loop and thus the leading contribution to $B_1 - B_2$ is $\mathcal{O}(\alpha_s)$. To control the systematic error to better than 10% one needs a two loop matching calculation. The non-perturbative calculation seems completely consistent with the factorization assumption in the quenched approximation (for both ΔB =0 and 2 operators), as there is no hint of deviation in Eq. (4.51) from unity.

To improve the accuracy in the future one has to do (i) unquenching, (ii) two-loop matching, (iii) further improvement of lattice action and/or continuum extrapolation, just as in the lattice calculations of other quantities. (Note that the result (4.51) does not contain the quenching error.) We may expect that the error is similar to that for the $\Delta B = 2$ matrix element B_B, which is 8% for $\delta(f_B^2 B_B)$ (see Section 4.6.1). This means that the improvement over the current guess, $|B_1 - B_2| = \mathcal{O}(0.1)$, is unlikely to be significant enough in the near future to allow for either establishing $B_1 - B_2 \neq 0$ at a roboust level or to demostrate if $|B_1 - B_2|$ is smaller than expected.

4.4.2 The relevance of the decay $B \to X_s\gamma$ to the extraction of V_{ub}

≻– I. Rothstein –≺

The extraction of $|V_{ub}|$ from inclusive $B \to X_u$ decays is complicated by the fact that in order to reject the overwhelming charm background one must cut the spectrum in a corner of phase space. This not only hurts statistically, but also makes the theory much more complicated. In particular, when one cuts the spectrum close to the endpoint, the rate becomes sensitive to the non-perturbative motion of the heavy quark inside the meson. This motion is described by a well-defined universal matrix element called the "shape function"[92], defined as

$$f(k_+) = \langle B(v) \mid \bar{b}_v \delta(k_+ - iD_+) b_v \mid B(v) \rangle. \tag{4.52}$$

This function is interpreted as the probability for the b quark to carry light cone momentum fraction k_+ in the meson. The amount of sensitivity to this presently unknown function depends upon the choice of observable[93]. Cutting on the lepton energy is simplest from the experimental point of view, since in this case there is no need to reconstruct the neutrino momentum. This method has the disadvantage in that it only contains $\approx 10\%$ of the rate, whereas a cut on the hadronic mass [94] contains $70 - 80\%$ [8] of the rate. A cut on leptonic mass [95] is favored, since it is less sensitive to large energy, small mass hadronic states, and thus the error induced by ignoring the shape function is in the noise. The downsides of this cut are that the effective expansion parameter becomes Λ/m_c, and not Λ/m_b [96], and that it captures only 10 to 20% of the rate. Hybrid cuts [97] have been proposed to minimize the uncertainties due to the ignorance of the shape function and formally sub-leading corrections.

We will only address the lepton energy and hadronic mass cuts, as these have order one sensitivity to the shape function. Since the shape function is universal, it can, in principle, be extracted from one decay for use in another. In

[8] These percentages are estimates based upon models.

particular, the cut rate for the decay $B \to X_S + \gamma$ may be written, at tree level, as

$$\Gamma_H \left[\frac{2E_{cut}}{M_B}\right] = \int_{2E_{cut}-m_b}^{\overline{\Lambda}} dk_+ f(k_+) \Gamma_p \left[\frac{2E_{cut}}{m_b + k_+}\right], \tag{4.53}$$

where $\Gamma_p \left[\frac{2E_{cut}}{m_b+k_+}\right]$ is the partonic rate with a cut on $x = 2E/m_b$ at $x_p = 2E_{cut}/(m_b + k_+)$. A similar expression can be derived for the semileptonic decay. Thus, one would hope to extract $f(k_+)$ by fitting the end-point spectrum in the radiative decay, and use it to predict V_{ub}. Indeed, most extractions to date follow the results in [98], where it was assumed that the radiative corrections can simply be incorporated in (4.53) by changing Γ_p to include the one loop QCD corrections. Unfortunately, as pointed out by [99], this is incorrect, due to the fact the presumed relation between the moments of the shape function and matrix elements of local operators does not hold beyond tree level. When CLEO [100], *BABAR* [23] and Belle [101] performed their extraction, they assumed that the shape function was constrained to have certain properties; these constraints followed from the aforementioned erroneous relationship between moments and local operators. Thus, the true size of systematic errors for those measurements is not clear. We expect that extractions utilizing the hybrid cut will be less sensitive to this issue, and thus the errors made using this method of fitting the shape function will be diminished in amplitude, though it is not clear by how much.

Fortunately, there is no need to extract the shape function in the first place, since by taking the ratio of the moments of the radiative and semi-leptonic decay rates, we can eliminate the need for the shape function altogether [102]. It has been shown that we can write a closed form expression for $\mid V_{ub} \mid$ in terms of the cut lepton energy spectrum as [103, 104, 105]

$$\frac{|V_{ub}|^2}{|V_{ts}^* V_{tb}|^2} = \frac{3\,\alpha\, C_7^{(0)}(m_b)^2}{\pi}(1 + \mathcal{H}_{mix}^{\gamma}) \int_{x_B^c}^1 dx_B \frac{d\Gamma}{dx_B} \times \left\{ \int_{x_B^c}^1 du_B W(u_B) \frac{d\Gamma^{\gamma}}{du_B} \right\}^{-1}, \tag{4.54}$$

where $\mathcal{H}_{mix}^{\gamma}$ represents the corrections due to interference coming from the operators O_2 and O_8 [106] .

$$\mathcal{H}_{mix}^{\gamma} = \frac{\alpha_s(m_b)}{2\pi C_7^{(0)}} \left[C_7^{(1)} + C_2^{(0)} \Re(r_2) + C_8^{(0)} \left(\frac{44}{9} - \frac{8\pi^2}{27} \right) \right], \tag{4.55}$$

and x_B^c is the value of the cut. In Eq. (4.55), all the Wilson coefficients, evaluated at m_b, are "effective" as defined in [107], and $\Re(r_2) \approx -4.092 + 12.78(m_c/m_b - 0.29)$ [108]. The numerical values of the Wilson coefficients are: $C_2^{(0)}(m_b) \approx 1.11,\ C_7^{(0)}(m_b) \approx -0.31,\ C_7^{(1)}(m_b) \approx 0.48$, and $C_8^{(0)}(m_b) \approx -0.15$. The diagonal pieces from O_2 and O_8 are numerically insignificant. The function $W(u_B)$ is given by

$$W[u_B] = u_B^2 \int_{x_B^c}^{u_B} dx_B \left(1 - 3(1 - x_B)^2 + \frac{\alpha_s}{\pi}\left(\frac{7}{2} - \frac{2\pi^2}{9} - \frac{10}{9} log(1 - \frac{x_B}{u_B})\right)\right). \tag{4.56}$$

This expression for V_{ub} does is not afflicted by large end point logs which were resummed and shown to have a small effect on the rate [109, 103, 104, 110].

The expression for V_{ub} for the case of the hadronic mass cut is given by [111]

$$\frac{|V_{ub}|^2}{|V_{ts}|^2} = \frac{6\,\alpha\, C_7(m_b)^2 (1 + \mathcal{H}_{mix}^{\gamma})\, \delta\Gamma(c)}{\pi\,[I_0(c) + I_+(c)]}. \tag{4.57}$$

The expressions for $\Gamma(c),\ I_0(c)$ and $I_+(c)$ can be found in [111]. The effect of resummation of the end-point logs in this case was again shown to be negligible [112],[113]. Note that the dominant source of errors in both of these extractions will come from sub-leading shape functions, which were studied in [114].

4.4.3 Experimental prospects

≻– D. del Re –≺

The *BABAR* experiment has already performed measurements of inclusive semileptonic B decays with statistical errors comparable to the experimental systematic errors, while the theoretical error is already dominant. This is due to the fact that even Cabibbo-suppressed inclusive semileptonic B decays are abundant at B Factories, but also due to the large theoretical uncertainties affecting the study of inclusive decays in restricted regions of phase space. A substantial gain in the overall error will only be achieved if the theoretical error can be better controlled—more data and measurements in dedicated regions of phase can help in this regard.

The recoil approach should help in reaching this goal. It significantly reduces the experimental systematics, and, since the level of background is lower, permits looser cuts on the phase space and multiplicity, thereby reducing theoretical systematic uncertainties.

Inclusive charmless semileptonic B decays

In order to understand the level of sensitivity achievable in the study of inclusive charmless semileptonic B decays, it is worth to briefly describe the measurement recently presented by the *BABAR* experiment [23]. It makes use of the recoil technique and it is the $|V_{ub}|$ measurement that, so far, obtained the smallest systematic uncertainty.

In this analysis, a semi-leptonic decay of one B meson (B_{recoil}) is identified by the presence of a charged lepton in the recoil of a B_{reco} candidate. In addition, the detection of missing energy and momentum in the event is taken as evidence for the presence of a neutrino. The $B \to X_u \ell \nu$ transitions are dominantly located in the low mass region $m_X < m_D$. Undetected particles and mis-measurement of detected particles distort the measured mass distribution and lead to a large background from the dominant $b \to c\ell\nu$ decays. To improve the resolution in the measurement of m_X, this analysis exploits the kinematic constraints and simplicity of the $B\overline{B}$ state and uses the measured momenta and energies of all particles in a 2C kinematic fit to the whole event. With the additional constraint that the missing particle should have zero mass the hadronic mass m_X is determined, largely independent of the unfitted missing mass of the event. To extract the number of leptons from $b \to u\ell\nu$ transitions the data are divided into subsamples of events, one that is enriched in $b \to u$ transitions by a veto on the presence of kaons in the recoil system, and the rest of the sample, which is used to control the background. To derive the charmless semileptonic branching ratio, the observed number of events, corrected for background and efficiency, is normalized to the total number of semileptonic decays $b \to q\ell\nu$ (here q stands for c or u) in the B_{reco} event sample. Additional selection criteria are imposed to select $b \to u\ell\nu$ decays. They include constraints on the sum of the charges of all observed particles in the events, correlations between the sign of the lepton and the flavor of the reconstructed B meson, requirement on the missing momentum and mass, and most importantly a veto on strange particles. This *BABAR* analysis, based on 82 fb^{-1}, selects ~ 170 signal events signal events for $m_X < 1.55\,\mathrm{GeV}$ (see Fig. 4-3) , with a signal-to-background ratio that corresponds to ~ 1.7. The inclusive branching ratio comes out to be $\mathcal{B}(B \to X_u \ell \overline{\nu}\,) = (2.24 \pm 0.27(\mathrm{stat}) \pm 0.26(\mathrm{syst}) \pm 0.39(\mathrm{theo})) \times 10^{-3}$, that can be translated into $|V_{ub}| = (4.62 \pm 0.28(\mathrm{stat}) \pm 0.27(\mathrm{syst}) \pm 0.48(\mathrm{theo})) \times 10^{-3}$. Even at these moderate luminosities, the systematic error is larger than the statistical error.

The experimental systematic error will be improved in the future. It is dominated by detector effects that will be better understood with more experience. A substantial component of this uncertainty is due to imperfect knowledge of semileptonic branching ratios ($B \to D^{(*,**)} l\nu$) and to the D meson decay branching ratios ($D \to X$)—measurements which will improve with more data, leading to a reduction in the related systematics. A quite large error due to the MC statistics will decrease as soon as more simulated events become available. A reasonable estimate is that the total experimental systematic error can be below 5% for the rate (and half of that for $|V_{ub}|$).

This measurement technique will be only limited by the theoretical uncertainty but even this error can be improved. The cleanliness of the technique allows a measurement of the m_X spectrum with a good resolution. By adding statistics not only the m_X integral but also the m_X shape can be measured allowing the extraction of the theoretical parameters m_b and a (as suggested in [115]), reducing the uncertainty due the extrapolation to the full spectrum. Moreover new theoretical papers [57] suggest a different cut in the phase space. A combination of a cut on $q^2 > (m_B - m_D)^2$ (i.e. on the virtual W invariant mass) and a cut on m_X should decrease the theoretical error. Finally a combination of the m_X

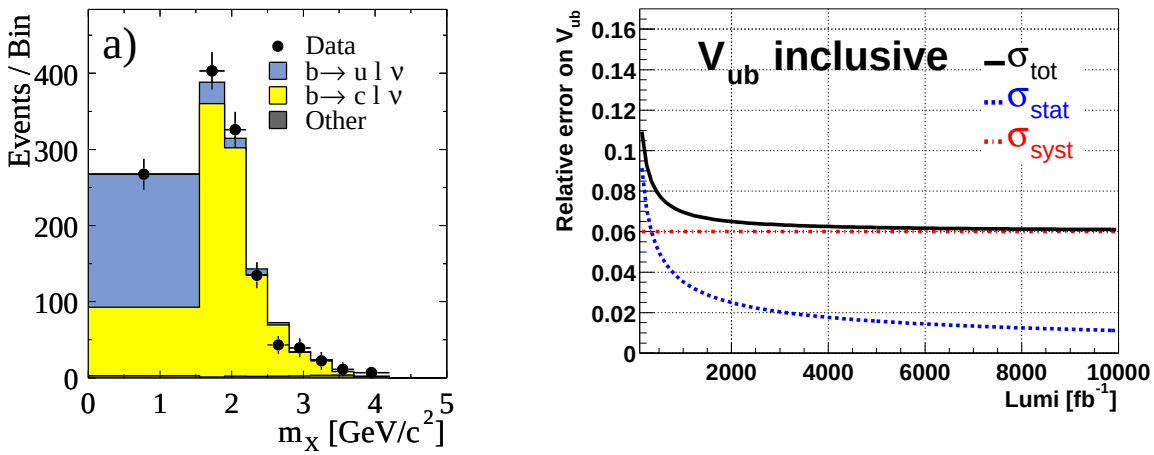

Figure 4-3. *Left: a χ^2 fit to the m_X distribution. Right: perspectives for the error on $|V_{ub}|$ as a function of the accumulated luminosity as described in text.*

spectrum and the photon spectrum in $b \to s\gamma$ decays [116, 104, 106] could be used to perform a $|V_{ub}|$ measurement with suppressed uncertainty related to the shape function.

In summary, we expect the total error on $|V_{ub}|$ to decrease down to 5–10% within several years. In Fig. 4-3 an extrapolation to higher luminosities is presented. The analysis method corresponds to that presented in [23], with the addition of a cut on $q^2 > 10$ GeV. We assume a systematic error of 6%. The plot clearly shows how this inclusive measurement cannot be improved by increasing the statistics above 1-2 ab^{-1}, unless systematic errors are further reduced.

Inclusive rare radiative B decays

≻– U. Langenegger –≺

The measurement of the photon energy spectrum in inclusive radiative decays $B \to s\gamma$ provides a direct determination of the shape function of the b quark. The first and second moment of this spectrum are related to the mass of the b quark and HQET parameters describing its Fermi momentum within the hadron. From a theoretical point of view, it would be most desirable to measure the photon spectrum down to the lowest possible energies.

The experimental challenge here is on the one hand the small branching fraction of about 3×10^{-4}, and on the other hand, the very large background both from continuum $q\bar{q}$ production (where $q = u, d, s, c$) and from $B\overline{B}$ events. Both background spectra rise exponentially towards lower energies and therefore lead to an experimental spectrum truncated around $E_\gamma > 2$ GeV. There are two distinct types of analyses, semi-exclusive and inclusive.

In semi-exclusive analyses, the hadronic final state X_s in $B \to X_s\gamma$ decays is reconstructed as the sum of several exclusive modes. This allows a measurement of the photon energy in the B meson rest frame with an excellent E_γ resolution, but is sensitive to only 50% of all X_s states. The dependence on the modeling of the included hadronic final states constitutes the major difficulty in the analysis.

In inclusive analyses, the continuum $q\bar{q}$ background is rejected with high efficiency by selecting ("tagging") events based on B decay signatures (see Section 4.2). This includes (1) high-momentum leptons and (2) a fully reconstructed hadronic B decay.

In the first case, the photon energy is measured in the $\Upsilon(4S)$ restframe with a resolution of about $100\ \mathrm{MeV}$. In the current *BABAR* analysis based on $82\,\mathrm{fb}^{-1}$, it is expected to determine the mean photon energy with an error of about 1.2% (without background and efficiency contributions), dominated by the statistical error. Here, the spectrum is measured for energies $E_\gamma > 2.0\ \mathrm{GeV}$.

In the second case, the photon can be boosted into the B meson rest frame, and, due to the overconstrained kinematics, better resolution, compared to the lepton-tagged analysis, can be achieved. Because of the low efficiency for hadronic tags, the event yield is substantially lower: for $82\,\mathrm{fb}^{-1}$ a total of about 60 events is expected. Comparable statistical errors to the lepton-tagged analysis are expected for an integrated luminosity of about $1\,\mathrm{ab}^{-1}$. Nevertheless, this approach is very valuable as it offers the potential to lower the threshold for the photon energy and, more importantly, allows the best resolution in the measurement of the photon energy.

4.5 $b \to u$ Exclusive Decays (π, $\eta^{(\prime)}$, ρ, ω, *etc.*)

4.5.1 Theory

≻C. Bauer, I. Stewart ≺

Branching ratios of exclusive semileptonic B decays proceed via the heavy-light current $\overline{u}\Gamma b$, and are proportional to the square of the magnitude of the CKM matrix element V_{ub}. However, the relevant matrix element of this $b \to u$ current for exclusive processes depends on non-perturbative hadronic physics parameterized by form factors, which are needed in order to extract CKM information from these decays. For decays to pseudoscalars P or vectors V these form factors are defined as

$$\begin{aligned}
\langle P(p)|\overline{q}\,\gamma^\mu b|\overline{B}(p_b)\rangle &= f_+(q^2)\left[p_b^\mu + p^\mu - \frac{m_B^2 - m_P^2}{q^2}\,q^\mu\right] + f_0(q^2)\,\frac{m_B^2 - m_P^2}{q^2}\,q^\mu,\\
\langle V(p,\epsilon^*)|\overline{q}\gamma^\mu b|\overline{B}(p_b)\rangle &= \frac{2V(q^2)}{m_B + m_V}\,i\epsilon^{\mu\nu\rho\sigma}\epsilon^*_\nu\,(p_b)_\rho\,p_\sigma,\\
\langle V(p,\epsilon^*)|\overline{q}\gamma^\mu\gamma_5 b|\overline{B}(p_b)\rangle &= 2m_V A_0(q^2)\,\frac{\epsilon^*\cdot q}{q^2}\,q^\mu + (m_B + m_V)\,A_1(q^2)\left[\epsilon^{*\mu} - \frac{\epsilon^*\cdot q}{q^2}\,q^\mu\right]\\
&\quad - A_2(q^2)\,\frac{\epsilon^*\cdot q}{m_B + m_V}\left[p_b^\mu + p^\mu - \frac{m_B^2 - m_V^2}{q^2}\,q^\mu\right].
\end{aligned} \tag{4.58}$$

where $q^\mu = p_B^\mu - p^\mu$ is the momentum transfer to the leptons. Decay rates to particular exclusive final states can be written in terms of these form factors. Decays to pseudoscalar mesons are given by

$$\frac{\mathrm{d}\Gamma(B \to P\ell\overline{\nu})}{\mathrm{d}q^2\,\mathrm{d}\cos\theta} = |V_{ub}|^2\frac{G_F^2|\vec{p}_P|^3}{32\pi^3}\sin^2\theta\,|f_+(q^2)|^2\,, \tag{4.59}$$

where $\ell = \mu, e$ and an f_0 term would be proportional to m_ℓ^2 and has been dropped. For the analogous decays to vector mesons one finds

$$\frac{\mathrm{d}\Gamma(B \to V\ell\overline{\nu})}{\mathrm{d}q^2\,\mathrm{d}\cos\theta} = |V_{ub}|^2\frac{G_F^2|\vec{p}_V|q^2}{768\pi^3 m_B^2}\left[(1+\cos\theta)^2|H_+|^2 + (1-\cos\theta)^2|H_-|^2 + 2\sin^2\theta|H_0|^2\right], \tag{4.60}$$

where the three helicity amplitudes are given by

$$\begin{aligned}
H_\pm(q^2) &= (m_B + m_V)A_1(q^2) \mp \frac{2m_B|\vec{p}_V|}{(m_B + m_V)}\,V(q^2)\,,\\
H_0(q^2) &= \frac{(m_B + m_V)}{2m_V q^2}\left[\left(m_B^2 - m_V^2 - q^2\right)A_1(q^2) - \frac{4|\vec{p}_V|^2 m_B^2}{(m_B + m_V)^2}A_2(q^2)\right].
\end{aligned} \tag{4.61}$$

In Eqs. (4.59-4.61) the three momenta are related to q^2

$$4m_B^2|\vec{p}_{P,V}|^2 = (q^2 - m_B^2 - m_{P,V}^2)^2 - 4m_B^2 m_{P,V}^2\,. \tag{4.62}$$

Given knowledge of the form factors, a measurement of the exclusive semileptonic branching ratios can be used to determine the CKM parameter $|V_{ub}|$.

Measurements of the heavy-to-light form factors themselves are also important ingredients in the description of many other exclusive B meson decays. In addition to parameterizing the semileptonic decays they appear in rare radiative decays such as $B \to K^*\gamma$, $B \to \rho\gamma$, $B \to K^{(*)}\ell^+\ell^-$, and $B \to \pi\ell^+\ell^-$. They also play a crucial role in factorization theorems for nonleptonic $B \to MM'$ decays, with $M^{(\prime)}$ light pseudoscalar and vector mesons, which are important for measurements of CP violation.

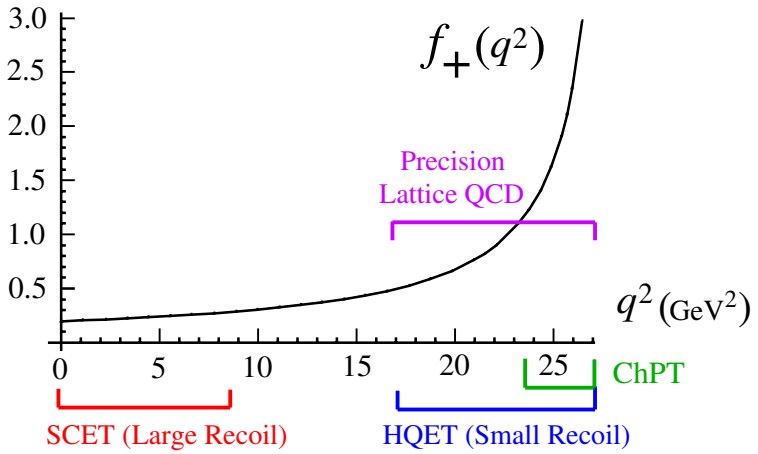

Figure 4-4. *Regions of validity in* q^2 *for different model independent methods for the* $B \to \pi$ *form factors. The abbreviations are Heavy Quark Effective Theory (HQET), Soft-Collinear Effective Theory (SCET), and Chiral Perturbation Theory (ChPT). The curve shown for* $f_+(q^2)$ *is for illustration only.*

For rare decays such as $B \to K^*\gamma$, $B \to K^*\ell^+\ell^-$, and $B \to K\ell^+\ell^-$ additional form factors appear via tensor currents. They can be defined by

$$\begin{aligned}
\langle P(p)|\overline{q}\, i\sigma^{\mu\nu} q_\nu b|\overline{B}(p_b)\rangle &= -\frac{f_T(q^2)}{m_B+m_P}\left[q^2(p_b^\mu + p^\mu) - (m_B^2 - m_P^2)\, q^\mu\right], \\
\langle V(p,\epsilon^*)|\overline{q}\, i\sigma^{\mu\nu} q_\nu b|\overline{B}(p_b)\rangle &= -2\, T_1(q^2)\, i\epsilon^{\mu\nu\rho\sigma}\epsilon^*_\nu\, (p_b)_\rho\, p_\sigma, \\
\langle V(p,\epsilon^*)|\overline{q}\, i\sigma^{\mu\nu}\gamma_5 q_\nu b|\overline{B}(p_b)\rangle &= T_2(q^2)\left[(m_B^2 - m_V^2)\,\epsilon^{*\mu} - (\epsilon^*\cdot q)\,(p_b^\mu + p^\mu)\right] \\
&\quad + T_3(q^2)\,(\epsilon^*\cdot q)\left[q^\mu - \frac{q^2}{m_B^2 - m_V^2}(p_b^\mu + p^\mu)\right].
\end{aligned} \tag{4.63}$$

Although the phenomenology and experimental methods for rare decays differ from the semileptonic decays, the theoretical description of the form factors in Eq. (4.63) is no more difficult than those in Eq. (4.58). Thus the theory techniques explored in this section apply equally well to both cases, and in certain kinematic cases actually provide useful relations between the two. For a detailed discussion of rare decays we refer the reader to Chapter 2.

Exclusive form factors depend in a complicated way on the details of the hadronic states, and their computation has been traditionally performed using QCD inspired phenomenological methods, such as quark models (for examples see [117]). Predictions for form factors can also be obtained with QCD sum rules [118, 119, 120, 121, 122, 123, 124], which we do not discuss here. For the level of precision obtainable from a high-luminosity asymmetric B-factory we expect that reliance on model independent methods with well understood theoretical uncertainty will be crucial. In this chapter we focus on results for form factors obtained with HQET, SCET, chiral perturbation theory, and lattice QCD over the regions of q^2 shown in Fig. 4-4. The best tool available to determine the heavy-light form factors directly from first principles QCD is the lattice. As illustrated in Fig. 4-4 precision control over the systematics of both the heavy B and light meson is currently only projected for smaller recoils, where the light meson is not too energetic in the B's rest frame. Lattice methods with a moving B meson have recently been proposed [125, 126, 127] which have the potential to improve the precision of form factor determinations at lower values of q^2, however these methods are not included in the projections discussed here. The prospects for lattice determinations of the form factors are discussed in section 4.5.2.

Additional constraints on the form factors can be obtained with the help of expansion parameters derived from $\Lambda_{\rm QCD}$, m_B, and E_M. Here $q^2 = m_B^2 + m_M^2 - 2m_B E_M$, where E_M is the energy of the light meson M in the B-meson rest frame, and their is a one-to-one correspondence between values of E_M and q^2. Different expansions are appropriate for

different regions of q^2 and are made systematic with the help of several effective field theories as shown in Fig. 4-4. For the region where $E_M/\Lambda \ll 1$ is a good expansion parameter SU(2) heavy baryon chiral perturbation theory (ChPT) can be used to compute the form factors for $B \to \pi$ and SU(3) heavy baryon chiral perturbation theory can be used for $B \to K$ [128, 129, 130].[9] Here $\Lambda \sim 1\,\mathrm{GeV}$ is of order the chiral symmetry breaking scale. For example for $B \to \pi$ one obtains

$$f_+ - f_- = \frac{f_B}{f_\pi}\frac{g_\pi m_B}{E_\pi + \Delta}\,, \qquad f_+ + f_- = \frac{f_B}{f_\pi}\Big(1 - \frac{g_\pi E_\pi}{E_\pi + \Delta}\Big)\,, \tag{4.64}$$

where $f_- = (f_0 - f_+)(m_B^2 - m_\pi^2)/q^2$, $\Delta = m_{B^*} - m_B$, and g_π is the $B^*B\pi$ coupling. Analysis beyond leading order can be found in Refs. [131, 132, 133].

The results in Eq. (4.64) are only valid in a very limited range at large q^2 or small E_π. For the larger region where $m_b \gg E_\pi \sim \Lambda_{\rm QCD}$ we can make use of heavy quark effective theory, HQET. Although HQET does not provide a normalization for any of the form factors it does give important relations between different form factors. The HQET form factor form factor relations are discusssed further in section 4.5.3.

For the other end of the spectrum, namely large recoil or small q^2, the power expansion in HQET breaks down since the light meson gets too energetic. In this region another effective theory is applicable, known as the soft-collinear effective theory (SCET) [134, 135, 136, 137]. The expansion parameters here are $\Lambda_{\rm QCD}/E_M$ and $\Lambda_{\rm QCD}/m_b$. In section 4.5.3 we discuss the LO predictions of SCET for heavy-to-light form factors, as well as reviewing the large recoil SCET form factor relations.

Finally, dispersion relations combined with analyticity provide important constraints on the shape of form factors over the entire region of q^2 [138, 139, 140, 141]. We do not review these methods here.

4.5.2 Lattice form factors ($|\vec{p}_M| \lesssim 1$ GeV)

≻C. Bernard, S. Hashimoto, P. Mackenzie ≺

The estimates for future lattice precision presented in this section and Section 4.6.1 on leptonic decay constants are based largely on a DOE planning document prepared by S. Sharpe, C. Bernard, A. El-Khadra, P. Mackenzie, and R. Sugar.

We assume three levels of computation based on improved staggered simulations with $n_F = 3$ flavors of dynamical sea quarks:

- "MILC0." These are existing configurations generated over the past four years by the MILC configurations. A complete analysis of heavy-light quantities on these lattices will probably take one to two years.
- "MILC1." This level will take $\sim$6 Teraflop-years and require machines now being built under the DOE SciDAC project [142]: the Columbia QCDOC and large clusters at Fermilab and Jefferson Lab. We estimate that this level will be completed in three to five years from the present,including time for analysis of heavy-light quantities,
- "MILC2." This level will take $\sim$ 50–100 Teraflop-years and require the next generation of machines. We estimate that this level will be completed in five to eight years from the present, including time for analysis of heavy-light quantities.

As mentioned in Section 4.1.2, dynamical domain wall fermions provide a safer, but slower, alternative to improved staggered. A level "DWF1" of dynamical domain wall fermions (or equivalent) at comparable mass and lattice spacings to MILC1 may have comparable precision to MILC2 because DWF have smaller discretization errors and are free from taste-violation issues. This may require $\sim$ 600-1000 Teraflop-years and the "next next" generation of

[9] For SU(3) it is obvious that precision results would require going beyond leading order in the chiral expansion.

machines, finishing perhaps ten or twelve years from the present. In other words, our guess is that use of DWF, as opposed to improved staggered fermions in lattice QCD computation, would delay the available lattice precision by roughly five years.

Tables 4-2, 4-3, and 4-4 show estimates of precision attainable for lattice calculations of semileptonic form factors with data sets MILC0, MILC1, and MILC2, respectively. These are meant to be average errors for the form factors at fixed q^2 in the allowed range of momentum. We focus on the gold plated quantities $B \to \pi$ and $B \to D$; it is possible that the errors in $B \to D^*$ will not be much larger than for $B \to D$. As discussed in Section 4.1.2, we give two alternatives for perturbative errors (one-loop and two-loop) and two alternatives for chiral extrapolation errors: (no) SχPT assumes that staggered chiral perturbation theory is (is not) useful.

Table 4-2. *Estimated percent errors for form factors at MILC0 level: one to two years from the present. "Light q" includes light quark chiral and discretization errors. "Heavy Q" means heavy quark discretization errors. $B \to \pi$ form factors are for restricted range $0.5\ \mathrm{GeV} \lesssim \vec{p}_\pi \lesssim 1\ \mathrm{GeV}$ (in B rest frame), but can have any bilinear current.*

quantity	**statist.**	**scale**	**light** q		**heavy** Q	**pert. th.**	
			no SχPT	SχPT		1-loop	2-loop
$B \to \pi\ell\nu$	4.5	1	6	3	3	7.5	2
$B \to D\ell\nu$	1	0.5	2	1	1	2.5	0.7

Table 4-3. *Same as Table 4-2, but for MILC1 level: three to five years from the present. $B \to \pi$ momentum range is slightly larger than for MILC0: $0.35\ \mathrm{GeV} \lesssim \vec{p}_\pi \lesssim 1\ \mathrm{GeV}$ (in B rest frame).*

quantity	**statist.**	**scale**	**light** q		**heavy** Q	**pert. th.**	
			no SχPT	SχPT		1-loop	2-loop
$B \to \pi\ell\nu$	3	0.7	4	2	2	7.5	2
$B \to D\ell\nu$	0.6	0.5	2	1	0.6	2.5	0.7

Table 4-4. *Same as Table 4-3, but for MILC2 level: five to eight years from the present.*

quantity	**statist.**	**scale**	**light** q		**heavy** Q	**pert. th.**	
			no SχPT	SχPT		1-loop	2-loop
$B \to \pi\ell\nu$	1.5	0.5	2.7	1.3	1.5	7.5	2
$B \to D\ell\nu$	0.3	0.3	1.4	0.7	0.5	2.5	0.7

Table 4-5 shows total lattice form factor errors under various assumptions, together with our best guess of which alternatives are most likely to be realized in practice. It must be kept in mind that the errors themselves are uncertain, by a fractional amount which is at least $\sim 30\%$ and rises with time into the future.

Table 4-5. *Estimated total lattice errors in percent under various assumptions. Momentum ranges for $B \to \pi$ are same as in Tables 4-2, 4-3 and 4-4. Where there are four entries per column they correspond to: (1)* **no** *SχPT and 1-loop perturbation theory, (2) SχPT and 1-loop perturbation theory, (3)* **no** *SχPT and 2-loop perturbation theory, and (4) SχPT and 2-loop perturbation theory. Our best guesses of which alternative will in fact be realized are surrounded with boxes.*

quantity	**now**	**1-2 yrs.** MILC0	**3-5 yrs.** MILC1	**5-8 yrs.** MILC2
$B \to \pi\ell\nu$	15	11, 10, 8, 7	9, 9, 6, 5	8, 8, 4, 3
$B \to D\ell\nu$	6	4, 3, 3, 2	3, 3, 2, 1.6	3, 3, 2, 1.2

4.5.3 Heavy-to-light form factors in SCET

≻C. Bauer, D. Pirjol, I. Stewart ≺

In the absence of perfect theoretical computations, it is of interest to exploit the existence of model-independent relations among form factors. Such relations can be established in two kinematical regions, corresponding to the limits of a) energetic and b) slow final light hadron. These two situations are described in terms of two effective theories: a) the Soft-Collinear Effective Theory (SCET) and b) the Heavy Quark Effective Theory (HQET). In this and the following section we consider these two types of predictions in turn.

In the large recoil region, the existence of symmetry relations for heavy-light form factors was first suggested by Charles *et al.* in Ref. [143], formalizing earlier results obtained in the quark model [144]. The derivation here was based on an effective theory, LEET [145], which unfortunately is flawed since LEET does not correctly capture the IR physics of QCD in the case of energetic mesons. An analysis of the leading order contributions in perturbation theory [146] showed the existence of calculable corrections to these "symmetry" relations. Rather than following the historical order of events, we review the results obtained from the all-order effective theory treatment based on SCET [135, 147, 148, 149, 150, 151, 152, 153, 154].

For small values of q^2 a weak current $\bar{q}P_R\gamma^\mu b$ can be matched onto the leading order SCET current

$$\bar{q}P_R\gamma^\mu b = \int \mathrm{d}\omega\, C_\Gamma^{(0)}\, [\bar{\xi}W]_\omega P_R \Gamma h_v \equiv \int \mathrm{d}\omega\, C_\Gamma^{(0)}\, J_{\Gamma,\omega}^{(0)}\,, \tag{4.65}$$

h_v is the usual field in HQET and $[\xi W]_\omega$ is a gauge invariant collinear field with label momentum equal to ω. There are only three independent Dirac structures Γ, since both the ξ and the h_v are two component spinors. The matrix element of this operator between a B meson state and a collinear light meson state vanishes, since the interpolating field for a collinear light meson contains two collinear fermions. This fact on the one hand explains the suppression of the form factor in the large recoil region, but it also makes the SCET analysis difficult, since a good understanding of subleading effects are needed.

The analysis of the form factors is performed in a two step matching procedure, where one first matches QCD onto a theory called $\mathrm{SCET_I}$, containing collinear particles with off-shellness $p^2 \sim Q\lambda_{\rm QCD}$ and usoft particles with off-shellness $p^2 \sim \Lambda_{\rm QCD}^2$ [155]. In $\mathrm{SCET_I}$ the heavy to light current has to appear in a time-ordered product with an interactions which turn the soft spectator fermion in the B meson into a collinear fermion. These interactions appear at subleading order in SCET [156]. It turns out that the first non-vanishing time-ordered product occurs two powers of λ suppressed, and one therefore also requires the subleading heavy-light current in SCET, $J_{\omega_1\omega_2}^{(1)}$, which depends on two label momenta ω_1 and ω_2, as well as the subleading SCET Lagrangian. Combining these results, one conveniently divides the resulting time-ordered product into two terms

$$T_{\rm I}^\Gamma(\omega) = i\int d^4y\, T[J_{\Gamma,\omega}^{(0)}(0), i\mathcal{L}_{\xi q}^2(y)] + i\int d^4y \int d^4z T[J_{\Gamma,\omega}^{(0)}(0), i\mathcal{L}^1(y), i\mathcal{L}_{\xi\xi}^1(z) + i\mathcal{L}_{cg}^1(z)]$$

$$T_2^\Gamma(\omega_1\omega_2) \,=\, i\int d^4\, y T[J^{(1)}_{\Gamma,\omega_1\omega_2}(0), i\mathcal{L}^{(1)}_{\xi q}(y)] \tag{4.66}$$

To proceed, these time-ordered products are matched onto four quark operators in $\mathrm{SCET_{II}}$. The form factor is the matrix element of the resulting operator in $\mathrm{SCET_{II}}$.

$$F^{B\to M} = \int d\omega\; C_\Gamma^{(0)}(\omega)\langle M|T_1^\Gamma(\omega)|B\rangle + \int d\omega_1 \int d\omega_2\; C^{(1)}(\omega_1,\omega_2)\langle M|T_2^\Gamma(\omega_1,\omega_2)|B\rangle\,. \tag{4.67}$$

where in this equation it is understood that the T_i^Γ are matched onto operators in $\mathrm{SCET_{II}}$ before taking the matrix element. There is still some discussion in the literature how to properly factorize T_1 and match it onto operators in $\mathrm{SCET_{II}}$. This can be avoided by simply defining the matrix element

$$\begin{aligned}\langle P|T_1^\Gamma(\omega)|B\rangle \,&=\, \overline{n}\cdot p\;\zeta(\overline{n}\cdot p)\delta(\omega-\overline{n}\cdot p)\,,\\ \langle V_{\perp,\parallel}|T_1^\Gamma|B\rangle \,&=\, \overline{n}\cdot p\;\zeta_{\perp,\parallel}(\overline{n}\cdot p)\delta(\omega-\overline{n}\cdot p)\end{aligned} \tag{4.68}$$

he functions $\zeta(\overline{n}\cdot p)$, $\zeta_\parallel(\overline{n}\cdot p)$, $\zeta_\perp(\overline{n}\cdot p)$ are called soft form factors, and the reason for there only being three soft form factors is due to the fact that each of the three independent Dirac structures in the SCET current gives rise to only one type of meson by parity and angular momentum.

For T_2, one integrates out the modes with $p^2 \sim Q\Lambda_{\mathrm{QCD}}$, which give rise to a jet function. The exact structure depends on what kind of meson and which Dirac structure appear in the matrix element. The general structure, however, of such a matrix element is

$$\langle M|T_2(\omega_1,\omega_2)|B\rangle = \frac{f_B f_M m_B}{\overline{n}\cdot p^2}\int_0^1 dx\int_0^\infty dk^+\; J_\Gamma(\omega_1,x,k^+)\phi_M(x)\phi_B^+(k^+)\delta(\omega_1+\omega_2-\overline{n}\cdot p) \tag{4.69}$$

In this expression, the jet function $J_\Gamma(\omega_1,x,k^+)$ depends on the Dirac structure of the suubleading current $J^{(1)}_{\Gamma,\omega_1,\omega_2}$ and can be expanded in a series in $\alpha_s(\sqrt{E\Lambda_{\mathrm{QCD}}})$. Inserting (4.68) and (4.69) into (4.67) we obtain the result for a general form factor

$$f_i(q^2) = C_{ij}^{(0)}(Q)\zeta_j^M(Q\Lambda,\Lambda^2) + \int dxdzdk_+ C_{ij}^{(1)}(z,Q^2)J_j(z,x,k_+)\phi_B^+(k_+)\phi_j^M(x) \tag{4.70}$$

As explained before, the coefficients C_{ij} are calculable in an expansion in $\alpha_s(Q)$, the jet functions J_j are calculable in an expansion in $\alpha_s(Q\Lambda)$ and the remaining elements in these expressions denote the non-perturbative parameters. They are the well known light cone wave functions of the B meson and the pseudoscalar or vector meson, as well as the soft form factors explained earlier.

Below we summarize the factorization results for the $B\to P$ and $B\to V$ form factors (following the notation in Ref. [150] and Ref. [151]). We use below the notations of [150] for the Wilson coefficients of $\mathrm{SCET_I}$ operators $C_i(E), B_i(x,z)$. For decays to pseudoscalars

$$\begin{aligned} f_+(E) = &\left(C_1^{(v)} + \frac{E}{m_B}C_2^{(v)} + C_3^{(v)}\right)\zeta^P \\ &+N_0\int dxdzdl_+\left\{\frac{2E-m_B}{m_B}\left[B_1^{(v)} - \frac{E}{m_B-2E}B_2^{(v)} - \frac{m_B}{m_B-2E}B_3^{(v)}\right]\delta(x-z)\right. \\ &\left.+\frac{2E}{m_b}\left[B_{11}^{(v)} - \frac{E}{m_B}B_{12}^{(v)} - B_{13}^{(v)}\right]\right\}J_\parallel(x,z,l_+)\phi_\pi(x)\phi_B^+(l_+) \end{aligned} \tag{4.71}$$

$$\begin{aligned} \frac{m_B}{2E}f_0(q^2) = &\left(C_1^{(v)} + \frac{m_B-E}{m_B}C_2^{(v)} + C_3^{(v)}\right)\zeta^P \\ &+N_0\int dxdzdl_+\left\{\frac{m_B-2E}{m_B}\left[B_1 + \frac{m_B-E}{m_B-2E}B_2^{(v)} + \frac{m_B}{m_B-2E}B_3^{(v)}\right]\delta(x-z)\right. \end{aligned} \tag{4.72}$$

$$+\frac{2E}{m_b}\left[B_{11}^{(v)}-\frac{m_B-E}{m_B}B_{12}^{(v)}-B_{13}^{(v)}\right]\Bigg\}J_\parallel(x,z,l_+)\phi_\pi(x)\phi_B^+(l_+)$$

$$\frac{m_B}{m_B+m_P}f_T(q^2)=\left(C_1^{(t)}-C_2^{(t)}-C_4^{(t)}\right)\zeta^P \tag{4.73}$$

$$+N_0\int_0^1 dxdl_+\left\{-\left[B_1^{(t)}-B_2^{(t)}-2B_3^{(t)}+B_4^{(t)}\right]\delta(x-z)-\frac{2E}{m_b}[B_{15}^{(t)}+B_{16}^{(t)}-B_{18}^{(t)}]\right]J_\parallel(x,z,l_+)\phi_B^+(l_+)\phi(x)\,,$$

with $N_0=f_Bf_Pm_B/(4E^2)$. The corresponding results for the $B\to V$ form factors have a similar form

$$\frac{m_B}{m_B+m_V}V(q^2)=C_1^{(v)}\zeta_\perp^V$$

$$-N_\perp\int_0^1 dxdzdl_+\left[-\frac{1}{2}B_4^{(v)}\delta(x-z)+\frac{E}{m_b}(2B_{11}^{(v)}+B_{14}^{(v)})\right]J_\perp(x,z,l_+)\phi_B^+(l_+)\phi_\perp(x)$$

$$\frac{m_B+m_V}{2E}A_1(q^2)=C_1^{(a)}\zeta_\perp^V$$

$$-N_\perp\int_0^1 dxdl_+\left[-\frac{1}{2}B_4^{(a)}\delta(x-z)+\frac{E}{m_b}(2B_{11}^{(a)}+B_{14}^{(a)})\right]J_\perp(x,z,l_+)\phi_B^+(l_+)\phi_\perp(x)$$

$$A_0(q^2)=\left(C_1^{(a)}+\frac{m_B-E}{m_B}C_2^{(a)}+C_3^{(a)}\right)\zeta_\parallel^V \tag{4.74}$$

$$+N_\parallel\int_0^1 dxdzdl_+\left\{\left[\frac{m_B-2E}{m_B}B_1^{(a)}+\frac{m_B-E}{m_B}B_2^{(a)}+B_3^{(a)}\right]\delta(x-z)\right.$$

$$\left.-\frac{2E}{m_b}\left[-B_{11}^{(a)}+\frac{m_B-E}{m_B}B_{12}^{(a)}+B_{13}^{(a)}\right]\right\}\phi_B^+(l_+)\phi_\parallel(x)$$

$$\frac{m_BE}{m_B+m_V}A_2(q^2)-\frac{1}{2}(m_B+m_V)A_1(q^2)=-\left(C_1^{(a)}+\frac{E}{m_B}C_2^{(a)}+C_3^{(a)}\right)m_V\zeta_\parallel^V \tag{4.75}$$

$$+m_VN_\parallel\int_0^1 dxdzdl_+\left\{\left[\frac{m_B-2E}{m_B}B_1^{(a)}-\frac{E}{m_B}B_2^{(a)}-B_3^{(a)}\right]\delta(x-z)\right.$$

$$\left.-\frac{2E}{m_b}\left[B_{11}^{(a)}-\frac{E}{m_B}B_{12}^{(a)}-B_{13}^{(a)}\right]\right\}J_\parallel(x,z,l_+)\phi_B^+(l_+)\phi_\parallel(x)$$

$$T_1(q^2)=\frac{m_B}{2E}T_2(q^2)=\left\{C_1^{(t)}-\frac{m_B-E}{m_B}C_2^{(t)}-C_3^{(t)}\right\}\zeta_\perp^V \tag{4.76}$$

$$-\frac{1}{2}N_\perp\int_0^1 dxdzdl_+\left\{\left[B_5^{(t)}+\frac{m_B-E}{m_B}B_6^{(t)}\right]\delta(x-z)\right.$$

$$\left.-\frac{2E}{m_b}\left[2B_{15}^{(t)}+2B_{17}^{(t)}+B_{19}^{(t)}+B_{21}^{(t)}+\frac{m_B-E}{m_B}(2B_{16}^{(t)}+B_{20}^{(t)})\right]\right\}J_\perp(x,z,l_+)\phi_B^+(l_+)\phi_\perp(x)$$

$$ET_3(q^2)-\frac{m_B}{2}T_2(q^2)=-(C_1^{(t)}-C_2^{(t)}-C_4^{(t)})m_V\zeta_\parallel^V \tag{4.77}$$

$$+m_VN_\parallel\int_0^1 dxdzdl_+\left\{\left[B_1^{(t)}-B_2^{(t)}-2B_3^{(t)}+B_4^{(t)}\right]\delta(x-z)\right.$$

$$\left.+\frac{2E}{m_b}(B_{15}^{(t)}+B_{16}^{(t)}-B_{18}^{(t)})\right\}J_\parallel(x,z,l_+)\phi_B^+(l_+)\phi_\parallel(x)$$

where $N_\perp=m_B/(4E^2)f_Bf_V^T$ and $N_\parallel=m_B/(4E^2)f_Bf_V$. To all orders in $\alpha_s(\Lambda m_b)$ there are only 2 jet functions. One of them $J_\parallel$ contributes to $B\to P,V_\parallel$, and other one $J_\perp$ contributing only to $B\to V_\perp$. At tree level they are equal $J_{\parallel,\perp}(z,x,l_+)=\frac{\pi\alpha_sC_F}{N_c}\frac{1}{\bar{x}l_+}\delta(x-z)$, but in general they are different.

The Wilson coefficients satisfy $C_{1-3}^{(v)} = C_{1-3}^{(a)}$ and $B_{1-4}^{(v)} = B_{1-4}^{(a)}$ in the NDR scheme. Reparameterization invariance constrains them as $B_{1-3}^{(v,a,t)} = C_{1-3}^{(v,a,t)}$, $B_4^{(v,a)} = -2C_3^{(v,a)}$, $B_4^{(t)} = C_4^{(t)}$, $B_5^{(t)} = 2C_3^{(t)}$, $B_6^{(t)} = -2C_4^{(t)}$ [157, 150]. At tree level they are given by $C_1^{(v,a,t)} = 1$, $B_1^{(v,a,t)} = 1$, $B_{13}^{(v,a)} = -1$, $B_{17}^{(t)} = 1$.

From the above discussion it is clear that while SCET does not allow us to calculate the shape or normalization of the heavy-light form factors, it does give predictions amongst different form factors. In particular, relations between form factors arising in decays of B mesons via tensor currents, such as $B \to K^*\gamma$ and form factors required for the extraction of $|V_{ub}|$ can be derived. This allows to get the necessary information about the form factors from decays which are independent of $|V_{ub}|$. First steps at understanding quark mass effects in SCET have been carried out in [158]. Model independent relations that survive including the leading SU(3) violation in the light-cone distribution functions were given in [159].

The generic structure of the SCET factorization theorem is

$$f_i(q^2) = C_{ij}^{(0)}(Q)\, \zeta_j^M(Q\Lambda, \Lambda^2) + \int dx dz dk_+ C_{ij}^{(1)}(z,Q) J_j(z,x,k_+) \phi_B^+(k_+) \phi_j^M(x)\,. \tag{4.78}$$

Both terms in the SCET factorization formula scale like $(\Lambda/Q)^{3/2}$, such that their relative numerical contributions could be comparable. In the absence of the factorizable term, all 10 $B \to P, V$ form factors are determined by only three unknown "soft" form factors $\zeta^P, \zeta_\parallel^V, \zeta_\perp^V$, and thus satisfy symmetry relations [143, 146, 135]. In general they are however broken by the factorizable terms, which are not spin-symmetric.

Two of these symmetry relations turn out to remain valid, even after including the factorizable terms. This can be seen by a simple helicity argument [160] or by examining the factorization theorems

$$V(q^2) = \frac{(m_B + m_V)^2}{2m_B E} A_1(q^2)\,, \qquad T_1(q^2) = \frac{m_B}{2E} T_2(q^2)\,. \tag{4.79}$$

These relations are broken only by power corrections of $O(\Lambda/Q)$, which can, however, be numerically sizable $\sim 30\%$.

An important point is related to the convergence of the convolutions appearing in the factorizable term in Eq. (4.78). This issue is connected to the asymptotic behaviour of the light-cone wave function $\phi_B(k_+)$ and of the jet functions $J(x,z,k_+)$, issues which were studied in Refs. [153] and [152], respectively.

We comment next on the important issue of the relative size of the two terms in Eq. (4.78). Due to the explicit factor of $\alpha_s(\mu_c)$ (with $\mu_c^2 \sim Q\Lambda$) appearing in the jet function J, one might be led to take the point of view that the factorizable term is a small correction to the nonfactorizable contribution [146], and therefore the symmetry relations would be satisfied to a good approximation. However, this point of view neglects the possibility of similar $O(\alpha_s(\Lambda Q))$ terms being present in the ζ functions, which in principle receive also contributions from the collinear scale $\mu_c^2 \sim Q\Lambda$. Recently, in Ref. [154] it was argued that no effects from the collinear scale are present in ζ, which would indicate that the first term in Eq. (4.78) dominates. However, a more definitive conclusion requires the resummation of the Sudakov logs present in the coefficients $C^{(0,1)}$.

An extreme case of Sudakov suppression is assumed in the pQCD approach [161, 162]. Here one takes the point of view that the nonfactorizable term is suppressed as $m_b \to \infty$ by the Sudakov logs contained in the Wilson coefficients $C_{ij}^{(0)}$, which effectively renders the form factors calculable in perturbation theory. Such a conclusion could be invalidated by the fact that similar Sudakov logs (not yet computed) are present also in the factorizable term $C_{ij}^{(1)}$. See also Ref. [163] for a detailed discussion of Sudakov effects in this context.

In the following we will not make any assumptions about the relative size of the two terms in Eq. (4.78). Eventually the soft form factors ζ will be obtained from model computations or lattice QCD. However, even in the absence of such information, the factorization results have significant predictive power. For example, using as input the form factor $f_+(q^2)$ as measured in $B \to \pi e \nu$, the remaining $B \to \pi$ form factors can be computed using the explicit form of the factorization formulae in Ref. [150] and $\phi_B(k_+), \phi_\pi(x)$.

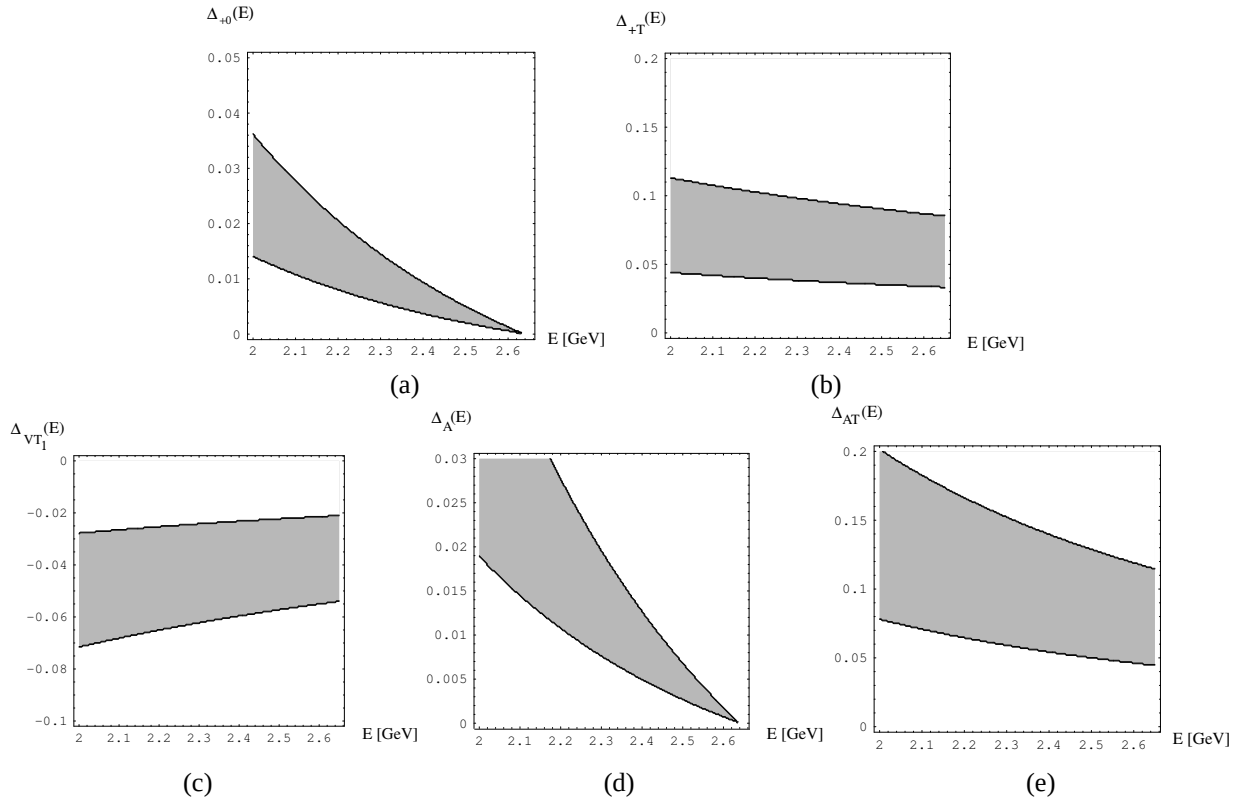

Figure 4-5. *Symmetry breaking corrections to the $B \to \pi$ form factor relations showing (a) $\Delta_{+0}(E)$ and (b) $\Delta_{+T}(E)$, and to the $B \to \rho$ form factor relations showing (c) $\Delta_{VT_1}(E)$, (d) $\Delta_A(E)$ and (e) $\Delta_{TA}(E)$. The shaded region corresponds to the variation in the collinear scale μ_c used to define the jet function between 0.54 and 2.18 GeV, with the choices of hadronic parameters defined in the text.*

To illustrate this approach, we present explicit results for form factor combinations from which the soft matrix elements ζ cancel out, and are therefore calculable. Working at tree level in matching at the scale Q, but to all orders in the jet function, there are 2 such combinations for the $B \to P$ form factors

$$\Delta_{+0}(E) = \frac{m_B}{2E} f_0(E) - f_+(E)\,, \qquad \Delta_{+T}(E) = f_+(E) - \frac{m_B}{m_B + m_P} f_T(E)\,. \tag{4.80}$$

and 3 combinations for the $B \to V$ form factors

$$\begin{aligned} \Delta_{VT_1}(E) &= \frac{m_B}{m_B + m_V} V(E) - T_1(E)\,, \\ \Delta_A(E) &= m_V A_0(E) + \frac{m_B E}{m_B + m_V} A_2(E) - \frac{1}{2}(m_B + m_V) A_1(E) \\ \Delta_{AT}(E) &= m_V A_0(E) + E T_3(E) - \frac{m_B}{2} T_2(E)\,. \end{aligned} \tag{4.81}$$

We show in Fig. 4-5 illustrative results for these form factor combinations, working at tree level in matching at the scale Q and in the jet function. [10] In computing these results we used $f_B = 180$ MeV, $f_\pi = 131$ MeV, $f_\rho = 210$ MeV, $f_\rho^\perp(1.47\text{ GeV}) = 152$ MeV, $\langle k_+^{-1} \rangle_B = (350\text{ MeV})^{-1}$ and $a_2^\pi = a_2^\rho = a_2^{\rho\perp} = 0.2$.

[10] Editors note: Recently one-loop corrections to the jet functions became available [164], which substantially reduce the scale dependence shown in Fig. 4-5.

4.5.4 Form factor relations from HQET

≻D. Pirjol≺

In the low recoil region for the final meson, corresponding to maximal $q^2 \sim (m_B - m_M)^2$, heavy quark symmetry can be applied to describe the transition process. For the heavy-to-heavy form factors, such as those parameterizing $B \to D^{(*)}\ell\nu$ decays, the normalization at zero recoil is fixed from the symmetry, with the leading power corrections of order Λ/m_b vanishing for certain form factors [165]. No such information is available for heavy-to-light form factors, although some results can be established in a model-independent way.

The heavy mass scaling of the form factors can be straightforwardly derived from the mass dependence of the $|B\rangle$ states implicit in their relativistic normalization $|\overline{B}(p)\rangle \sim \sqrt{m_b}$. These relations are simpler when expressed in terms of the form factors defined in [166] (as opposed to the more commonly used form factors used in the preceding section). The scaling of the $B \to P$ form factors is

$$f_+(E) + f_-(E) \sim m_b^{-1/2}\,, \qquad f_+(E) - f_-(E) \sim m_b^{1/2}\,, \qquad s(E) \sim m_b^{1/2} \tag{4.82}$$

and for the $B \to V$ form factors

$$\begin{aligned} f(E) \sim m_b^{1/2}\,, \qquad & g(E) \sim m_b^{-1/2}\,, \quad a_+(E) - a_-(E) \sim m_b^{-1/2}\,, \quad a_+(E) + a_-(E) \sim m_b^{-3/2}\,, \\ & g_+(E) - g_-(E) \sim m_b^{1/2}\,, \quad g_+(E) + g_-(E) \sim m_b^{-1/2}\,, \quad h(E) \sim m_b^{-3/2} \end{aligned} \tag{4.83}$$

We take the argument of the form factors as the light meson $M = P, V$ energy E rather than $q^2 = m_B^2 + m_M^2 - 2m_B E$. In the low recoil region it scales as $E \sim \Lambda$.

Heavy quark spin symmetry implies also the existence of symmetry relations among form factors at fixed E [166, 167]. There is one such relation for the $B \to P$ form factors

$$\text{(P-1)}: f_+(E) - f_-(E) - 2m_B s(E) \sim O(m_b^{-1/2}) \tag{4.84}$$

and three relations for the $B \to V$ form factors

$$\text{(V-1)}: \quad g_+(E) - g_-(E) + 2m_B g(E) \sim O(m_b^{-1/2}) \tag{4.85}$$

$$\text{(V-2)}: \quad g_+(E) + g_-(E) - 2Eg(E) - \frac{1}{m_B} f(E) \sim O(m_b^{-3/2}) \tag{4.86}$$

$$\text{(V-3)}: \quad a_+(E) - a_-(E) - 2g(E) + 2m_B h(E) \sim O(m_b^{-3/2})\,. \tag{4.87}$$

The leading power corrections to the heavy quark symmetry relations Eqs. (4.84)-(4.87) are also known from Ref. [168]. Contrary to naive expectations, they have a very simple form and depend only on the form factors of the dimension-4 currents $\overline{q} i D_\mu (\gamma_5) b$. We discuss in the following one possible application of these symmetry relations, and give a brief description of the Λ/m_b improved form factor relations.

The HQET symmetry relations are relevant for a method discussed in Refs. [169, 170] for determining the CKM matrix element $|V_{ub}|$ from exclusive B decays. This method combines data on semileptonic $B \to \rho\ell\nu$ and rare radiative decays $B \to K^*\ell^+\ell^-$ near the zero recoil point, and $|V_{ub}|$ is extracted from the ratio [169, 170]

$$\frac{\mathrm{d}\Gamma(B \to \rho e\nu)/\mathrm{d}q^2}{\mathrm{d}\Gamma(B \to K^*\ell^+\ell^-)/\mathrm{d}q^2} = \frac{8\pi^2}{\alpha^2} \frac{|V_{ub}|^2}{|V_{tb}V_{ts}^*|^2} \frac{1}{|C_9|^2 + |C_{10}|^2} \frac{|A_1^{B\to\rho}(q^2)|^2}{|A_1^{B\to K^*}(q^2)|^2} \frac{(m_B + m_\rho)^2}{(m_B + m_{K^*})^2} \frac{1}{1 + \Delta(q^2)} \tag{4.88}$$

The parameter $\Delta(q^2)$ contains the contribution of the radiative penguin O_7 to the $B \to K^* e^+ e^-$ amplitude, and is computable at leading order in $1/m_b$ with the help of the symmetry relations Eqs. (4.85) and (4.86). The SU(3) breaking in the ratio of form factors on the right-hand side $A_1^{B\to\rho}(q^2)/A_1^{B\to K^*}(q^2)$ can be fixed using a Grinstein-type double ratio [171] and data on semileptonic $D \to K^*(\rho)e\overline{\nu}$ decays.

The leading power correction to the symmetry relations Eqs. (4.84)-(4.87) depends on the $B \to M$ matrix elements of dimension-4 currents. They are parameterized in terms of 2 form factors for $B \to P$

$$\langle P(p')|\bar{q} i \overleftarrow{D}_\mu h_v|\overline{B}(p)\rangle = \delta_+(E)(p+p')_\mu + \delta_-(E)(p-p')_\mu \tag{4.89}$$

and four form factors for $B \to V$ transitions

$$\langle V(p',\eta)|\bar{q} i \overleftarrow{D}_\mu b|\overline{B}(p)\rangle = d(E) i\epsilon^{\mu\nu\rho\sigma}\eta^*_\nu p_\rho p'_\sigma \tag{4.90}$$

$$\langle V(p',\eta)|\bar{q} i \overleftarrow{D}_\mu \gamma_5 b|\overline{B}(p)\rangle = d_1(E)\eta^*_\mu + d_+(E)(\eta^*\cdot p)(p_\mu + p'_\mu) + d_-(E)(\eta^*\cdot p)(p_\mu - p'_\mu)\,. \tag{4.91}$$

In the heavy quark limit, not all these form factors are independent; using the constraint $\not{v} h_v = h_v$ and the equation of motion for the heavy quark field $iv\cdot D h_v = 0$, the number of independent subleading form factors is reduced to one for $B \to P$, and 3 for $B \to V$.

Furthermore, the $B \to \pi, K$ subleading form factors $\delta_\pm(E)$ can be computed in a model-independent way at leading order in the heavy mass and the chiral expansion [172, 168]. On the other hand, the corresponding $B \to V$ form factors have to estimated with the help of quark models or lattice QCD.

The improved HQET symmetry relations can be obtained from operator identities of the type

$$i\partial^\nu(\bar{q} i\sigma_{\mu\nu} b) = -(m_b + m_q)\bar{q}\gamma_\mu b - 2\bar{q} i\overleftarrow{D}_\mu b + i\partial_\mu(\bar{q} b)\,, \tag{4.92}$$

which follows from a simple application of the QCD equations of motion for the quark fields. Taking the $B \to V$ matrix element one finds the exact relation

$$g_+(q^2) = -(m_b + m_q) g(q^2) + d(q^2)\,. \tag{4.93}$$

Counting powers of m_b and keeping only the leading order terms reproduces the symmetry relation (V-1) + (V-2) among vector and tensor form factors [166, 167]. Keeping also the subleading terms of $O(m_b^{-1/2})$ gives the improved version of the form factor relation Eq. (4.85)

$$\text{(V-1')}: g_+(E) - g_-(E) + 2m_B g(E) = -2(E-\overline{\Lambda})g(E) - \frac{1}{m_B} f(E) + 2d(E) + O(m_b^{-3/2}) \tag{4.94}$$

Similar improved versions of the other symmetry relations can be found in Ref. [168]. We quote here only the analog of (V-2) Eq. (4.86), which has implications for the method of determining $|V_{ub}|$ using exclusive decays (see Eq. (4.88))

$$\begin{aligned}\text{(V-2')}: \quad & g_+(E) + g_-(E) - 2Eg(E) - \frac{1}{m_B} f(E) = \frac{2}{m_B}\{(2E^2 - m_V^2) - E(\overline{\Lambda} - m_q)\} g(E) \\ & + \frac{1}{m_B^2}(2E - \overline{\Lambda} - m_q) f(E) - 2\frac{E}{m_B} d(E) + \frac{2}{m_B^2} d_1(E) + O(m_b^{-5/2})\end{aligned} \tag{4.95}$$

The improved symmetry relation Eq. (4.94) can be used to determine the tensor form factor $g_+(q^2)$ in terms of the vector and axial form factors $f(q^2), g(q^2)$ as measured in exclusive semileptonic $B \to V\ell\nu$ decays. Combining the symmetry relations Eqs. (4.85), (4.86) in order to extract g_+ at next-to-leading order in Λ/m_b requires the knowledge of the leading correction of $O(m_b^{-1/2})$ to Eq. (4.85) (since the latter is of the same order as the terms shown on the RHS of Eq. (4.86)).

The relations Eqs. (4.94) and (4.95) were used in Ref. [173] to estimate the subleading corrections of $O(\Lambda/m_b)$ to the $|V_{ub}|$ determination using Eq. (4.88). These corrections can be as large as 5%, and are dominated by the unknown form factor $d_1(q^2)$ of $\bar{q} i\overleftarrow{D}_\mu\gamma_5 b$. Quark model estimates of this matrix element suggest that the correction is under a few percent, and more precise determinations (lattice QCD) could help to reduce or eliminate this source of uncertainty.

The rare B decays $b \to s\gamma$ and $b \to se^+e^-$ receive significant long-distance effects arising from $c\bar{c}$ and $u\bar{u}$ quark loops. In Ref. [174] it was proposed to treat these effects in the small recoil region using an operator product expansion in $1/Q$, combined with HQET. This method is similar to the computation of $e^+e^- \to$ hadrons, and allows model-independent predictions of the e^+e^- invariant spectrum in $B \to K^{(*)}\ell^+\ell^-$ decays in the small recoil region.

The results of [174] are applied to a method for determining V_{ub} from combined exclusive B decays, first proposed in [175, 176]. This method is improved here in two ways: a) combining the OPE method with recent results in the theory of $b \to se^+e^-$ decays, the complete next-to-leading perturbative corrections can be included; b) power corrections of order Λ/Q and m_c^2/m_b^2 are included with the help of corrected heavy quark symmetry relations derived earlier in [177, 178]. The resulting uncertainty in $|V_{ub}|$ from this determination is dominated by scale dependence and is of the order of 15%.

4.5.5 SU(3) breaking in $B \to \rho/K^*\gamma, \rho/K^*\ell^+\ell^-$, double ratios, and $|V_{td}/V_{ts}|$

≻B. Grinstein≺

The radiative decays $b \to d\gamma$ and $b \to s\gamma$ are dominated by the short-distance top-quark penguin graph. Using SU(3) symmetry to relate the relevant form factors, it has been suggested to use a measurement of the ratio

$$\frac{\Gamma(B \to \rho\gamma)}{\Gamma(B \to K^*\gamma)} = \left|\frac{V_{td}}{V_{ts}}\right|^2 R_{\mathrm{SU}(3)}(1+\Delta) \tag{4.96}$$

to determine the CKM matrix element V_{td}. There are two theoretical sources of uncertainty in such a determination, coming from long distance effects (parameterized by Δ) and SU(3) breaking in the form factor and kinematics (contained in $R_{\mathrm{SU}(3)}$). In Ref. [179] the different sources of long-distance contributions to the decays in Eq. (4.96) have been classified using a diagrammatic approach, essentially equivalent to a SU(3) flavor analysis.

The figure above defines the different long distance contributions as annihilation (A), W exchange (E), penguin ($P_q^{(i)}$), penguin annihilation (PA) and gluonic t-penguin ($M^{(i)}$); the crosses indicate where the photon emission may take place at leading order in $1/m_b$, and the superscripts on P_q and M refer to whether the photon is emitted from the quark in the loop ("(1)") or not ("(2)"). Particular processes are affected by some, but not necessarily all, of these long distance "contamination." For example, the weak annihilation amplitude A contribute only to the $B^\pm$ radiative decays,

$$\mathcal{A}(B^- \to \rho^-\gamma) = \lambda_u^{(d)}(P_u^{(1)} + Q_u P_u^{(2)} + A) + \lambda_c^{(d)}(P_c^{(1)} + Q_u P_c^{(2)}) + \lambda_t^{(d)}(\hat{P}_t + Q_u M^{(2)}), \tag{4.97}$$

$$\mathcal{A}(B^- \to K^{*-}\gamma) = \lambda_u^{(s)}(P_u^{(1)} + Q_u P_u^{(2)} + A) + \lambda_c^{(s)}(P_c^{(1)} + Q_u P_c^{(2)}) + \lambda_t^{(s)}(\hat{P}_t + Q_u M^{(2)}), \tag{4.98}$$

while W-exchange contributes only to $\overline{B}^0$ decays,

$$\sqrt{2}\mathcal{A}(\overline{B}^0 \to \rho^0\gamma) = \lambda_u^{(d)}(P_u^{(1)} + Q_d P_u^{(2)} - E - PA_u) + \lambda_c^{(d)}(P_c^{(1)} + Q_d P_c^{(2)} - PA_c) + \lambda_t^{(d)}(\hat{P}_t + Q_d M^{(2)}), \tag{4.99}$$

$$\sqrt{6}\mathcal{A}(\overline{B}^0 \to \phi^{(8)}\gamma) = -\lambda_u^{(d)}(P_u^{(1)} + Q_d P_u^{(2)} + E + PA_u) - \lambda_c^{(d)}(P_c^{(1)} + Q_d P_c^{(2)} + PA_c) - \lambda_t^{(d)}(\hat{P}_t + Q_d M^{(2)}). \tag{4.100}$$

Perhaps more interestingly, some amplitudes contain no annihilation or W exchange contamination:

$$\mathcal{A}(\overline{B}^0 \to \overline{K}^{*0}\gamma) = \lambda_u^{(s)}(P_u^{(1)} + Q_d P_u^{(2)}) + \lambda_c^{(s)}(P_c^{(1)} + Q_d P_c^{(2)}) + \lambda_t^{(s)}(\hat{P}_t + Q_d M^{(2)}), \tag{4.101}$$

$$\mathcal{A}(\overline{B}_s \to K^{*0}\gamma) = -\lambda_u^{(d)}(P_u^{(1)} + Q_s P_u^{(2)}) - \lambda_c^{(d)}(P_c^{(1)} + Q_s P_c^{(2)}) - \lambda_t^{(d)}(\hat{P}_t + Q_s M^{(2)}). \tag{4.102}$$

We have used the shorthand $\lambda_{q'}^{(q)} = V_{q'b}V_{q'q}^*$ and, noting that P_t and $M^{(1)}$ appear always in the same combination, we have defined $\hat{P}_t = P_t + M^{(1)}$.

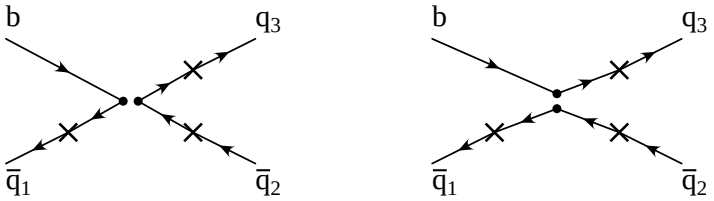

Weak Annihilation $A^{(i)}$ W-exchange $E^{(i)}$

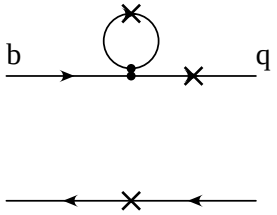

Penguin $P^{(1)}_{d,s}$ and $P^{(2)}_{u,c}$

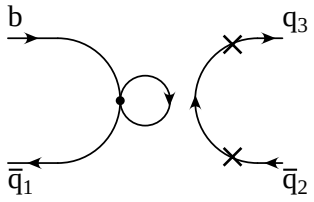

Penguin Annihilation PA

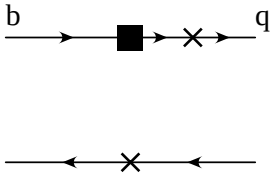

Gluonic t-Penguin $M^{(1)}$ and $M^{(2)}$

Photon helicity	$\lvert P_{t\lambda}\rvert$	$\lvert P_{c\lambda}\rvert$	$\lvert P_{u\lambda}\rvert$	$\lvert A_\lambda\rvert$	$\lvert E_\lambda\rvert$
$\lambda = L$	1.8	0.16	0.03	0.6	0.05
$\lambda = R$	0	0.04	0.007	0.07	0.007

The table above shows an estimate of the individual amplitudes (in units of 10^{-6} MeV) contributing to $B \to \rho\gamma$ decays for different photon helicities. The $V-A$ structure of charged currents in the standard model gives a strong suppression to right handed helicities. This could be used as a probe of New Physics. The dominant amplitudes, with left handed photons, show an interesting pattern of magnitudes, $|P_{t\lambda}| > |A_\lambda| > |P_{c\lambda}| > |E_\lambda| \approx |P_{u\lambda}|$. As expected, the short distance contribution — the top-penguin — dominates.

Including the CKM factors, the weak annihilation amplitude contributes about 15% to the $B \to \rho\gamma$ decay amplitude. It is possible to show that the annihilation amplitude factorizes (to leading order in $1/m_b$) and the relevant hadronic matrix element can be related to the measurable decay rate of the radiative leptonic decay $B \to \gamma e\overline{\nu}$. Although this amplitude can be estimated theoretically [180], for a model-independent determination of $|V_{td}|$ it is preferable to use measurements of this process.

In order to determine the CKM ratio $|V_{td}/V_{ts}|$ the leading top-penguin amplitude, can be determined in terms of the form factors for $B \to \rho\ell\nu$ semileptonic decays using the form factor relations at large recoil (see the appropriate section in this report).

Keeping the dominant contributions in Eqs. (4.97)-(4.98) one can write for the amplitudes of the radiative decays

$$\mathcal{A}(B^- \to \rho^-\gamma_L) = V_{td}V_{tb}^* P(1 + \varepsilon_A e^{i(\alpha+\phi_A)}) \tag{4.103}$$

$$\mathcal{A}(B^- \to K^{*-}\gamma_L) = V_{td}V_{tb}^* P' \tag{4.104}$$

where the penguin amplitudes P, P' include the effects of charm loops. The weak annihilation amplitude is negligible in $B^- \to K^{*-}\gamma$ because of its small CKM coefficient. Using these expressions, the factors appearing in the ratio Eq. (4.96) are given by

$$R_{\mathrm{SU}(3)} = \frac{|P|^2}{|P'|^2} \simeq \left(\frac{g_+^{(B\rho)}(0)}{g_+^{(BK^*)}(0)} \right)^2 = 0.76 \pm 0.22\,, \qquad \Delta = 2\varepsilon_A \cos\phi_A \cos\alpha + \varepsilon_A^2\,, \tag{4.105}$$

where the tensor form factor $g_+(q^2)$ is defined in Section 4.5.3. Model estimates give for the weak annihilation contribution $\varepsilon_A = 0.12$ which leads to an error of 12% in V_{td}. The SU(3) breaking factor $R_{\mathrm{SU}(3)}$ has been computed using QCD sum rules and lattice QCD. The result quoted above is from the UKQCD collaboration [181].

The issue of SU(3) breaking in heavy-light form factors is also relevant for a method for determining V_{ub} from rare radiative and semileptonic B decays in the low recoil region. This has been discussed in some detail in Section 4.5.4; we comment here on the SU(3) breaking effects. This method requires the ratio of exclusive decay rates [182, 176, 183]

$$\frac{\mathrm{d}\Gamma(\overline{B} \to \rho e\nu)/\mathrm{d}q^2}{\mathrm{d}\Gamma(\overline{B} \to K^*\ell^+\ell^-)/\mathrm{d}q^2} = \frac{|V_{ub}|^2}{|V_{tb}V_{ts}^*|^2} \frac{8\pi^2}{\alpha^2} \frac{1}{|C_9|^2 + |C_{10}|^2} \frac{|f^{B\to\rho}(y)|^2}{|f^{B\to K^*}(y)|^2} \frac{1}{1+\Delta(y)} \tag{4.106}$$

where $y = E_V/M_V$ and q^2 is the invariant mass of the lepton pair. C_i are coefficients of interactions in the effective Hamiltonian for $b \to see$ decays [184, 185, 186, 187]. In the SU(3) symmetry limit the ratio $f^{B\to\rho}(y)/f^{B\to K^*}(y)$ is unity. Since SU(3) is violated at the 30% level, a better approach is to measure the corresponding ratio in D decays. The double ratio

$$R(y) \equiv \frac{|f^{B\to\rho}(y)/f^{B\to K^*}(y)|}{|f^{D\to\rho}(y)/f^{D\to K^*}(y)|} = 1 + \mathcal{O}\left(\frac{m_s}{\Lambda_\chi} (\frac{\Lambda}{m_c} - \frac{\Lambda}{m_b}) \right) \tag{4.107}$$

is protected *both* by heavy quark symmetry and by SU(3), so even if each of these is good only to about the 30% level, the ratio is unity to better than 10%. Calculations in heavy meson chiral perturbation theory [188, 189] show that double ratios are typically protected at the few percent level [132, 190, 191].

To summarize, the leading uncertainty in the extraction of CKM ratios from $\Gamma(B^- \to \rho^-\gamma_L)/\Gamma(B^- \to K^{*-}\gamma)$ is due to SU(3) symmetry breaking. The largest long distance correction, of order 15% in the amplitude, is from weak-annihilation, but can be computed reliably by measuring the photon energy spectrum in $B \to e\nu\gamma$. Form factor uncertainties are eliminated in $B \to K^* e^+ e^-$ using double ratios with the corresponding D decays. A method for determining V_{ub} using these decays contains SU(3) breaking effects which can be eliminated by combining B and D decays.

4.5.6 Experimental prospects

≻– D. del Re –≺

Exclusive charmless semileptonic B decays have been previously studied by the CLEO [192], Belle [193] and *BABAR* [194] collaborations. All these measurements are performed by the reconstruction of one half of the event. One hard lepton in the event is identified and the charmless meson present in the semileptonic decay is reconstructed. Requirements on the missing mass of the event are also imposed. Since these requirements alone do not sufficiently reduce the background, significant restrictions on the lepton energy and other variables are applied. As a consequence, an extrapolation to the full phase space is needed thereby introducing large theoretical systematic uncertainties, that are already bigger than the statistical errors. If higher integrated luminosities are recorded, this approach will not allow us to improve the error on these branching ratios and on $|V_{ub}|$.

The recoil method can thus play an important role in the study of exclusive charmless semileptonic decays in the Super B Factory era. This approach assures a sample with a much higher purity than in previous measurements. Since the level of background is low, no kinematic cuts are required, and nearly the full phase space is analyzed. Thus,

the dependence on form factors and on the different decay models in the extraction of the branching ratios is largely eliminated. In terms of total error, the recoil method will surpass the traditional approach for an integrated luminosity of about 500 fb^{-1}, well before the projected advent of a Super B Factory.

$B \to X_u \ell \nu$ decays

In the following study, we propose a method very similar to the inclusive approach presented in section 4.4.3. A preliminary result based on this analysis has been already presented in [195]. As in the inclusive case, we select events with one or more leptons in the recoil. A very loose cut on the lepton momentum is applied ($p^* > 1$ GeV). We also apply cuts on the charge conservation and missing mass squared of the event. We inclusively reconstruct the invariant mass of the X system and apply additional constraints on charged particle multiplicity, in order to select specific resonances. For instance, we require no tracks in the $B^- \to \pi^0 \ell^+ \nu$ case and two tracks for $B^- \to \rho^0 \ell^+ \nu$. Moreover, we apply cuts based on the neutral energy in the recoil to separate resonances with identical charged multiplicities (such as ρ^0 and ω).

This technique selects a very clean sample of exclusive charmless decays. In Fig. 4-6 the result of a detailed generic Monte Carlo event sample of an equivalent integrated luminosity of $500\,\text{fb}^{-1}$ is shown for the modes $B^\pm \to \pi^0 l\nu$, $B^\pm \to \omega l\nu$ and $B^\pm \to$ "ρ^0" $l\nu$ (here "ρ^0" indicates a combination of π^+ π^- with $m_{\pi^+\pi^-}$ in the window $0.65 < m_{\pi^+\pi^-} < 0.95\,\text{GeV}/c^2$ at generator level). The signal-to-background ratio is much better than in the standard exclusive analyses. The $B^\pm \to \pi^0 l\nu$ case, for instance, is basically background-free. A projection of the total error

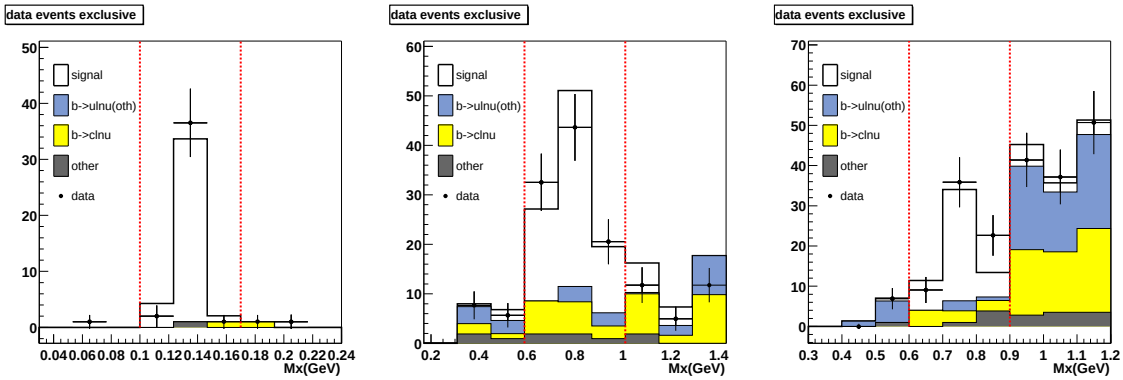

Figure 4-6. *Measurement of exclusive charmless semileptonic decays in the recoil of a fully reconstructed hadronic B decay (detailed MC simulation for 500 fb^{-1}). Projections in the m_X variable of the result. Vertical dotted lines represent the signal region. The plots show $B^\pm \to \pi^0 l\nu$ (left), $B^\pm \to$ "ρ^0" $l\nu$ (middle), and $B^\pm \to \omega l\nu$ (right).*

on the exclusive branching ratio as a function of the accumulated luminosity is shown in Fig. 4-7 for $B^\pm \to \pi^0 l\nu$. A systematic uncertainty of 3% for $B^\pm \to \pi^0 l\nu$ has been assumed. The extrapolation indicates how the error can be significantly reduced at a Super B Factory .

A study of the kinematic quantities can also be performed, as has been done by the CLEO collaboration [192], but the recoil approach offers the advantage of analyzing the full phase space. In Fig. 4-8 the measured q^2 spectrum for the $\overline{B}^0 \to \pi^+ \ell^- \nu$ case on a MC sample equivalent to an equivalent integrated luminosity of $2\,\text{ab}^{-1}$ is compared with the distribution expected by using different models. With these statistics it is possible to have sufficient sensitivity to reject certain models. However, as mentioned in Section 4.5.2, lattice QCD should provide model-independent calculations for form factors on a timescale well-suited for this type of analysis.

This method can be further improved by performing a purely exclusive analysis on the recoil, and reconstructing the resonances, instead of inclusively reconstructing the X system. A gain in efficiency is achievable using this technique, especially in $B^+ \to \pi^0 \ell^+ \nu$.

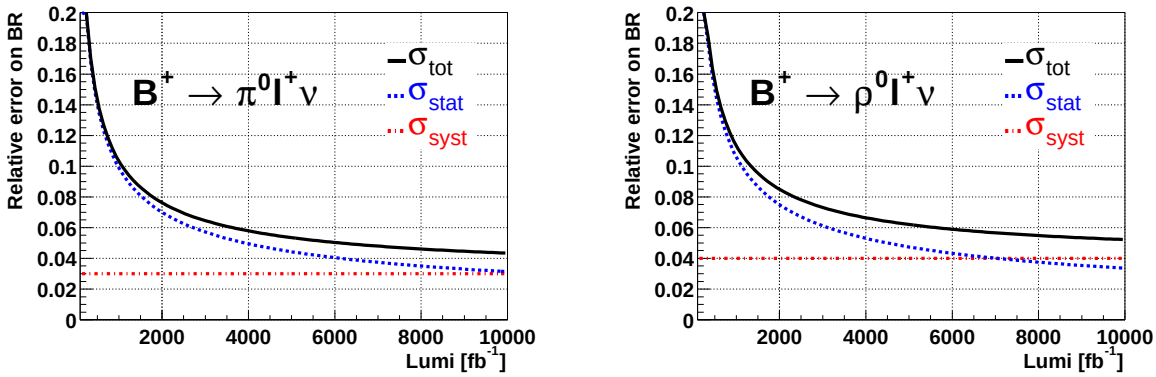

Figure 4-7. *Projections of the error on the exclusive branching ratio as a function of integrated luminosity.*

$B \to X_u \tau \nu$ decays

The recoil technique, together with large data samples, also permits the study of more difficult exclusive decays, such as $B \to \pi\tau\nu$, which presents many additional challenges due the presence of a τ. First the branching ratio for this decay should be 6 times smaller than the equivalent e/μ decays. In addition, instead of electrons and muons which can be simply identified, we have τ leptons whose decays involve additional neutrinos, thus destroying the powerful constraint from the missing mass squared. Preliminary studies show that, since the discrimination from $b \to c\ell\nu$ is much less effective in this case, additional efforts are needed to reduce the charm background, and make the analyses feasible. Furthermore, the background from Cabibbo-favored semileptonic decays should be studied with a full MC simulation (to account for the presence of, *e.g.*, K_L^0 in these decays).

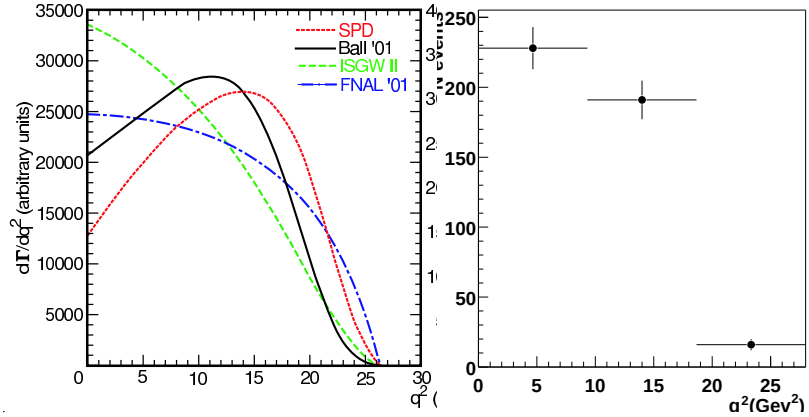

Figure 4-8. *Left: Theoretical expectations for the* q^2*-spectrum in* $\overline{B}^0 \to \pi^+\ell^-\nu$ *decays for different calculations [192]. Right: The* q^2*-spectrum in* $\overline{B}^0 \to \pi^+\ell^-\nu$ *decays (detailed MC simulation for an integrated luminosity of* $2\ ab^{-1}$*).*

4.6 Purely Leptonic Decays

4.6.1 $B \to \mu\overline{\nu}$ and $B \to \tau\overline{\nu}$ theory: f_B from lattice QCD

≻C. Bernard, S. Hashimoto, P. Mackenzie ≺

The estimates for future lattice precision presented in this section parallel those in Section 4.5.2 on semileptonic form factors. In addition to expected errors for the leptonic decay constants f_B, and f_{B_s}, we include estimates for errors on the combination relevant for B-$\overline{B}$ mixing, $f_B\sqrt{B_B}$, where B_B is the bag parameter for B mesons, as well as the ratios f_{B_s}/f_B and

$$\xi \equiv \frac{f_{B_s}\sqrt{B_{B_s}}}{f_B\sqrt{B_B}} \, .$$

As in Section 4.5.2, we assume three levels of computation, MILC0, MILC1, and MILC2, based on improved staggered simulations with $n_F = 3$ flavors of dynamical sea quarks.

Tables 4-6, 4-7, and 4-8 show estimates of precision attainable for lattice calculations with data sets MILC0, MILC1, and MILC2, respectively. As in Section 4.5.2, we give two alternatives for perturbative errors (one-loop and two-loop) and two alternatives for chiral extrapolations errors: (no) SχPT assumes that staggered chiral perturbation theory is (is not) useful.

Table 4-6. *Estimated percentage errors for form factors at MILC0 level: one to two years from the present. "Light q" includes light quark chiral and discretization errors. "Heavy Q" means heavy quark discretization errors.*

quantity	**statist.**	**scale**	**light** q		**heavy** Q	**pert. th.**	
			no SχPT	SχPT		1-loop	2-loop
f_B	3	2	5	2.5	3	7.5	2
$f_B\sqrt{B_B}$	4	2	5.5	3	3	8.5	2.5
f_{B_s}/f_B	1	–	5	2.5	1	–	–
ξ	2	–	5.5	3	1	–	–

Table 4-7. *Same as Table 4-6, but for MILC1 level: three to five years from the present.*

quantity	**statist.**	**scale**	**light** q		**heavy** Q	**pert. th.**	
			no SχPT	SχPT		1-loop	2-loop
f_B	2	1.5	3	1.5	2	7.5	2
$f_B\sqrt{B_B}$	3	2	3.5	2	2	8.5	2.5
f_{B_s}/f_B	0.8	–	3	1.5	0.8	–	–
ξ	2	–	3.5	2	1	–	–

Table 4.6.1 shows the total lattice errors of the leptonic decay constants (and related quantities) under various assumptions, together with our best guess of which alternatives are most likely to be realized in practice. It must be kept in mind that the errors themselves are uncertain, by a fractional amount which is at least $\sim 30\%$ and rises with time into the future.

Table 4-8. *Same as Table 4-6, but for MILC2 level: five to eight years from present.*

quantity	**statist.**	**scale**	**light** q		**heavy** Q	**pert. th.**	
			no SχPT	SχPT		1-loop	2-loop
f_B	1	1	2	1	1.5	7.5	2
$f_B\sqrt{B_B}$	1.3	2	2.5	1	1.6	8.5	2.5
f_{B_s}/f_B	0.5	–	2.5	1	0.5	–	–
ξ	1	–	3	1	0.6	–	–

Table 4-9. *Estimated total lattice errors under various assumptions. Where there are four entries per column they correspond to: (1)* **no** *SχPT and 1-loop perturbation theory, (2) SχPT and 1-loop perturbation theory, (3)* **no** *SχPT and 2-loop perturbation theory, and (4) SχPT and 2-loop perturbation theory. Where there are two entries per column the quantity is free from perturbative errors, and the entries correspond to: (1)* **no** *SχPT and and (2) SχPT. Our best guesses of which alternative will in fact be realized are surrounded with boxes.*

quantity	**now**	**1-2 yrs.** MILC0	**3-5 yrs.** MILC1	**5-8 yrs.** MILC2
f_B	15	10, 9, 7, 6	9, 8, 5, 4	8, 8, 4, 3
$f_B\sqrt{B_B}$	15-20	12, 11, 8, 7	10, 10, 6, 5	9, 9, 5, 4
f_{B_s}/f_B	6	5, 3	3, 2	3, 1
ξ	7	6, 4	4, 3	3, 1.5

4.6.2 Experimental prospects

≻M. Datta, T. Moore≺

The purely leptonic decays $B^+ \to \ell^+\nu_\ell$ have not yet been observed experimentally. These decays are highly suppressed in the Standard Model due to their dependence on $|V_{ub}|^2$. Furthermore, helicity suppression introduces a dependence on m_ℓ^2 where m_ℓ is the lepton mass. Assuming $|V_{ub}|$ = 0.0036 [196] and f_B = 198 MeV [197], the Standard Model prediction for the $B^+ \to \tau^+\nu_\tau$ branching fraction is roughly 1×10^{-4}. Due to helicity suppression, $B^+ \to \mu^+\nu_\mu$ and $B^+ \to e^+\nu_e$ are further suppressed by factors of 225 and 10^7, respectively. The Standard Model predictions have an uncertainty of about 50% from the uncertainties in $|V_{ub}|$ and f_B. The small Standard Model rate expected for $B^+ \to e^+\nu_e$ is even beyond the sensitivity of a Super B Factory . Although searches for $B^+ \to e^+\nu_e$ are still interesting as tests of New Physics, only the τ and muon modes are discussed below.

$B^+ \to \ell^+\nu_\ell$ decays produce a mono-energetic lepton in the B rest frame with a momentum given by

$$p_\ell = \frac{m_B^2 - m_\ell^2}{2m_B}. \tag{4.108}$$

In the case of $B^+ \to \mu^+\nu_\mu$, the muon momentum is approximately $m_B/2 = 2.645$ GeV/c, which provides a strong experimental signature. By contrast, the decay of the τ^+ lepton produced in $B^+ \to \tau^+\nu_\tau$ decays results in additional missing energy from the additional neutrino. The absence of strong kinematic constraints results in a more challenging experimental analysis. Thus, despite the larger branching fraction for $B^+ \to \tau^+\nu_\tau$, the two decay modes have comparable physics reach. Since very different analysis techniques have been developed for these searches, they will be discussed separately in the following sections.

$B^+ \to \tau^+\nu_\tau$

In this section we briefly describe the analyses performed in the *BABAR* experiment for the search of the decay $B^+ \to \tau^+\nu_\tau$ and discuss the potential of similar analyses in the scenario of a Super B Factory .

The $B^+ \to \tau^+\nu_\tau$ decay has very little experimental constraint, due to the presence of multiple neutrinos in the final state. Therefore, in the $\Upsilon(4S)$ CMS, the decay of one of the B mesons (referred as the "tag" B meson) is reconstructed and the signature of $B^+ \to \tau^+\nu_\tau$ decay is searched for in the recoil. In the *BABAR* experiment, both hadronic and semileptonic tags (cf. Section 4.2.1) have been used in analyses based on a data set of about $80\,\text{fb}^{-1}$.

In the analysis with hadronic tags [198], the τ lepton is identified in both leptonic and hadronic decay modes: $\tau^+ \to e^+\nu_e\overline{\nu}_\tau$, $\tau^+ \to \mu^+\nu_\mu\overline{\nu}_\tau$, $\tau^+ \to \pi^+\overline{\nu}_\tau$, $\tau^+ \to \pi^+\pi^0\overline{\nu}_\tau$, $\tau^+ \to \pi^+\pi^-\pi^+\overline{\nu}_\tau$. This set is somewhat restricted in events with semi-exclusive semileptonic tags because of the higher background level (see below).

In the recoil all remaining particles are required to be consistent with coming from $B^+ \to \tau^+\nu_\tau$ decay. The selection criteria require that there be no extra charged particles besides one(three) track(s) from τ decay, and little neutral energy in the calorimeter, after excluding the energy of any neutrals coming from the decay of the tag B and the τ. Particle identification is used to identify leptonic and hadronic τ decays. Signal selection criteria vary among the analyses using different tag B samples and τ decay modes. Continuum suppression cuts, γ or(and) π^0 multiplicity requirements, *etc.* are also used in different analyses.

A GEANT4-based MC simulation is used to study the signal efficiency and to estimate backgrounds. The MC simulated events used for background estimation corresponds to roughly three times the luminosity of on-resonance data. The current analyses are optimized for $80\,\text{fb}^{-1}$ on-resonance data luminosity. On larger data sets at a Super B Factory , stricter selection criteria can be applied to improve the signal-to-background ratio. The main sources of background in all analyses are missing charged track(s) and undetected K_L^0'(s).

Signal selection efficiencies for range from 23% for $\tau \to e\overline{\nu}_e\nu_\tau$ to 7% for $\tau \to \pi^+\pi^-\pi^+\nu_\tau$ decay mode. The total signal selection efficiency is 11.3 %, which results in an overall selection efficiency of 0.028% when including the B_{reco} tag efficiency. For a data set of 82 fb^{-1}, we expect about 1.8 signal events and 38 ± 5.0 background events.

For semi-exclusive semileptonic B tags [199], only the leptonic τ decay modes are identified. The signal selection efficiency is ∼22.5% and the overall efficiency, including systematic corrections, is $(5.60 \pm 0.25(\text{stat.}) \pm 0.44(\text{syst.})) \times 10^{-4}$. With a data set of $82\,\text{fb}^{-1}$, this leads to an expectation of 40 signal events with a background of 274 events. The analysis uses an unbinned maximum likelihood fit to extract signal and background yields. The probability density functions (PDFs) for signal and background are obtained from the distribution of the neutral energy remaining in the calorimeter, after excluding neutrals associated with the tag side (E_{extra}) in signal and background MC simulation, respectively. Figure 4-9 shows the E_{extra} distributions in signal and background MC and in on-resonance data. The PDFs are shown in figure 4-10.

In the signal region $E_{extra} < 0.35$ GeV, the expected number of background from data sideband extrapolation is 39.9 ± 2.8 and the expected number of signal events is ∼ 5, assuming a branching fraction of $\mathcal{B}(B^+ \to \tau^+\nu_\tau) = 10^{-4}$. With a luminosity of $82\,\text{fb}^{-1}$, the observed number of events in the signal region is 47. The maximum likelihood fit to the data yields 10.9 ± 7.5 signal events and 258.1 ± 17.4 background events in the total fit region of $E_{extra} < 1.0$ GeV, consistent with signal and background expectations.

We next discuss expected signal and background for $B^+ \to \tau^+\nu_\tau$ decay at luminosities of $2\,\text{ab}^{-1}$ in a Super B Factory . The estimates are done under the assumption that the detector performance at a Super B Factory will be same as the performance of the *BABAR* detector.

We take the expected numbers of background and signal events at $80\,\text{fb}^{-1}$ of luminosity (see above) and extrapolate those numbers to a luminosity of $2\,\text{ab}^{-1}$. For this estimate, $\tau^+ \to \pi^+\pi^0\overline{\nu}_\tau$ and $\tau^+ \to \pi^+\pi^-\pi^+\overline{\nu}_\tau$ decay modes are excluded, due to worse signal-to-background ratios in these two modes. The estimated number of signal and background events for different tag B are listed in Table 4-10.

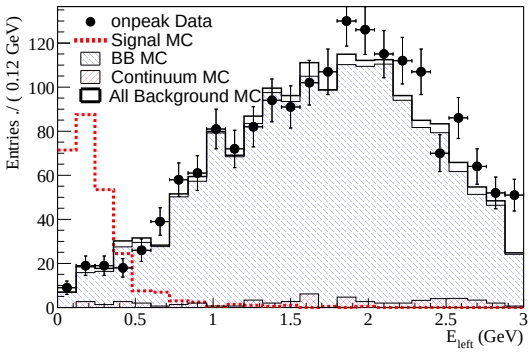

Figure 4-9. *E_{extra}, the neutral energy remaining in the calorimeter after excluding neutrals associated with the semi-leptonic side. In the above distribution all analysis selection criteria are applied. The normalization of the signal MC sample is arbitrary.*

Table 4-10. *Expected number of signal and background events at 2 ab^{-1} of integrated luminosity, obtained by projecting estimations from current BABAR analyses.*

Tag B decay mode	τ decay modes	Expected number of background events	Expected number of signal events for $\mathcal{B}(B^+ \to \tau^+\nu_\tau) = 10^{-4}$
$B^- \to D^{(*)0}X^-$	$\tau^+ \to e^+\nu_e\overline{\nu_\tau}$, $\mu^+\nu_\mu\overline{\nu_\tau}$, $\tau^+ \to \pi^+\overline{\nu_\tau}$	559	34
$B^- \to D^0\ell^-\nu X^0$ ($E_{extra} < 0.35$ GeV)	$\tau^+ \to e^+\nu_e\overline{\nu_\tau}$, $\mu^+\nu_\mu\overline{\nu_\tau}$	974	122
$B^- \to D^{*0}\ell^-\overline{\nu_\ell}$	$\tau^+ \to e^+\nu_e\overline{\nu_\tau}$, $\mu^+\nu_\mu\overline{\nu_\tau}$, $\tau^+ \to \pi^+\overline{\nu_\tau}$	547	74

As discussed above, the analysis using semi-exclusive semileptonic tags ($B^- \to D^0\ell^-\nu X^0$) performs a maximum likelihood fit to extract signal and background yields. Toy MC experiments are used to study the signal sensitivity of the likelihood fit at a Super B Factory . Toy MC samples are generated using the current PDFs (figure 4-10). By scaling the number of events in the fit region of $E_{extra} < 1.0$ GeV (see above), one expects about 6568 background events and about 151 signal events at 2 ab^{-1}. For each toy MC sample the number of generated background and signal events are obtained from Poisson fluctuation of those expected number of events. The same PDFs are used to fit the toy MC samples in order to obtain signal and background yields. The distributions of number of fitted signal and background events for 5000 such toy experiments are looked at. The mean and the rms of the distribution of number of fitted signal events from the toy experiments are 152 and 38 respectively, while for the distribution of the fitted number of background events, the mean and rms are 6568 and 38 respectively. Based on these studies, we expect about 4σ significance for the signal at 2 ab^{-1}.

A large sample of background and signal events also have been generated using the fast (Pravda) MC simulation. The Pravda MC does not presently have a realistic simulation of the detector response to neutral particles. Figure 4-11 shows a comparison of the distributions of quantities related to neutral simulation between detailed and fast MC simulation. Quantities related to neutral energy, such as number of π^0 mesons associated with the signal side, E_{extra}, *etc.*, are some of the major signal-defining quantities for identifying $B^+ \to \tau^+\nu_\tau$ signal. Since these distributions in fast MC simulation are quite different from those in the detailed MC simulation (which is in good agreement with data

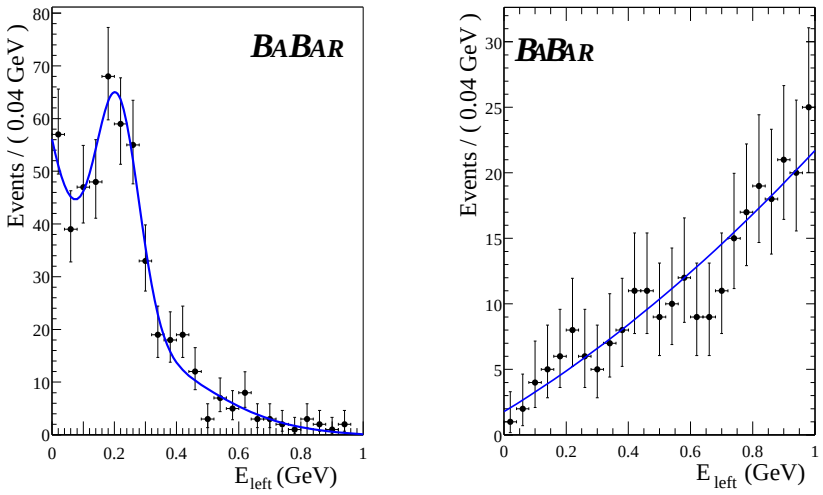

(a) (b)

Figure 4-10. *The signal PDF (left) fitted to E_{extra} from the signal MC sample and the background PDF (right) fitted to E_{extra} from the background MC sample. All selection criteria are applied to the events in signal and background MC samples. The normalization of the signal MC sample is arbitrary and the normalization of the background MC sample is fixed to the integrated luminosity of* $80\,\mathrm{fb}^{-1}$.

from the *BABAR* experiment) any estimation using fast MC simulation will not be realistic and reliable. Thus the fast MC sample has not been used.

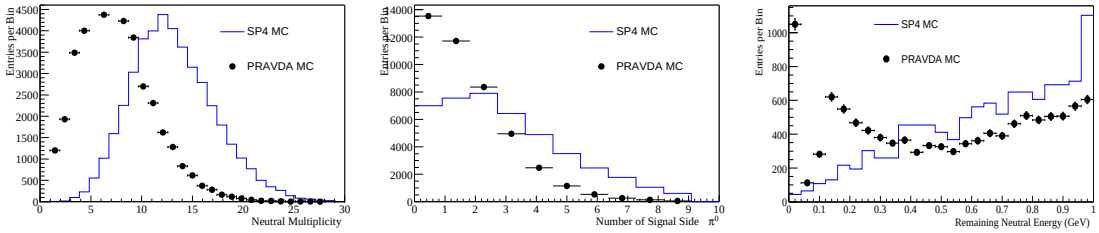

Figure 4-11. *(a) Distributions of number of reconstructed photons in the event, compared between detailed MC simulation (solid line) and fast MC simulation (dots) (b) Distributions of number of reconstructed π^0 associated with signal side, compared between detailed MC simulation (solid line) and fast MC simulation (dots). (c) Distributions of remaining neutral energy E_{extra}, compared between detailed MC simulation (solid line) and fast MC simulation (dots). The distributions related to simulation of neutrals are compared for detailed MC and fast (PRAVDA) MC simulations. The distributions for fast MC simulation are quite different than those for detailed MC simulation.*

From our studies, the potential of $B^+ \to \tau^+\nu_\tau$ decay in a Super B Factory looks promising. The major issues concerning these analysis are the following.

- Search or observation of $B^+ \to \tau^+\nu_\tau$ signal are highly sensitive to quantities related to neutral particles. A detailed simulation of the calorimeter response, beam background at high luminosity environment etc. will be useful to get a more realistic estimation of the signal sensitivity at a Super B Factory .

- Since the major source of background are from missing tracks and undetected K_L^0 mesons, detector coverage and neutral identification will affect the signal sensitivity.

With an integrated luminosity of $2\,\text{ab}^{-1}$, we expect to observe $B^+ \to \tau^+\nu_\tau$ with 4σ significance.

$B^+ \to \mu^+\nu_\mu$

The existing upper limits on the $B^+ \to \mu^+\nu_\mu$ branching fraction from CLEO [200], Belle [201], and *BABAR* [202] were all obtained using similar analysis techniques on data samples collected at the $\Upsilon(4S)$ resonance. In this section, we describe the existing *BABAR* measurement and estimate the sensitivity of a similar technique with a 5 ab^{-1} sample collected at a Super B Factory. The high luminosity study was carried out using the Pravda fast Monte Carlo described in section 4.2.3. We also briefly discuss the prospects for measuring $B^+ \to \mu^+\nu_\mu$, using a sample of events in which the other B in the event has been fully reconstructed, similar to the $B^+ \to \tau^+\nu_\tau$ analysis.

As noted above, $B^+ \to \mu^+\nu_\mu$ is a two-body decay so the muon is monoenergetic in the B rest frame. Since B mesons from $\Upsilon(4S) \to B\overline{B}$ are produced with relatively low momenta ($\approx 320\ \text{MeV}/c$), the $\Upsilon(4S)$ rest frame is a good approximation to the B rest frame. Therefore, the existing analysis begins by selecting well-identified muon candidates with momentum near $m_B/2$ in the $\Upsilon(4S)$ rest frame. The neutrino goes undetected so we can assume that all remaining particles are associated with the decay of the other B in the event, which we denote the "companion" B. Signal decays can then be selected using the kinematic variables ΔE and energy-substituted mass m_{ES} (see section 4.2.1).

After removing the muon candidate from the event, the companion B can be reconstructed from the remaining visible energy. To aid the event energy resolution, only loose selection criteria are applied to the remaining charged tracks and neutral calorimeter clusters. In the *BABAR* analysis, the companion B includes all charged tracks that are consistent with being produced at the interaction point and all neutral calorimeter clusters with energy greater than 30 MeV. Particle identification is applied to the charged tracks in order to select the appropriate mass hypothesis and thus improve the ΔE resolution. Events with additional identified leptons from the companion B are discarded since they typically arise from semileptonic B or charm decays and indicate the presence of additional neutrinos. Figure 4-12 shows distributions of ΔE and m_{ES} for the *BABAR* on-resonance data, background MC and signal MC samples after muon candidate selection. For a properly reconstructed signal decay, we expect m_{ES} to peak near the B mass and the energy of the companion B to be consistent with the beam energy so that ΔE peaks near 0. In practice, energy losses from detector acceptance, unreconstructed neutral hadrons and additional neutrinos result in the signal ΔE distribution being shifted toward negative ΔE, while the m_{ES} distribution develops a substantial tail below the B mass.

Once the companion B is reconstructed, we can calculate the muon momentum in the rest frame of the signal B. We assume the signal B travels in the direction opposite that of the companion B momentum in the $\Upsilon(4S)$ rest frame with a momentum determined by the two-body decay $\Upsilon(4S) \to B\overline{B}$. Figure 4-13 shows the muon candidate momentum distribution in the B rest frame, p_μ, for all muon candidates in the signal MC. The dashed curve is the momentum distribution of the same events in the $\Upsilon(4S)$ rest frame.

Backgrounds may arise from any process that produces charged tracks in the momentum range of the signal muon. The two most significant backgrounds are found to be B semi-leptonic decays involving $b \to u\mu\overline{\nu}$ transitions where the endpoint of the muon spectrum approaches that of the signal, and non-resonant $q\overline{q}$ ("continuum") events where a charged pion is mistakenly identified as a muon. In order for continuum events to populate the signal region of ΔE and m_{ES}, there must be significant energy loss, mainly from particles outside the detector acceptance and unreconstructed neutral hadrons. We reduce these backgrounds by tightening the selection on the muon momentum. The momentum spectrum of the background decreases with increasing momentum, so we apply an asymmetric cut about the signal peak, $2.58 < p_\mu < 2.78\ \text{GeV}/c$.

The continuum background is further suppressed using event-shape variables. These events tend to produce a jet-like event topology, as opposed to $B\overline{B}$ events, which tend to be spherical. We define a variable, θ_T^*, which is the

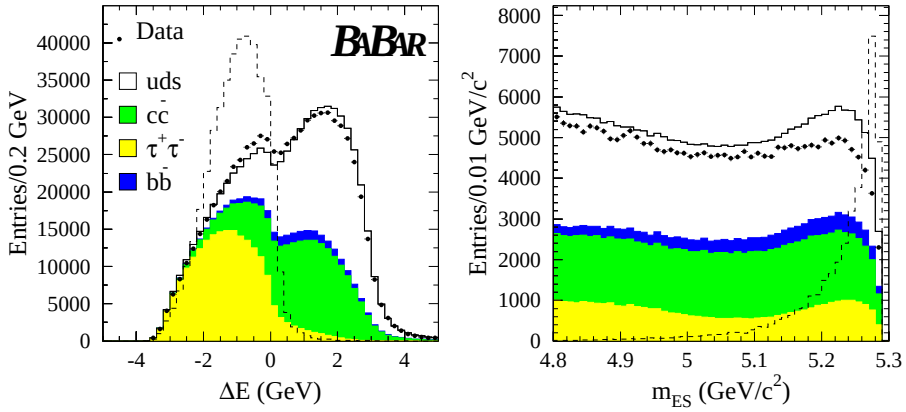

Figure 4-12. *The distributions of ΔE and m_{ES} for on-peak data and MC samples after muon candidate selection. The signal distributions are overlaid (dashed histograms) with an arbitrary normalization.*

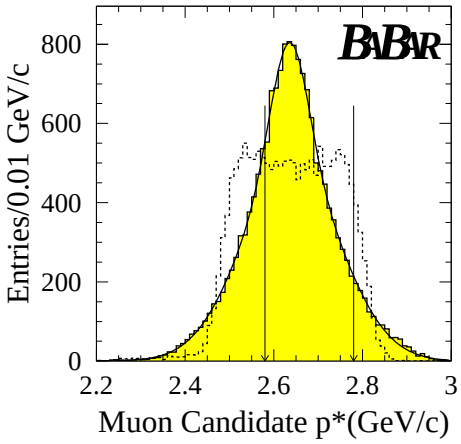

Figure 4-13. *The muon candidate momentum distribution in the reconstructed B rest frame for all muon candidates in the signal MC. The dashed curve is the momentum distribution of the same events in the $\Upsilon(4S)$ rest frame. The arrows indicate the selected signal region.*

angle between the muon candidate momentum and the thrust axis of the companion B in the $\Upsilon(4S)$ rest frame. For continuum background, $|\cos\theta_T^*|$ peaks sharply near one while the distribution is nearly flat for signal decays. The polar angle of the missing momentum vector in the laboratory frame, θ_ν, can also discriminate against continuum backgrounds. In continuum decays, the missing momentum is often due to undetected particles that were outside the detector acceptance. Therefore, we require that the missing momentum is directed into the detector's fiducial volume. Figure 4-14 shows the *BABAR* on-peak data and MC distributions of $|\cos\theta_T^*|$ and $|\cos\theta_\nu|$. For comparison, the signal MC is overlaid with an arbitrary normalization.

We select $B^+ \to \mu^+\nu_\mu$ signal events with simultaneous requirements on ΔE and m_{ES}, thus forming a "signal box" defined by $-0.75 < \Delta E < 0.5$ GeV and $m_{ES} > 5.27$ GeV/c^2. After applying all selection criteria, the $B^+ \to \mu^+\nu_\mu$ efficiency is determined from the simulation, after correcting for discrepancies between the data and MC, to be about 2.1%. The amount of background expected in the signal box is estimated to be $5.0^{+1.8}_{-1.4}$ events, by extrapolating from

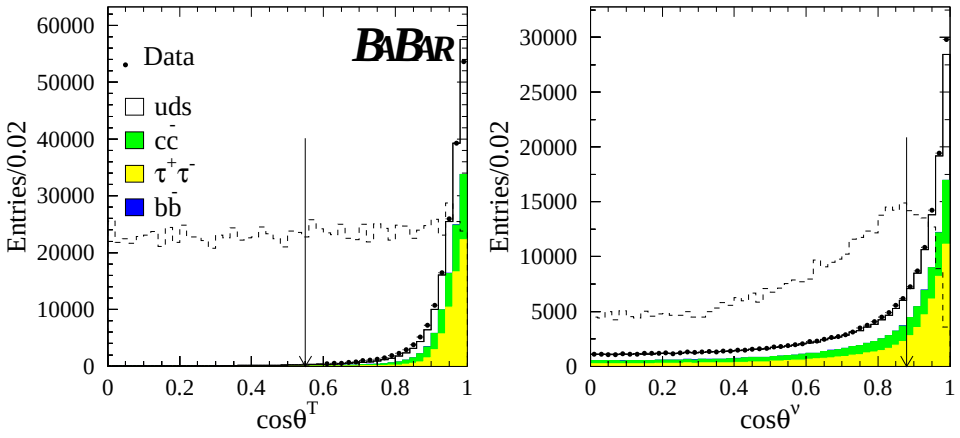

Figure 4-14. *The distributions of* $|\cos\theta_T^*|$ *and* $|\cos\theta_\nu|$ *for on-peak data and MC. The events in these plots have passed the requirement* $2.58 < p* < 2.78$ GeV/c. *The signal distributions are overlaid (dashed histograms) with an arbitrary normalization.*

the signal box sidebands. From the MC simulation, we expect that this background is composed of approximately 57% light-quark ($u\overline{u}$, $d\overline{d}$, $s\overline{s}$), 23% $c\overline{c}$, and 20% $B\overline{B}$ events. In the on-resonance data we find 11 events in the signal box which results in an upper limit of $\mathcal{B}(B^+ \to \mu^+\nu_\mu) < 6.6 \times 10^{-6}$ at the 90% confidence level.

To estimate the sensitivity to $B^+ \to \mu^+\nu_\mu$ at a Super B Factory, this analysis has been repeated using a sample of approximately 5 ab^{-1} simluated with the Pravda fast MC simulation. Here we have assumed 90% muon efficienciecy and 1% pion misidentification at the Super B Factory .

The reliability of the Pravda simulation has been evaluated by comparing the event yields expected for the current analysis (80 fb^{-1}) with the full simulation. For these comparisons, we have applied the current *BABAR* muon identification performance to the Pravda simulation. In general, the results are in reasonable agreement. In the signal box, Pravda predicts 7.6 background events where we find 5.3 in the full simulation. In the "grand sideband" defined by $-3.0 < \Delta E < 1.5$ GeV and $m_{ES} > 5.23$ GeV/c^2, we see 257 Pravda background events as compared to 200 in the full simulation. Although, the background totals are in adequate agreement, we do observe some notable discrepancies in particular modes. For example, the $B^+ \to \mu^+\nu_\mu$ and $B^0 \to \pi^+\mu^-\overline{\nu}_\mu$ efficiencies are overestimated in Pravda by roughly a factor of 2. Furthermore, the Pravda simulation appears to neglect interactions of neutral hadrons in the calorimeter. Therefore, we see an enhanced background rate from processes involving neutral hadrons. The increase in the signal efficiency is likely due to the lack of detector related backgrounds such as fake charged tracks, calorimeter noise and beam backgrounds, which improves the event energy resolution. We actually expect these backgrounds to increase with luminosity but we currently have no estimate of this effect.

With higher luminosity, the optimum values of analysis cuts may change. Therefore, we have re-optimized the cut on $|\cos\theta_T^*|$ (the most effective variable for continuum rejection) using signal boxes of various sizes. The optimum combination was found to be $|\cos\theta_T^*| < 0.6$, $-0.5 < \Delta E < 0$ GeV and $m_{ES} > 5.27$ GeV/c^2. Therefore, the ΔE range of the signal box has decreased but all other cuts retain essentially the same value as in the current analysis. We also found a small benefit by requiring the total event charge to be 0. With this combination of cuts we find a signal efficiency of approximately 4% in the Pravda simulation. For a 5 ab^{-1} data sample, this simulation yields approximately 90 signal and 210 background events in the signal box. The background composition is significantly different than that found in the full simulation. Because we have assumed an improved muon identification probability, as well as a factor of two improvement in the pion misidentification rate, the background is now roughly half $B\overline{B}$ as opposed to being dominated by continuum. We also note that about 85% of the continuum background involves a neutral hadron.

Figure 4-15 shows the distributions of m_{ES} and p_μ for signal and background MC. In each plot, all other cuts have been applied. Note that a large contribution from $b \to c\ell\nu$ decays would normally be evident in the p_μ distribution. However, those decays do not produce muons in the momentum range of the signal, so they have been neglected here. Also, the sharp peak in m_{ES} due to $B\overline{B}$ events with fake muons is due mostly to decays such as $B^+ \to K^0_L\pi^+$. This decay mode is enhanced due to the lack of simulation of neutral hadrons in the Pravda MC.

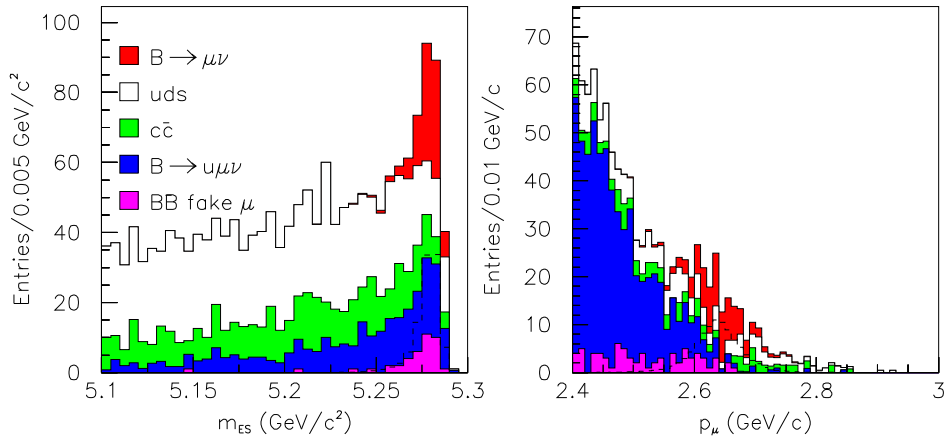

Figure 4-15. *The distributions of m_{ES} and p_μ for signal and background Pravda MC simulation, normalized to $5\,\mathrm{ab}^{-1}$. In each plot, all other cuts have been applied.*

With a larger data sample we would likely extract the signal yield using a maximum likelihood analysis rather than the "cut and count" method employed so far. As a simple example, we have performed a binned likelihood fit to the p_μ distribution from the Pravda simulation. The background PDF was assumed to be a single Gaussian function while the signal distribution was fit to a double Gaussian. The parameters of the Gaussians were fixed and a fit was performed for the signal and background normalizations. For a sample of $5\,\mathrm{ab}^{-1}$, the signal yield is extracted with approximately 15% statistical uncertainty, assuming the Standard Model branching fraction. If the branching fraction (or, equivalently, the signal efficiency) were a factor of two larger(smaller), the statistical uncertainty is expected to be about 10(30)%. These results could likely be improved with a simultaneous fit to p_μ, ΔE, and m_{ES}. Based on these results, $|V_{ub}|$ could be extracted with a statistical uncertainty of 5-15% assuming f_B has been calculated to the necessary precision.

We have also considered searching for $B^+ \to \mu^+\nu_\mu$ using a fully-reconstructed tag B as described for the $B^+ \to \tau^+\nu_\tau$ analysis. The reconstruction efficiency for this type of analysis is too small to be useful with existing data samples but may become feasible for the larger data samples provided by a Super B Factory. The primary benefit of this "recoil" method is that the backgrounds can be significantly reduced by requiring the existence of another fully reconstructed B. The $B^+ \to \tau^+\nu_\tau$ analyses have demonstrated B tagging efficiencies of 0.25% for the hadronic modes and 0.31% for the semi-leptonic modes. Furthermore, due to the simplicity of the $B^+ \to \mu^+\nu_\mu$ signal side (1 charged track), we might expect some improvement in the tagging efficiency and reduction of the combinatorial background.

Given a good tag B, the signal-side selection for this analysis should be quite simple. We have considered, for example, requiring only one remaining charged track that passes muon identification and satisfies $2.6 < p_\mu < 2.7$ GeV/c. Note that the p_μ selection has been tightened, because having a fully reconstructed tag B provides much better knowledge of the B rest frame. Therefore, the p_μ resolution is significantly improved. We expect about 91% of the signal muons to be reconstructed due detector acceptance, about 90% to pass muon identification, and about 95% to pass the p_μ requirement yielding a total signal-side efficiency of about 78%.

Given the above tag-side and signal-side efficiencies, we expect a total signal efficiency of about 0.5% for a recoil anlysis. Therefore, in a sample of $5\,\mathrm{ab}^{-1}$, we expect about 10 signal events to pass all cuts, assuming a signal branching

fraction of 4×10^{-7}. The expected background has been investigated by applying the above signal-side selection to the existing semi-leptonic $B^+ \to \tau^+\nu_\tau$ analysis. In roughly 200 fb^{-1} of generic $B\overline{B}$ MC and 50 fb^{-1} of continuum MC, both in the full simulation, we see no background events passing all cuts. If we optimistically assume that the backgrounds are negligible, the signal branching fraction could be measured with a statistical uncertainty of about 30%.

In conclusion, fast MC studies indicate that the branching fraction for $B^+ \to \mu^+\nu_\mu$ could be measured with a statistical uncertainty of 10-30% with a 5 ab^{-1} data sample collected at a Super B Factory . The measurement could be performed using either an inclusive reconstruction of the companion B, as in the current analysis, or a fully reconstructed companion B. At present, the inclusive analysis is better understood and appears to give a smaller statistical uncertainty. Assuming that the theoretical uncertainty in f_B can be significantly improved in lattice QCD calculations, $|V_{ub}|$ could be determined to 5-15% in this mode. As the theoretical uncertainties here are very different from those in semileptonic B decays, this provides a very powerful alternate route to $|V_{ub}|$. The critical considerations for the detector design are maximum hermiticity, neutral hadron identification, and, of course, muon identification. Finally, we do not expect these measurements to be possible at hadronic machines such as LHCb and BTeV, due to the necessity of neutrino reconstruction. Therefore, a future Super B Factory has the unique opportunity to observe leptonic B decays, and thus constrain the Standard Model parameters $|V_{ub}|$ and f_B.

4.6.3 $B \to \gamma\ell\overline{\nu}$, $\gamma\ell^+\ell^-$, $\gamma\gamma$

≻E. Lunghi≺

The decays $B \to \gamma e\nu$, $B \to \gamma\gamma$ and $B \to \gamma ee$ are extremely rare modes that are nevertheless within the reach of a Super B Factory. Rough estimates of their branching ratios give: $\mathcal{B}(B \to \gamma e\nu) \sim 10^{-6}$, $\mathcal{B}(B \to \gamma\gamma) \sim 3 \times 10^{-8}$, $\mathcal{B}(B \to \gamma ee) \sim 10^{-11} \div 10^{-10}$. The absence of hadrons in the final state facilitate the analysis of QCD effects; indeed, it can be shown that all these modes factorize up to power corrections.

$B \to \gamma e\nu$

The effective Hamiltonian responsible for this decay:

$$H_{\rm eff} = \frac{4G_F}{\sqrt{2}}\, V_{ub}\, (\overline{u}_L\gamma^\mu b_L)\, (\overline{e}_L\gamma_\mu\nu_L) \tag{4.109}$$

arises at tree level in the Standard Model. The amplitude for the $B \to \gamma e\nu$ transition can be exactly parameterized in terms of the following photonic form factors:

$$\frac{1}{e}\langle\gamma(q,\varepsilon)|\,\overline{u}\,\gamma_\mu\, b\,|\overline{B}(v)\rangle \;=\; i\epsilon_{\mu\alpha\beta\delta}\,\varepsilon^*_\alpha\, v_\beta\, q_\delta\, f_V(E_\gamma) \tag{4.110}$$

$$\frac{1}{e}\langle\gamma(q,\varepsilon)|\,\overline{u}\,\gamma_\mu\gamma_5\, b\,|\overline{B}(v)\rangle \;=\; \left[q_\mu(v\cdot\varepsilon^*) - \varepsilon^*_\mu(v\cdot q)\right] f_A(E_\gamma) + v_\mu\frac{v\cdot\varepsilon^*}{v\cdot q} f_B m_B\,, \tag{4.111}$$

where ε is the photon polarization. The last term in (4.111) is a contact term that compensates the photon emission from the electron line. In Refs. [203, 204, 205] it was shown that, at leading order in $\Lambda_{\rm QCD}/E_\gamma$ and at all orders in α_s, the form factors $f_{V,A}(E_\gamma)$ are equal at all orders in perturbation theory and factorize into the product of hard Wilson coefficients and a universal convolution of a jet function with the B meson light cone distribution amplitude (LCDA):

$$f_V(E_\gamma) = f_A(E_\gamma) = C(E_\gamma)\int \mathrm{d}\xi\; J(E_\gamma,\xi)\;\phi_B(\xi) = C(E_\gamma)\; I(E_\gamma)\,, \tag{4.112}$$

where $C(E_\gamma)$ is the hard coefficient, J is the jet-function containing terms of the type $(\log\xi)^n/\xi$ with $n \geq 0$ and $\phi_B(\xi)$ is the B meson LCDA (see Ref. [204] for details).

Since we do not expect any sizable New Physics correction to a Standard Model tree level amplitude, this decay will provide us with valuable pieces of information on the first negative moment of the poorly known B meson

LCDA[206]: $\lambda_b^{-1} = \int \phi_B(\xi)/\xi$. This quantity is important because it enters factorization formulas for several rare B decays ($B \to (\rho, K^*)\gamma$, $B \to \rho e\nu$, $B \to K\pi$, $B \to \pi\pi$, ...). Unfortunately, the convolution $I(E_\gamma)$ evaluated at $\mathcal{O}(\alpha_s)$ depends on the first two logarithmic moments of ϕ_B as well ($\int \phi_B(\xi) \log \xi/\xi$ and $\int \phi_B(\xi) \log^2 \xi/\xi$). This could limit the accuracy of the extraction of λ_b from this measurement (See Ref. [207] for a detailed description of this problem).

Note that the above result are valid for large photon energy ($\Lambda_{\rm QCD}/E_\gamma << 1$); a cut in the photon spectrum ($E_{\gamma c} < E_\gamma < m_B/2$) is necessary to restrict to the theoretically clean region. Using the parametrization of the B meson LCDA given in Ref. [206], we obtain the follow approximate expression, valid in the region $1\mathrm{GeV} < E_{\gamma c} < m_B/2$, for the integrated branching ratio:

$$\int_{E_{\gamma c}}^{m_B/2} \mathrm{d}E_\gamma \frac{\mathrm{d}\mathcal{B}(B \to \gamma e\nu)}{\mathrm{d}E_\gamma} = 10^{-2} \left| \frac{V_{ub}}{3.9 \times 10^{-3}} \right|^2 \left(\frac{\lambda_B^{-1}}{2.15\ \mathrm{GeV}} \right)^2 \left[5.97 - 4.08\ E_{\gamma c} + 0.65\ E_{\gamma c}^2 \right] . \tag{4.113}$$

Using the QCD sum rules estimate $\lambda_b^{-1} = (2.15 \pm 0.5)\mathrm{GeV}^{-1}$ [206] and a photon cut-off of $1\,\mathrm{GeV}$ we obtain $\mathcal{B}(B \to \gamma e\nu) \sim 1.8 \times 10^{-6}$ with O(100%) uncertainties coming mainly from λ_b^{-1} and V_{ub}.

Note that a first principles computation of the $f_{V,A}$ form factors on the lattice would allow for a direct test of the relation $f_V(E_\gamma) = f_A(E_\gamma)$ and shed some light on the size of the incalculable power corrections.

$B \to \gamma\gamma$

The decay $B \to \gamma\gamma$ arises, in the Standard Model, at loop level and is mediated by the same effective Hamiltonian that governs $b \to d\gamma$ transitions:

$$H_{\rm eff} = \frac{4G_F}{\sqrt{2}} \left(V_{tb}V_{td}^* \sum_{i=1}^{8} C_i O_i + V_{ub}V_{ud}^* \sum_{i=1}^{2} C_i O_i^u \right) , \tag{4.114}$$

where the most relevant operators are

$$O_2 = (\bar{d}_L \gamma^\mu c_L)(\bar{c}_L \gamma_\mu b_L) , \tag{4.115}$$

$$O_7 = \frac{e}{16\pi^2} m_b (\bar{d}_L \sigma^{\mu\nu} b_R) F_{\mu\nu} , \tag{4.116}$$

$$O_8 = \frac{g_s}{16\pi^2} m_b (\bar{d}_L T^a \sigma^{\mu\nu} b_R) G^a_{\mu\nu} . \tag{4.117}$$

The matrix element of O_7 can be parameterized in terms of the following tensor form factors:

$$\begin{aligned} \frac{1}{e}\langle \gamma(q,\varepsilon)|\overline{u}\sigma_{\mu\nu}b|\overline{B}(p)\rangle &= i\,\varepsilon_{\mu\nu\alpha\beta}\,\varepsilon^{*\alpha}\,(p+q)^\beta\,g_+(E_\gamma) + i\,\varepsilon_{\mu\nu\alpha\beta}\,\varepsilon^{*\alpha}\,(p-q)^\beta\,g_-(E_\gamma) \\ &\quad -2\,(\varepsilon^*\cdot p)\,h(E_\gamma) i\varepsilon_{\mu\nu\alpha\beta}p^\alpha q^\beta . \end{aligned} \tag{4.118}$$

From the results of Ref. [204] it follows that the three tensor form factors $g_\pm$ and h factorize at all orders in α_s and are proportional to the convolution integral $I(E_\gamma)$. Therefore, the following ratios are clean of hadronic uncertainties up to power corrections:

$$\frac{g_+(E_\gamma)}{f_V(E_\gamma)} = \frac{1}{2}\frac{Q_d}{Q_u}\left(1 - \frac{\alpha_s C_F}{4\pi}\frac{E_\gamma}{E_\gamma - m_b/2}\log\frac{2E_\gamma}{m_b}\right) + O(\alpha_s^2) \tag{4.119}$$

$$g_-(E_\gamma) = -g_+(E_\gamma) + O(\alpha_s^2) \tag{4.120}$$

$$h(E_\gamma) = 0 + O(\alpha_s^2) . \tag{4.121}$$

The situation is more complicated for the matrix elements of other operators (the most relevant are O_2 and O_8), and the issue has not yet been addressed at all orders. In Ref. [207] the authors show explicitly that all diagrams that would lead to non-factorizable effects are indeed suppressed by at least one power of $\Lambda_{\rm QCD}/m_B$.

From a phenomenological point of view, it is more useful to normalize the $B \to \gamma\gamma$ branching ratio to $\mathcal{B}(B \to \gamma e \nu)$. This ratio allows for a determination of the Wilson coefficient C_7^d with precision similar to the inclusive channel $B \to X_d\gamma$. In fact, the latter mode is plagued by non-perturbative contributions to the matrix elements of the four-quark operators induced by up quark loops [208].

Finally, note that some power suppressed contributions to the amplitude $B \to \gamma\gamma$ are nevertheless computable. They are responsible for the presence of a direct CP asymmetry of order -10% (see Ref. [209] for further details).

$B \to \gamma e e$

This mode is described by the effective Hamiltonian Eq. (4.114) with the inclusion of the semileptonic operators

$$O_9 = (\bar{d}_L \gamma^\mu b_L)\,(\bar{e}\gamma_\mu e)\,, \tag{4.122}$$

$$O_{10} = (\bar{d}_L \gamma^\mu b_L)\,(\bar{e}\gamma_\mu \gamma_5 e)\,. \tag{4.123}$$

The analysis of this decay follows closely that of $B \to \gamma\gamma$. In this case as well, a complete proof of factorization at all orders has not been completed yet. The shape of the dilepton invariant mass spectrum is very similar to the $B \to X_d e e$ case; in particular, the presence of non-perturbative $q\bar{q}$ rescattering results in the presence of resonant peaks corresponding to the tower of $c\bar{c}$ resonances (J/ψ, ψ', ...). In analogy with $b \to (d,s)ee$ modes, it is, therefore, necessary to place cuts on the dilepton invariant mass distribution.

Moreover, factorization theorems are only valid in regions in which the photon energy is large or, equivalently, in which the dilepton invariant mass is small. This region is also free from effects induced by bremsstrahlung from the external leptons. The analysis of the high invariant mass region has to rely on other methods (see for instance Ref. [210]).

An important observable is the forward–backward asymmetry of the dilepton system. The measurement of a zero in the spectrum provides a determination of the sign of the Wilson coefficient C_7^d. In this case as well, considering the ratio to the leading $B \to \gamma e \nu$ mode allows to reach a precision comparable to the inclusive $B \to X_d e e$ channels.

4.6.4 Experiment

≻U. Langenegger≺

The leptonic decays modes $B \to \gamma\gamma$, and $B \to \gamma\ell^+\ell^-$, $B \to \ell\overline{\nu}\gamma$ are extremely rare and have not yet been observed experimentally; they come within reach at a Super B Factory. The first two modes will not benefit from analyses on the recoil of a B_{reco} candidate due to their very small expected branching fraction. Here progress will only come with a difficult improvement of the background rejection in the traditional reconstruction of the signal decay.

The best current experimental upper limit on $B \to \gamma\gamma$ has been determined at $\mathcal{B}(B \to \gamma\gamma) < 1.7 \times 10^{-6}$ by the *BABAR* collaboration [211]. Here, the dominant background processes are continuum $q\overline{q}$ production (where $q = u, d, s, c$). At some point, even the rare decay $B^0 \to \pi^0\pi^0$ will constitute a background for this decay mode.

No limits exist yet for the decay $\to \gamma\ell^+\ell^-$. Here, the backgrounds consist both of continuum processes and radiative B meson decays (combined with a misidentified pion).

The study of $B \to \ell\overline{\nu}\gamma$ has a substantially larger expected branching fraction, but is complicated by the unmeasured neutrino. At a Super B Factory, a large background in the electron channel is due to two-photon processes. This background is much reduced for the muon channel. Eventually, events tagged by the fully reconstructed hadronic decay of a B meson will provide the best environment to measure this decay.

4.7 Summary

On the experimental side, the Super B Factory will definitely establish the method of "recoil physics" as the primary approach for the precision study of semileptonic B decays. Here, $B\overline{B}$ events are selected by the full reconstruction of a hadronic B decays (serving as event tags), thus allowing the study of a semileptonic decay of the second B meson in the event. While the overall efficiency for this approach is small, this is no longer a limiting factor at a Super B Factory.

The *inclusive* determination of $|V_{ub}|$ will reach statistical and experimental systematic errors below the 3% level even before the arrival of a Super B Factory and will be limited by the theoretical errors. With unquenched lattice QCD calculations for the form factors, the measurement of *exclusive* charmless semileptonic B decays will provide a premier opportunity for the model-independent determination of $|V_{ub}|$. The statistical error of the recoil methods will approach the detector systematic error of about 2% only at the Super B Factory, especially for those decay channels most amenable to lattice QCD calculations. The total error on $|V_{ub}|$ will be limited by theoretical uncertainties only after several years at a Super B Factory.

The measurement of *leptonic* B decays will provide complementary determinations of $|V_{ub}|$ at the Super B Factory. The observation of $B \to \tau\overline{\nu}$ is expected to be achievable already at luminosities of around 2 ab^{-1}. It is difficult to predict the precision of the determination of $|V_{ub}|$ with this decay mode, as detailed background simulation studies are necessary for a reliable assessment of the experimental systematic errors. The decay $B \to \mu\overline{\nu}$ offers a much cleaner experimental environment, though at a much reduced rate due to helicity suppression. It allows for a statistics-limited determination of $|V_{ub}|$ at the level of about 10% at an integrated luminosity of about 5 ab^{-1}, if unquenched lattice QCD calculations provide f_B with the necessary precision. Here, analyses based on the recoil method will surpass traditional analyses only after several years at a Super B Factory.

References

[1] C. W. Bernard and M. F. L. Golterman, Phys. Rev. D **49**, 486 (1994) [arXiv:hep-lat/9306005].

[2] S. R. Sharpe, Phys. Rev. D **56**, 7052 (1997) [Erratum-*ibid.* D **62**, 099901 (2000)] [arXiv:hep-lat/9707018].

[3] S. R. Sharpe and N. Shoresh, Phys. Rev. D **62**, 094503 (2000) [arXiv:hep-lat/0006017].

[4] A. S. Kronfeld and S. M. Ryan, Phys. Lett. B **543**, 59 (2002) [arXiv:hep-ph/0206058].

[5] S. Hashimoto *et al.* [JLQCD Collaboration], Nucl. Phys. Proc. Suppl. **119**, 332 (2003) [arXiv:hep-lat/0209091].

[6] N. Yamada, Nucl. Phys. Proc. Suppl. **119**, 93 (2003) [arXiv:hep-lat/0210035].

[7] G.P. Lepage, Nucl. Phys. (Proc. Suppl.) **60A**, 267 (1998) and Phys. Rev. D **59**, 074501 (1999); K. Orginos and D. Toussaint, Phys. Rev. D **59**, 014501 (1999) ; K. Orginos, D. Toussaint and R.L. Sugar, Phys. Rev. D **60**, 054503 (1999) ; C. Bernard *et al.*, Nucl. Phys. (Proc. Suppl.) **60A**, 297 (1998), Phys. Rev. D **58**, 014503 (1998), and Phys. Rev. D **61**, 111502 (2000).

[8] A. X. El-Khadra, A. S. Kronfeld and P. B. Mackenzie, Phys. Rev. D **55**, 3933 (1997) [arXiv:hep-lat/9604004].

[9] M. B. Oktay, A. X. El-Khadra, A. S. Kronfeld, P. B. Mackenzie and J. N. Simone, Nucl. Phys. Proc. Suppl. **119**, 464 (2003) [arXiv:hep-lat/0209150].

[10] M. B. Oktay, A. X. El-Khadra, A. S. Kronfeld and P. B. Mackenzie, [arXiv:hep-lat/0310016].

[11] G. P. Lepage and B. A. Thacker, Nucl. Phys. Proc. Suppl. **4**, 199 (1988).

[12] C. T. H. Davies *et al.* [HPQCD Collaboration], [arXiv:hep-lat/0304004].

[13] M. Wingate, C. T. H. Davies, A. Gray, G. P. Lepage and J. Shigemitsu, [arXiv:hep-ph/0311130].

[14] C. Aubin *et al.* [MILC Collaboration], [arXiv:hep-lat/0309088].

[15] S. Hashimoto, A. X. El-Khadra, A. S. Kronfeld, P. B. Mackenzie, S. M. Ryan and J. N. Simone, Phys. Rev. D **61**, 014502 (2000) [arXiv:hep-ph/9906376].

[16] See H. D. Trottier, [arXiv:hep-lat/0310044], and references therein.

[17] W. J. Lee and S. R. Sharpe, Phys. Rev. D **60**, 114503 (1999) [arXiv:hep-lat/9905023].

[18] C. Aubin and C. Bernard, Phys. Rev. D **68**, 034014 (2003) [arXiv:hep-lat/0304014].

[19] C. Aubin and C. Bernard, Phys. Rev. D **68**, 074011 (2003) [arXiv:hep-lat/0306026].

[20] C. Aubin and C. Bernard, work in progress.

[21] U. Langenegger, (*BABAR* Collaboration]), [arXiv:hep-ex/0204001]; Belle Collaboration, (K. Abe *et al.*), [arXiv:hep-ex/0409015].

[22] C. H. Cheng [*BABAR* Collaboration], Int. J. Mod. Phys. A **16S1A**, 413 (2001) [arXiv:hep-ex/0011007].

[23] *BABAR* Collaboration, (B. Aubert *et al.*), Phys. Rev. Lett. **92**, 071802 (2004) [arXiv:hep-ex/0307062].

[24] S. Agostinelli *et al.* [GEANT4 Collaboration], Nucl. Instrum. Meth. A **506**, 250 (2003).

[25] N. Isgur, M. Wise, in: 'B Decays', S. Stone (ed.), 2nd ed., World Scientific, Singapore (1994); H. Georgi, 'Perspectives in the Standard Model', in: Proceed. TASI 1991, R.K. Ellis *et al.* (eds.), World Scientific, Singapore (1992).

[26] I.I. Bigi, M. Shifman, N.G. Uraltsev, Ann. Rev. Nucl. Part. Sci. **47**, 591(1997).

[27] N.G. Uraltsev, in: 'The B. Joffe Festschrift' At the Frontier of Particle Physics/Handbook of QCD, M. Shifman (ed.), World Scientific, Singapore, 2001; [arXiv:hep-ph/0010328].

[28] Z. Ligeti, 'Introduction to Heavy Meson Decays and CP Asymmetries', in Proceedings of the 30th SLAC Summer Institute: Secrets of the B Meson (SSI 2002), eConf C020805 (2002) L02

[29] C. W. Bauer, Z. Ligeti, M. Luke, A. V. Manohar and M. Trott, Phys. Rev. D **70**, 094017 (2004) [arXiv:hep-ph/0408002]; C. W. Bauer, Z. Ligeti, M. Luke, A. V. Manohar, Phys. Rev. D **67**, 054012 (2003) ; Z. Ligeti, hep-ph/0309219; A. H. Hoang, Z. Ligeti, A. V. Manohar, Phys. Rev. D **59**, 074017 (1999) .

[30] The translations have conveniently been given in: M. Battaglia *et al.*, [arXiv:hep-ph/0304132], to appear as a CERN Yellow Report.

[31] D. Benson, I.I. Bigi, Th. Mannel, N.G. Uraltsev, Nucl.Phys. B **665**, 367 (2003).

[32] I.I. Bigi, M. Shifman, N.G. Uraltsev, A. Vainshtein, Phys.Rev. D **52**, 196 (1995) .

[33] For the determined student of the subject of quark-hadron duality: I.I. Bigi, N.G. Uraltsev, Int.J.Mod.Phys. A **16**, 5201 (2001) ; a more casual observer might satisfy his/her curiosity with: I.I. Bigi, Th. Mannel, [arXiv:hep-ph/0212021].

[34] M. Battaglia *et al.*, Phys.Lett. B **556**, 41 (2003).

[35] I.I. Bigi, N.G. Uraltsev, , Phys.Lett. B **579**, 340 (2004) [arXiv:hep-ph/0308165].

[36] *BABAR* Collaboration (B. Aubert *et al.*), Phys. Rev. Lett. **93**, 011803 (2004) [arXiv:hep-ex/0404017].

[37] The possible impact of a photon energy cut has been raised before in terms of theoretical uncertainties, yet without reaching definite conclusions in: C. Bauer, Phys. Rev. D **57** (1998) 5611; Phys. Rev. D **60** (1999) 099907 (E); A. Kagan, M. Neubert, Eur. Phys. J. C **7** (1999) 5.

[38] D. Benson, I.I. Bigi, N. Uraltsev, Nucl. Phys. B **665**, 367 (2003) [arXiv:hep-ph/0302262].

[39] I.I. Bigi, M. Shifman, N.G. Uraltsev, A. Vainshtein, Phys.Rev. D **52**, 196 (1995).

[40] The *BABAR* Physics Book, P. Harrison, H. Quinn (eds.), SLAC-R-504.

[41] A. S. Kronfeld, P. B. Mackenzie, J. N. Simone, S. Hashimoto, S. M. Ryan, talk given by A. Kronfeld at 'Flavor Physics and CP Violation (FPCP)', May 16–18, Philadelphia, [arXiv:hep-ph/0207122]; S. Hashimoto, A. S. Kronfeld, P. B. Mackenzie, S. M. Ryan, J. N. Simone, Phys.Rev. D **66** (2002) 014503.

[42] N. Uraltsev, Phys. Lett. B **545** (2002) 337; [arXiv:hep-ph/0306290]; [arXiv:hep-ph/0312001].

[43] T. Miki, T. Miura, M. Tanaka, [arXiv:hep-ph/0210051].

[44] BABAR Collaboration, (B. Aubert *et al.*), Phys. Rev. D **69**, 111103 (2004) [arXiv:hep-ex/0403031].

[45] CLEO Collaboration, (F. Bartelt *et al.*), Phys. Rev. Lett. 71 (1993) 4111; H. Albrecht *et al.*, Argus Collaboration, Phys. Lett. B **255**, 297 (1991).

[46] CLEO Collaboration, (B.H. Behrens *et al.*), [arXiv:hep-ex/9905056].

[47] P. Ball and R. Zwicky, JHEP **0110**, 19 (2001).

[48] A. Kronfeld, [arXiv:hep-ph/0010074].

[49] J. Chay, H. Georgi, and B. Grinstein, Phys. Lett. B **247**, 399 (1990) ; M. Voloshin and M. Shifman, Sov. J. Nucl. Phys. **41**, 120 (1985) ; I.I. Bigi *et al.*, Phys. Lett. B **293**, 430 (1992) ; Phys. Lett. B **297**, 477 (1993) (E); I.I. Bigi *et al.*, Phys. Rev. Lett. **71**, 496 (1993) ; A.V. Manohar and M.B. Wise, Phys. Rev. D **49**, 1310 (1994); B. Blok *et al.*, Phys. Rev. D **49**, 3356 (1994); A. F. Falk, M. Luke and M. J. Savage, Phys. Rev. D **49**, 3367 (1994).

[50] CLEO Collaboration, (R. A. Briere *et al.*), [arXiv:hep-ex/0209024].

[51] A. H. Hoang, Z. Ligeti and A. V. Manohar, Phys. Rev. Lett. **82**, 277 (1999); *ibid.*, Phys. Rev. D **59**, 074017 (1999); A. H. Hoang and T. Teubner, Phys. Rev. D **60**, 114027 (1999).

[52] For a review, see A. El-Khadra and M. Luke, Ann. Rev. Nucl. Part. Sci. **52**, 201 (2002).

[53] A. F. Falk, M. E. Luke and M. J. Savage, Phys. Rev. D **53**, 2491 (1996). Phys. Rev. D **53**, 6316 (1996); A. F. Falk and M. E. Luke, Phys. Rev. D **57**, 424 (1998); A. Kapustin and Z. Ligeti, Phys. Lett. B **355**, 318 (1995); C. Bauer, Phys. Rev. D **57**, 5611 (1998); Erratum-*ibid*. D **60** 099907 (1999); Z. Ligeti, M. Luke, A.V. Manohar, and M.B. Wise, Phys. Rev. D **60**, 034019 (1999); CLEO Collaboration, (D. Cronin-Hennessy *et al.*), Phys. Rev. Lett. **87**, 251808 (2001); CLEO Collaboration, (R. A. Briere *et al.*), [arXiv:hep-ex/0209024]; *BABAR* Collaboration, (B. Aubert *et al.*), [arXiv:hep-ex/0207084]; DELPHI Collaboration, Contributed paper for ICHEP 2002, 2002-070-CONF-605; 2002-071-CONF-604; C. W. Bauer, Z. Ligeti, M. Luke and A. V. Manohar, Phys. Rev. D **67**, 054012 (2003);

[54] N. Uraltsev, Int. J. Mod. Phys. A **14**, 4641 (1999).

[55] V. Barger, C. S. Kim and R. J. Phillips, Phys. Lett. B **251**, 629 (1990) ; A.F. Falk, Z. Ligeti, and M.B. Wise, Phys. Lett. B **406**, 225 (1997) ; I. Bigi, R.D. Dikeman, and N. Uraltsev, Eur. Phys. J. C **4**, 453 (1998) ; R. D. Dikeman and N. Uraltsev, Nucl. Phys. B **509**, 378 (1998) ; DELPHI Collaboration, (P. Abreu *et al.*), Phys. Lett. B **478**, 14(2000).

[56] C.W. Bauer, Z. Ligeti, and M. Luke, Phys. Lett. B **479**, 395 (2000) .

[57] C. W. Bauer, Z. Ligeti and M. Luke, Phys. Rev. D **64**, 113004 (2001) .

[58] F. De Fazio and M. Neubert, JHEP **0006**, 017 (1999) .

[59] M. Neubert, Phys. Rev. D49, 3392 (1994) ; D **49**, 4623 (1994); I.I. Bigi *et al.*, Int. J. Mod. Phys. A **9**, 2467 (1994) ; T. Mannel and M. Neubert, Phys. Rev. D **50**, 2037 (1994) ; A. F. Falk, E. Jenkins, A. V. Manohar and M. B. Wise, Phys. Rev. D **49**, 4553 (1994) .

[60] CLEO Collaboration, (A. Bornheim *et al.*), Phys. Rev. Lett. **88**, 231803 (2002) .

[61] G. P. Korchemsky and G. Sterman, Phys. Lett. B **340**, 96 (1994); R. Akhoury and I. Z. Rothstein, Phys. Rev. D **54**, 2349 (1996); A. K. Leibovich and I. Z. Rothstein, Phys. Rev. D **61**, 074006 (2000); A. K. Leibovich, I. Low and I. Z. Rothstein, Phys. Rev. D **61**, 053006 (2000); A. K. Leibovich, I. Low and I. Z. Rothstein, Phys. Rev. D **62**, 014010 (2000); A. K. Leibovich, I. Low and I. Z. Rothstein, Phys. Lett. B **486**, 86 (2000).

[62] M. Neubert, Phys. Lett. B **513**, 88 (2001).

[63] C. W. Bauer and A. V. Manohar, [arXiv:hep-ph/0312109]

[64] C. W. Bauer, M. E. Luke and T. Mannel, [arXiv:hep-ph/0102089].

[65] C. W. Bauer, M. Luke and T. Mannel, Phys. Lett. B **543**, 261 (2002).

[66] A. K. Leibovich, Z. Ligeti and M. B. Wise, Phys. Lett. B **539**, 242 (2002).

[67] M. Neubert, Phys. Lett. B **543**, 269 (2002) .

[68] C. N. Burrell, M. E. Luke and A. R. Williamson, [arXiv:hep-ph/0312366].

[69] G. Buchalla and G. Isidori, Nucl. Phys. B **525**, 333 (1998) .

[70] M. Neubert, JHEP 0007, **022** (2000) .

[71] I. I. Bigi and N. G. Uraltsev, Nucl. Phys. B **423**, 33 (1994); M. B. Voloshin, Phys. Lett. B **515**, 74 (2001).

[72] K. S. M. Lee and I. W. Stewart, [arXiv:hep-ph/0409045].

[73] S. W. Bosch, M. Neubert and G. Paz, [arXiv:hep-ph/0409115].

[74] M. A. Shifman and M. B. Voloshin, Sov. J. Nucl. Phys. **41**, 120 (1985).

[75] M. A. Shifman and M. B. Voloshin, JETP **64**, 698 (1986).

[76] I. I. Bigi and N. G. Uraltsev, Nucl. Phys. B **423**, 33 (1994).

[77] I. I. Bigi and N. G. Uraltsev, Z. Phys. C **62**, 623 (1994).

[78] M. Neubert and C. T. Sachrajda, Nucl. Phys. B **483**, 339 (1997).

[79] V. Chernyak, Nucl. Phys. B **457**, 96 (1995).

[80] M. S. Baek *et.al*, Phys. Rev. D **57**, 4091 (1998).

[81] D. Pirjol and N. Uraltsev, Phys. Rev. D **59**, 034012 (1999).

[82] M. B. Voloshin, Phys. Lett. B **515**, 74 (2001).

[83] N. G. Uraltsev, J. Mod. Phys. A **14**, 4641 (1999).

[84] T. van Ritbergen, Phys. Lett. B **454**, 353 (1999).

[85] I. I. Bigi, N. G. Uraltsev, and A. I. Vainshtein, Phys. Lett. B **293**, 430 (1992).

[86] M. B. Voloshin, Surv. High En. Phys. **8**, 27 (1995).

[87] V. A. Novikov *et.al.*, Phys. Rep. C **41**, 1 (1978).

[88] B. Blok, R. D. Dikeman, and M. A. Shifman, Phys. Rev. D **51**, 6167 (1995).

[89] D. Cronin-Hennessy *et.al.*, CLEO Coll., Phys. Rev. Lett. **87**, 251808 (2001).

[90] M. B. Voloshin, Mod. Phys. Lett. A **17**, 245 (2002).

[91] M. Di Pierro and C. T. Sachrajda [UKQCD Collaboration], Nucl. Phys. B **534**, 373 (1998) [arXiv:hep-lat/9805028].

[92] M. Neubert, Phys. Rev. D **49**, 3392 (1994) [arXiv:hep-ph/9311325]. I. I. Y. Bigi, M. A. Shifman, N. G. Uraltsev and A. I. Vainshtein, Int. J. Mod. Phys. A **9**, 2467 (1994) [arXiv:hep-ph/9312359].

[93] For a review of the pros and cons of various cuts see, Z. Ligeti, [arXiv:hep-ph/0309219].

[94] V. D. Barger, C. S. Kim and R. J. N. Phillips, Phys. Lett. B **251**, 629 (1990).

[95] C. W. Bauer, Z. Ligeti and M. E. Luke, Phys. Lett. B **479**, 395 (2000) [arXiv:hep-ph/0002161].

[96] M. Neubert, JHEP **0007**, 022 (2000) [arXiv:hep-ph/0006068].

[97] C. W. Bauer, Z. Ligeti and M. E. Luke, Phys. Rev. D **64**, 113004 (2001) [arXiv:hep-ph/0107074].

[98] F. De Fazio and M. Neubert, JHEP **9906**, 017 (1999) [arXiv:hep-ph/9905351].

[99] C. W. Bauer and A. V. Manohar, [arXiv:hep-ph/0312109].

[100] CLEO Collaboration, (A. Bornheim *et al.*), Phys. Rev. Lett. **88**, 231803 (2002) [arXiv:hep-ex/0202019].

[101] Belle Collaboration, (H. Kakuno *et al.*), [arXiv:hep-ex/0311048].

[102] G. P. Korchemsky and G. Sterman, Phys. Lett. B **340**, 96 (1994) [arXiv:hep-ph/9407344].

[103] A. K. Leibovich, I. Low and I. Z. Rothstein, Phys. Rev. D **61**, 053006 (2000) [arXiv:hep-ph/9909404].

[104] A. K. Leibovich, I. Low and I. Z. Rothstein, Phys. Lett. B **513**, 83 (2001) [arXiv:hep-ph/0105066].

[105] I. Z. Rothstein, AIP Conf. Proc. **618**, 153 (2002) [arXiv:hep-ph/0111337].

[106] M. Neubert, Phys. Rev. D **49**, 4623 (1994)

[107] K. Chetyrkin, M. Misiak, and M. Munz, Phys. Lett. B **400**, 206 (1997).

[108] C. Greub, T. Hurth, and D. Wyler, Phys. Lett. B, **380**, 385 (1996).

[109] R. Akhoury and I. Z. Rothstein, Phys. Rev. D **54**, 2349 (1996) [arXiv:hep-ph/9512303].

[110] A. K. Leibovich and I. Z. Rothstein, Phys. Rev. D **61**, 074006 (2000) [arXiv:hep-ph/9907391].

[111] A. K. Leibovich, I. Low and I. Z. Rothstein, Phys. Lett. B **486**, 86 (2000) [arXiv:hep-ph/0005124].

[112] A. K. Leibovich, I. Low and I. Z. Rothstein, Phys. Rev. D **62**, 014010 (2000) [arXiv:hep-ph/0001028].

[113] A. K. Leibovich and I. Z. Rothstein, Phys. Rev. D **61**, 074006 (2000) [arXiv:hep-ph/9907391].

[114] C. W. Bauer, M. E. Luke and T. Mannel, Phys. Rev. D **68**, 094001 (2003) [arXiv:hep-ph/0102089]. A. K. Leibovich, Z. Ligeti and M. B. Wise, Phys. Lett. B **539**, 242 (2002) [arXiv:hep-ph/0205148]. C. W. Bauer, M. Luke and T. Mannel, Phys. Lett. B **543**, 261 (2002) [arXiv:hep-ph/0205150]. M. Neubert, Phys. Lett. B **543**, 269 (2002) [arXiv:hep-ph/0207002]. C. N. Burrell, M. E. Luke and A. R. Williamson, [arXiv:hep-ph/0312366].

[115] R. V. Kowalewski and S. Menke, Phys. Lett. B **541**, 29 (2002) [arXiv:hep-ex/0205038].

[116] U. Aglietti, M. Ciuchini and P. Gambino, Nucl. Phys. B **637**, 427 (2002) [arXiv:hep-ph/0204140].

[117] M. Wirbel, B. Stech and M. Bauer, Z. Phys. C **29**, 637 (1985); N. Isgur, D. Scora, B. Grinstein and M. B. Wise, Phys. Rev. D **39**, 799 (1989).

[118] V. M. Belyaev, A. Khodjamirian and R. Ruckl, Z. Phys. C **60**, 349 (1993) [arXiv:hep-ph/9305348].

[119] A. Khodjamirian, R. Ruckl, S. Weinzierl and O. I. Yakovlev, Phys. Lett. B **410**, 275 (1997) [arXiv:hep-ph/9706303].

[120] E. Bagan, P. Ball and V. M. Braun, "Radiative corrections to the decay B → pi e nu and the heavy quark Phys. Lett. B **417**, 154 (1998) [arXiv:hep-ph/9709243].

[121] A. Khodjamirian, R. Ruckl, S. Weinzierl, C. W. Winhart and O. I. Yakovlev, "Predictions on B → pi anti-l nu/l, D → pi anti-l nu/l and D → K Phys. Rev. D **62**, 114002 (2000) [arXiv:hep-ph/0001297].

[122] P. Ball and V. M. Braun, Phys. Rev. D **58**, 094016 (1998) [arXiv:hep-ph/9805422].

[123] P. Ball, JHEP **9809**, 005 (1998) [arXiv:hep-ph/9802394].

[124] P. Ball and R. Zwicky, JHEP **0110**, 019 (2001) [arXiv:hep-ph/0110115].

[125] J. H. Sloan, Nucl. Phys. Proc. Suppl. **63**, 365 (1998) [arXiv:hep-lat/9710061].

[126] K. M. Foley and G. P. Lepage, Nucl. Phys. Proc. Suppl. **119**, 635 (2003) [arXiv:hep-lat/0209135].

[127] P. A. Boyle, Nucl. Phys. Proc. Suppl. **129**, 358 (2004) [arXiv:hep-lat/0309100].

[128] M. B. Wise, Phys. Rev. D **45**, 2188 (1992).

[129] G. Burdman and J. F. Donoghue, Phys. Lett. B **280**, 287 (1992).

[130] T. M. Yan, H. Y. Cheng, C. Y. Cheung, G. L. Lin, Y. C. Lin and H. L. Yu, Phys. Rev. D **46**, 1148 (1992) [Erratum-*ibid.* D **55**, 5851 (1997)].

[131] G. Burdman, Z. Ligeti, M. Neubert and Y. Nir, Phys. Rev. D **49**, 2331 (1994) [arXiv:hep-ph/9309272].

[132] C. G. Boyd and B. Grinstein, Nucl. Phys. B **442**, 205 (1995) [arXiv:hep-ph/9402340].

[133] C. S. Huang, C. Liu and C. T. Yan, Phys. Rev. D **62**, 054019 (2000) [arXiv:hep-ph/0006003].

[134] C. W. Bauer, S. Fleming and M. E. Luke, Phys. Rev. D **63**, 014006 (2001).

[135] C. W. Bauer, S. Fleming, D. Pirjol and I. W. Stewart, Phys. Rev. D **63**, 114020 (2001).

[136] C. W. Bauer and I. W. Stewart, Phys. Lett. B **516**, 134 (2001).

[137] C. W. Bauer, D. Pirjol and I. W. Stewart, Phys. Rev. D **65**, 054022 (2002)

[138] C. G. Boyd, B. Grinstein and R. F. Lebed, Phys. Rev. Lett. **74**, 4603 (1995) [arXiv:hep-ph/9412324].

[139] C. G. Boyd and R. F. Lebed, Nucl. Phys. B **485**, 275 (1997) [arXiv:hep-ph/9512363].

[140] C. G. Boyd, B. Grinstein and R. F. Lebed, Phys. Rev. D **56**, 6895 (1997) [arXiv:hep-ph/9705252].

[141] I. Caprini, L. Lellouch and M. Neubert, Nucl. Phys. B **530**, 153 (1998) [arXiv:hep-ph/9712417].

[142] See `http://www.osti.gov/scidac/henp/SciDAC_HENP_details.htm#Lattice`.

[143] J. Charles, A. Le Yaouanc, L. Oliver, O. Pene and J. C. Raynal, Phys. Rev. D **60**, 014001 (1999).

[144] B. Stech, Phys. Lett. B **354**, 447 (1995); J. M. Soares, Phys. Rev. D **54**, 6837 (1996).

[145] M. J. Dugan and B. Grinstein, Phys. Lett. B **255**, 583 (1991).

[146] M. Beneke and T. Feldmann, Nucl. Phys. B **592**, 3 (2001)

[147] M. Beneke, A. P. Chapovsky, M. Diehl and T. Feldmann, Nucl. Phys. B **643**, 431 (2002); M. Beneke and T. Feldmann, Phys. Lett. B **553**, 267 (2003).

[148] C. W. Bauer, D. Pirjol and I. W. Stewart, Phys. Rev. D **67**, 071502 (2003).

[149] C. W. Bauer, D. Pirjol and I. W. Stewart, [arXiv:hep-ph/0303156].

[150] D. Pirjol and I. W. Stewart, Phys. Rev. D **67**, 094005 (2003).

[151] D. Pirjol and I. W. Stewart, [arXiv:hep-ph/0309053].

[152] M. Beneke and T. Feldmann, [arXiv:hep-ph/0311335].

[153] B. O. Lange and M. Neubert, Phys. Rev. Lett. **91**, 102001 (2003).

[154] B. O. Lange and M. Neubert, [arXiv:hep-ph/0311345].

[155] C. W. Bauer, D. Pirjol and I. W. Stewart, Phys. Rev. D **67**, 071502 (2003) [arXiv:hep-ph/0211069].

[156] M. Beneke, A. P. Chapovsky, M. Diehl and T. Feldmann, Nucl. Phys. B **643**, 431 (2002) [arXiv:hep-ph/0206152].

[157] A. V. Manohar, T. Mehen, D. Pirjol and I. W. Stewart, Phys. Lett. B **539**, 59 (2002).

[158] A. K. Leibovich, Z. Ligeti and M. B. Wise, Phys. Lett. B **564**, 231 (2003) [arXiv:hep-ph/0303099];

[159] J. W. Chen and I. W. Stewart, Phys. Rev. Lett. **92**, 202001 (2004) [arXiv:hep-ph/0311285].

[160] G. Burdman and G. Hiller, Phys. Rev. D **63**, 113008 (2001).

[161] T. Kurimoto, H. n. Li and A. I. Sanda, Phys. Rev. D **65**, 014007 (2002).

[162] H. N. Li, [arXiv:hep-ph/0303116].

[163] S. Descotes-Genon and C. T. Sachrajda, Nucl. Phys. B **625**, 239 (2002).

[164] R. J. Hill, T. Becher, S. J. Lee and M. Neubert, JHEP **0407**, 081 (2004) [arXiv:hep-ph/0404217].

[165] N. Isgur and M. B. Wise, Phys. Lett. B **237**, 527 (1990); M. E. Luke, Phys. Lett. B **252**, 447 (1990).

[166] N. Isgur and M. B. Wise, Phys. Rev. D **42**, 2388 (1990).

[167] G. Burdman and J. F. Donoghue, Phys. Lett. B **270**, 55 (1991).

[168] B. Grinstein and D. Pirjol, Phys. Lett. B **533**, 8 (2002)

[169] A. I. Sanda and A. Yamada, Phys. Rev. Lett. **75**, 2807 (1995).

[170] Z. Ligeti and M. B. Wise, Phys. Rev. D **53**, 4937 (1996); Z. Ligeti, I. W. Stewart and M. B. Wise, Phys. Lett. B **420**, 359 (1998).

[171] B. Grinstein, Phys. Rev. Lett. **71**, 3067 (1993).

[172] G. Burdman, Z. Ligeti, M. Neubert and Y. Nir, Phys. Rev. D **49**, 2331 (1994).

[173] B. Grinstein and D. Pirjol, Phys. Lett. B **549**, 314 (2002).

[174] B. Grinstein and D. Pirjol, [arXiv:hep-ph/0404250].

[175] Z. Ligeti and M. B. Wise, Phys. Rev. D **53**, 4937 (1996) [arXiv:hep-ph/9512225].

[176] Z. Ligeti, I. W. Stewart and M. B. Wise, Phys. Lett. B **420**, 359 (1998) [arXiv:hep-ph/9711248].

[177] B. Grinstein and D. Pirjol, Phys. Lett. B **533**, 8 (2002) [arXiv:hep-ph/0201298].

[178] B. Grinstein and D. Pirjol, Phys. Lett. B **549**, 314 (2002) [arXiv:hep-ph/0209211].

[179] B. Grinstein and D. Pirjol, Phys. Rev. D **62**, 093002 (2000) [arXiv:hep-ph/0002216].

[180] G. P. Korchemsky, D. Pirjol and T. M. Yan, Phys. Rev. D **61**, 114510 (2000) [arXiv:hep-ph/9911427].

[181] L. Del Debbio, J. M. Flynn, L. Lellouch and J. Nieves [UKQCD Collaboration], Phys. Lett. B **416**, 392 (1998) [arXiv:hep-lat/9708008].

[182] A. I. Sanda and A. Yamada, Phys. Rev. Lett. **75**, 2807 (1995) [arXiv:hep-ph/9507283].

[183] Z. Ligeti and M. B. Wise, Phys. Rev. D **60**, 117506 (1999) [arXiv:hep-ph/9905277].

[184] B. Grinstein, M. J. Savage and M. B. Wise, Nucl. Phys. B **319**, 271 (1989).

[185] B. Grinstein, R. P. Springer and M. B. Wise, Nucl. Phys. B **339**, 269 (1990).

[186] A. J. Buras and M. Munz, Phys. Rev. D **52**, 186 (1995) [arXiv:hep-ph/9501281].

[187] M. Misiak and M. Munz, Phys. Lett. B **344**, 308 (1995) [arXiv:hep-ph/9409454].

[188] G. Burdman and J. F. Donoghue, Phys. Lett. B **280**, 287 (1992).

[189] M. B. Wise, Phys. Rev. D **45**, 2188 (1992).

[190] C. G. Boyd and B. Grinstein, Nucl. Phys. B **451**, 177 (1995) [arXiv:hep-ph/9502311].

[191] E. Jenkins, A. V. Manohar and M. B. Wise, Phys. Rev. Lett. **75**, 2272 (1995) [arXiv:hep-ph/9506356].

[192] CLEO Collaboration, (S. B. Athar *et al.*), [arXiv:hep-ex/0304019].

[193] H. Ishino [Belle Collaboration], [arXiv:hep-ex/0205032].

[194] *BABAR* Collaboration, (B. Aubert *et al.*), Phys. Rev. Lett. **90**, 181801 (2003) [arXiv:hep-ex/0301001].

[195] D. del Re [*BABAR* Collaboration], Poster presented at Lepton Photon 2003 conference, `http://conferences.fnal.gov/lp2003/posters/physics/delre_poster2.pdf`

[196] Particle Data Group, K. Hagiwara *et al.* Phys. Rev. D **66**, 010001 (2002).

[197] S. M. Ryan, Nucl. Phys. Proc. Suppl. **106**, 86 (2002).

[198] *BABAR* Collaboration, (B. Aubert *et al.*), [arXiv:hep-ex/0304030].

[199] *BABAR* Collaboration, (B. Aubert *et al.*), [arXiv:hep-ex/0303034].

[200] CLEO Collaboration, (M. Artuso *et al.*), Phys. Rev. Lett. **75**, 785 (1995).

[201] Belle Collaboration, (K. Abe *et al.*), Search for W-Annihilation B Meson Decays, Belle-CONF-0247.

[202] *BABAR* Collaboration, (B. Aubert *et al.*), Phys. Rev. Lett. **92**, 221803 (2004) [arXiv:hep-ex/0401002].

[203] S. Descotes-Genon and C. T. Sachrajda, Nucl. Phys. B **650**, 356 (2003).

[204] E. Lunghi, D. Pirjol and D. Wyler, Nucl. Phys. B **649**, 349 (2003).

[205] S. W. Bosch, R. J. Hill, B. O. Lange and M. Neubert, Phys. Rev. D **67**, 094014 (2003).

[206] V. M. Braun, D. Y. Ivanov and G. P. Korchemsky, [arXiv:hep-ph/0309330].

[207] S. Descotes-Genon and C. T. Sachrajda, Phys. Lett. B **557**, 213 (2003).

[208] T. Hurth, [arXiv:hep-ph/0212304].

[209] S. W. Bosch and G. Buchalla, JHEP **0208**, 054 (2002).

[210] F. Krüger and D. Melikhov, Phys. Rev. D **67**, 034002 (2003).

[211] *BABAR* Collaboration, (B. Aubert *et al.*), Phys. Rev. Lett. **87**, 241803 (2001) [arXiv:hep-ex/0107068].